Pilins of the T4P of *Acidithiobacillus thiooxidans*: more than pili blocks

Tesis que para obtener el grado de Doctor en Ciencias Interdisciplinarias presenta

Araceli Hernández Sánchez

Línea de investigación

Biofísica

Codirectoras de Tesis

Dra. J. Viridiana García Meza

Dra. Mónica R. Calera Medina

San Luis Potosí, 29 de abril del 2024

CRÉDITOS INSTITUCIONALES

Esta tesis se realizó en el laboratorio de Geomicrobiología del Instituto de Metalurgia, de la Universidad Autónoma de San Luis Potosí bajo la asesoría de la Dra. J. Viridiana García Meza y el apoyo del Consejo Nacional de Ciencia y Tecnología (CONACyT-CB2017 -2018 Proyecto A1-S- 11505: "Análisis de dos pilinas de *Acidithiobacillus thiooxidans*: su función en la transferencia extracelular de electrones y su posible uso como nanobiocable"). La autora agradece el apoyo de una beca de doctorado otorgada por CONACyT a través del programa de Becas Nacionales No. 439497. Finalmente la autora agradece el apoyo económico por parte de los recursos propios del laboratorio de Geomicrobiología.

INSTITUTIONAL CREDITS

This thesis was conducted in the Geomicrobiology Laboratory at the Instituto de Metalurgia, Universidad Autónoma de San Luis Potosí under the guidance of Dr. J. Viridiana García Meza and with the support of the National Council of Science and Technology (CONACyT-CB2017-2018 Project A1-S-11505: "Análisis de dos pilinas de *Acidithiobacillus thiooxidans*: su función en la transferencia extracelular de electrones y su posible uso como nanobiocable"). The author acknowledges the support of a doctoral scholarship granted by CONACyT through the National Scholarship Program No. 439497. Finally, the author acknowledges the financial support from the own resources of the Geomicrobiology laboratory.

RESUMEN

La evolución es un proceso complejo y altamente dinámico que depende de múltiples variables. En los organismos extremófilos la evolución se muestra en todo su esplendor al adaptar lo funcional mediante cambios simples pero efectivos. Las proteínas extracelulares de la bacteria acidófila *Acidithiobacillus thiooxidans,* objeto de estudio en este trabajo, evidencian este fenómeno.

El propósito de esta tesis es describir las características intrínsecas de las proteínas que forman parte del apéndice extracelular conocido como pilum de *At. thiooxidans*. Esta descripción abarca análisis in silico y experimentales en los cuales las proteínas se exponen a diversas condiciones que permiten inferir las características que las hacen resilientes a las condiciones extremas donde este organismo se encuentra, así como comprender los mecanismos que facilitan la transmisión de diferentes estímulos desde el exterior hacia el interior de la célula. Nos enfocamos en dos proteínas: la pilina minoritaria PilV y la proteína adhesina PilY1, ambas ubicadas en la parte más apical del pilus y por ende, las más expuestas al ambiente donde *At. thiooxidans* se desarrolla. En cuanto a los resultados in silico, este trabajo destaca: a) la propuesta del desorden y la composición de aminoácidos como posibles mecanismos de resistencia a ambientes extremos oxidantes y ácidos, y b) la respuesta a ciertos estímulos externos ocurre a través de dominios conservados que concuerdan con la propuesta mencionada anteriormente. Los resultados experimentales, por su parte, son consistentes con los análisis in silico, destacando: a) la metodología para obtener la expresión heteróloga de proteínas de microorganismos extremófilos, b) la confirmación de los resultados in silico, ya que se demostró que las características intrínsecas que poseen estas proteínas les permite ser funcionales dada su resiliencia a cambios de pH desde muy ácidos hasta básicos y c) el inicio de la caracterización del transporte de electrones a través de las pilinas de *At. thiooxidans*.

En términos generales, la importancia de este trabajo radica en la descripción del pilus de *At. thiooxidans* desde un enfoque proteómico, lo que permitió proponer un modelo de resistencia al pH, extrapolable a otros géneros de bacterias acidófilas utilizadas en los procesos mineros.

ABSTRACT

Evolution is a complex and highly dynamic process that depends on multiple variables. In extremophilic organisms, evolution is showcased in all its splendor by adapting functionality through simple yet effective changes. The extracellular proteins of the acidophilic bacterium *Acidithiobacillus thiooxidans*, the subject of this study, demonstrate this phenomenon.

The purpose of this thesis is to describe the intrinsic characteristics of the proteins that are part of the extracellular appendage known as the pilus of *At. thiooxidans*. This description encompasses in silico and experimental analyses in which the proteins are exposed to various conditions that allow inferring the characteristics that make them resilient to the extreme conditions where this organism is found, as well as understanding the mechanisms that facilitate the transmission of different stimuli from the exterior to the interior of the cell. We focus on two proteins: the minor pilin PilV and the adhesin protein PilY1, both located in the most apical part of the pilus and therefore the most exposed to the environment where *At. thiooxidans* develop. Regarding the in silico results, this work highlights: a) the proposal of disorder and amino acid composition as possible mechanisms of resistance to extreme oxidative and acidic environments, and b) the response to certain external stimuli occurs through conserved domains that align with the aforementioned proposal. The experimental results, on the other hand, are consistent with the in silico analyses, emphasizing: a) the methodology for obtaining heterologous expression of proteins from extremophilic microorganisms, b) the confirmation of the in silico results, as it was demonstrated that the intrinsic characteristics of these proteins allow them to be functional given their resilience to pH changes from highly acidic to basic, and c) the initiation of the characterization of electron transport through the pilins of *At. thiooxidans*.

In general terms, the importance of this work lies in the description of the *At. thiooxidans* pilus from a proteomic approach, which allowed proposing a pH resistance model extrapolable to other genera of acidophilic bacteria used in mining processes.

INDEX

Figures Index

CHAPTER I

Global Introduction

The type 4 pili in Bacteria

Motility is a common characteristic in prokaryotes, offering each microorganism a movement advantage. Flagella and pili (or fimbriae) are filamentous structures involved in motility that differ in length, protein composition, and functions (Bardy et al., 2003).

Pili in Gram-negative bacteria have been classified into five major classes: P pili, curli pili, type I pili, type IV pili, and type V pili. Type IV pili (T4P) is unique as it is found in both Gram-positive and Gram-negative bacteria (Fronzes et al., 2008; Melville and Craig 2013; Shanmugasundarasamy et al., 2022). Additionally, in Archaea, there are appendages highly related to T4P called *archaellum* (Daum and Gold 2018; Wang et al., 2020).

Type IV pili serve a variety of functions. One of the most remarkable being twitching motility. This movement allows prokaryotic cells to "walk" in non-aqueous environments. Such motility becomes crucial when cells form colonies on solid substrates or semi-solid surfaces. The twitching motion involves the rapid extension, adhesion, and subsequent retraction of the pili, ensuring that the cell is pulled forward in the direction of the pili assembly. This motility is complex and multifactorial dependent, leading to diverse cell movements between surfaces and species (Maier and Wong 2015).

But motility is just the top of the iceberg. The T4P is involved in adhesion to a wide variety of biotic and abiotic surfaces (Lu et al., 2015), DNA exchange (Rudel et al., 1995; Averhoff and Friedrich 2003; Ronish et al., 2022) and sensing. Thus, it plays a role in promoting processes such as bacterial virulence, auto-aggregation, biofilm formation, intercellular communication and natural transformation in bacteria (Siryaporn et al., 2014; Ossa-Henao et al., 2014; Tang et al., 2018; Webster et al., 2021).

The T4P is a large complex that includes at least ten conserved core proteins for its biogenesis in prokaryotes. T4P has been classified into three subclasses pili' types: IVa (T4aP), IVb (T4bP) and Tad pili recently designated as type IVc (T4cP).

The subtypes of T4P share similar architecture and biogenesis involving protein complexes in intracellular, periplasmic and extracellular spaces, and includes: an ATPase that provides energy for elongation (polymerization), one peptidase that removes the leader peptide, a platform complex that interacts with the ATPase, a secretin complex that directs the output of pili to the extracellular space, an alignment and stability multiprotein complex in periplasmic and intracellular spaces, the major pilin subunits forming the pili structure, and finally, some minor pilin subunits. Actually, the subclasses T4P has been categorized accord to protein enrichment mostly. The T4aP exhibits greater complexity, followed by T4bP; the T4cP is the simplest among T4P. Similitudes and differences in protein diversity between T4P subclasses are resume in Table 1 (Ayers et al., 2010; Koo et al., 2013; Melville and Craig 2013; Pelicic 2019; Ligthart et al., 2020; Pelicic 2023).

Table 1. Differences between T4P pili subclasses. Modified of Pelicic (2023) and completed from Ayers et al., (2010)

Protein diversity in Type 4 pili subclasses			
Extracellular proteins			
Pilus component	**T4aP (*P. aeruginosa*)**	**T4bP (*V. cholerae*)**	**T4cP (*A. actinomycetemcomitans*)**
Major pili	PilA	TcpA	Flp1
Minor pilins	FimU	TcpB	TadE
	PilV	None	TadF
	PilW	None	
	PilX	None	None
	PilE	None	
Non pilin located tip	PilY1	TcpF	
Inner/inter membrane proteins			
Peptidase	PilD	TcpJ	TadV
Extension ATPase	PilB	TcpT	TadA
Retraction ATPase	PilT/PilU	None	None
Platform	PilC	TcpE	TadB/TadC
Alignment and stability complex	PilM	TcpR	TadG
	PilN	TcpD	TadZ
	PilO	TcpS	None
	PilP	None	None
Outer membrane proteins			
Secretin	PilQ	TcpC	RcpA
Pilotin	PilF	None	RcpB/RcpC/TadD

Other accessory proteins can complement those ten basic proteins; one of them is a non-pilin protein commonly referred as adhesins (e.g PilY1, PilC1/2 or TcpF) (Table 1). This non-pilin is attached to the pili tip and has a larger molecular weight than the structural minor and major pilins. Both T4aP and T4bP possess this tip protein, but T4cP does not. The functions of this non-pilin in the pili structure is unclear and although in some species is reported only as adhesin; in other it is involved in priming the assembly together with minor pilins and even like promoter regulator of pili to such a degree that it is elimination is translated in loss of piliation (Rudel et al., 1995; Nguyen et al., 2015; Oki et al., 2022). Other additional protein are pilotins, which are implicated in the secretin attachment in the outer membrane (Koo et al., 2008, 2013). Finally, the minor pilins even presents in the three subclass of T4P, they are more heterogeneous in T4aP (being able contains five different), while T4cP has only two and T4Pb usually had one; nevertheless, this does not means that pili structure has only few of these, for example, the minor PilV in *N. meningitides* is founded intercalated with the major pili PilE through entire pili (Barnier et al., 2021).

The T4aP structure and characteristics

The T4aP is a good example of a super nanomachine. Being the most complex of T4P, has the particularity that possess distinct ATPases, one for elongation ATPase (PilB) and other for pili retraction ATPase (PilT/PilU), which depolymerizes the pili fiber (Comolli et al., 1999; Jakovljevic et al., 2008; Chlebek et al., 2019). So actually, the retraction ATPase and more minor pilins are a landmark for the T4aP.

The T4aP subtype has been widely studied in pathogenic bacteria, with pili of *Pseudomonas aeruginosa* and *Myxococcus xanthus* being the most well-characterized at the genetic expression and regulation levels, as well as the functions and structures of several pili proteins or complete pilus assemblies have been resolved in these pathogens. Enlisted proteins in Table 1 use the nomenclature with which they are named in *P. aeruginosa*.

T4a pilus structural proteins

The genes responsible for the T4aP structure are typically encoded in four different operons. The first operon, *pilA-D*, includes genes for PilA (the major pilin), PilB (elongation ATPase), PilC (platform cytoplasmic protein), and PilD (the peptidase). The second operon, *pilUVWXEY1*, includes genes coding for the minor pilins (FimU, PilV, PilW, PilX and PilE)

and the non-pilin protein (PilY1). The third operon, *pilM-Q*, encompasses the proteins PilM, PilN, PilO, PilP and PilQ, all of which are part of the alignment and stability complex in the inner membrane. Finally, the fourth operon, *pilTU*, encodes the PilT and PilU retraction ATPases (Alm et al., 1996; Hmelo et al., 2015).

Major pilin PilA and minor pilins are named prepilins when they have leader signal (first six at ten amino acids, a type III signal peptide); they mature by action of peptidase PilD, which recognize and cleaved the bond between glycin (Gly)-phenilalanine (Phe), then Phe is methylated again by PilD that recognize glutamate (Glu) in the fifth position of mature pilin (Mcdonald et al., 1993). Accordingly, one manner to recognize pilins is by high conserved signal peptide (Giltner et al., 2010).

Once pilins are matured in the inner membrane along with PilY1, the next process involves their expulsion and polymerization. This is facilitated by PilB, which undergoes conformational changes during ATP hydrolysis, resulting in two states (open and closed). These motions are then transmitted to the platform protein PilC. The growing fiber passes through the complex located in the intermembrane space and formed by PilM, PilN, PilO, and PilP; lastly, the pilus is exiting through the secretin PilQ pore (Burrows 2012; Pelicic 2023).

Acidithiobacillus thiooxidans

At. thiooxidans is a gram-negative bacterium (Mahoney and Edwards 1966) usually founded in mine wastes, was isolated for first time by Waksman and Joffe (1921). *At. thiooxidans* is capable of oxidizing sulfur and other reduced inorganic sulfur compounds (RISCs) to obtain energy, using CO_2 as carbon source; accordingly, *At. thiooxidans* is a chemolithoautotrophic microorganism. Because also produce sulfuric acid during RISCs biooxidation, *At. thiooxidans* is an acidophil that survives in environments with pH around 1. *At. thiooxidans* is mesophilic (optimum temperature 28 °C) and aerobic, it is rode-shape of ca. <2 μm that forms very small colonies (0.5 mm to <2 mm) in solid medium (Waksman and Joffe 1922; García-Meza et al., 2013) (Fig. 1).

AGE OF CULTURE	pH
days	
At start	5.4
1	5.4
2	5.3
4	4.6
6	3.5
8	2.6
10	2.7
12	2.6
15	2.4
19	2.3
23	2.3
30	1.8
38	1.8
68	1.7
120	0.8

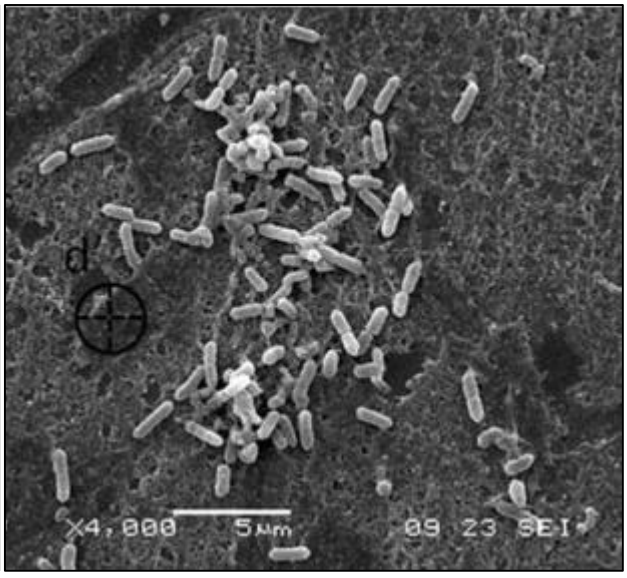

Figure 1. Left: Temporal course of *At. thiooxidans* and pH changes in culture (from Waksman and Joffe 1922). Right: Scanning electron microscopy (SEM) image of *At. thiooxidans* (scale bar 5µm). Rod shape morphology is clear in this micrography (from García-Meza et al., 2013).

Living at low pH is not the only prowess of *Acidithiobacillus* genus, they are soak up in high redox environment and heavy metals. The reducing power makes that cells are in constant electron exchange with the extracellular matrix; so, these microorganisms are considered bioelectrogenics (or *electricigens*) (García-Meza et al., 2013; Fernández-Reyes et al., 2018).

T4aP in *At. thiooxidans*

The growing interest in stems of *Acidithiobacillus* spp. (e.g. *At. ferrooxidans* -an iron-oxidizing- and *At. thiooxidans,* usually are found working together in bacterial consortia) from its natural bioleaching process, is because are particularly applied for the release of more or less occluded valuable metals such as Au, Ag, and Cu from oxidizing of sulfide minerals like pyrite (FeS_2) and chalcopyrite ($CuFeS_2$) (Diao et al., 2014, Yang et al., 2019; Jiménez-Paredes et al., 2021).

In the process of sulfide ore oxidation, intricate biochemical reactions occur at the interface between bacteria and minerals. The capacity of bacteria associated with minerals to control interfacial processes including adhesion and biofilm formation, is crucial.

In *At. thiooxidans* and *At. ferrooxidans,* bio-oxidation and bioleaching mechanisms have been studied using genomic and metabolic approaches; firstly, extracellular polymeric substances (EPS) (Harneit et al., 2006; González et al., 2011) or diverse periplasmic proteins

(Chi et al., 2007) were noted (overexpressed) in these processes. On the other hand, Dispirito et al., (1982) already found that *At. ferrooxidans* had pili, but the type was not identified. All those works eventually led to founded that the T4P was involved not only in adhesion, but also in motility, biofilm formation and in electrons transfer (Li et al., 2010; Li and Li 2014; Tang et al., 2018), at least in *At. ferrooxidans*.

Given that *Acidithiobacillus* genus members are genetically related, it is expected that they possess general similarities, and it is. In draft genome sequences, motility and biofilm formation genes were found (Valdés et al., 2007, 2011; Quatrini et al., 2017); among them, the genes for T4P, specifically the T4aP subclass, were found (Díaz et al., 2017). Second evidence about that *Acidithiobacillus* could had a T4aP is that contains PilT and PilU retraction ATPases (Li et al., 2013). However, T4aP involved genes had been poorly studied in *At. thiooxidans*. Indeed, the work of Li et al., (2010, 2014) and Tang et al., (2018) of *At. ferrooxidans*, assume that *pilV* and *pilW* genes are likely the major pilin subunits of T4aP; any study has been refused or confirmed it. Taken in count the above information about the T4aP in pathogenic bacteria, the assumption about what PilV or PilW are the major pilin could be wrong.

Following the findings of Li and collaborators for *At. ferrooxidans*, our group sequenced and confirmed the expression of three genes involved in T4aP in *At. thiooxidans*: *pilV*, *pilW* and *pilY1*, and the translated sequence analysis revealed more similitudes with the *P. aeruginosa* and *M. xanthus* minor pilins that with major pilin of the same bacteria (Alfaro-Saldaña et al., 2019).

At. thiooxidans T4aP opens a Pandora´s box

The combination of environmental and cellular characteristics of *At. thiooxidans* is unique. On one hand, it thrives under conditions of low pH, high redox potential and high metals concentration. On the other hand, *At. thiooxidans* "utilizes" one of the more complex Type IV pili structures, the T4aP, which have been confirmed by their involved in adhesion to sulfur minerals and twitching motility. Adding to the above features, this bacteria is electrogenic, presenting a set of intriguing unknowns that, when unraveled, could lead to even more interesting answers and open up a range of biotechnological possibilities.

Adaptive mechanisms in proteins of extremophiles acidophiles

The adaptive changes in all live forms are amazing. But in unicellular organisms a lightly change could be the difference between live or die. *At. thiooxidans* lives maintaining the equilibrium between extremely low pH out and near neutral pH (~6.5) into the cell: this means that *At. thiooxidans* is adapted to a great intracellular and extracellular pH (protons) gradient (Fig. 2) (Yin et al., 2019).

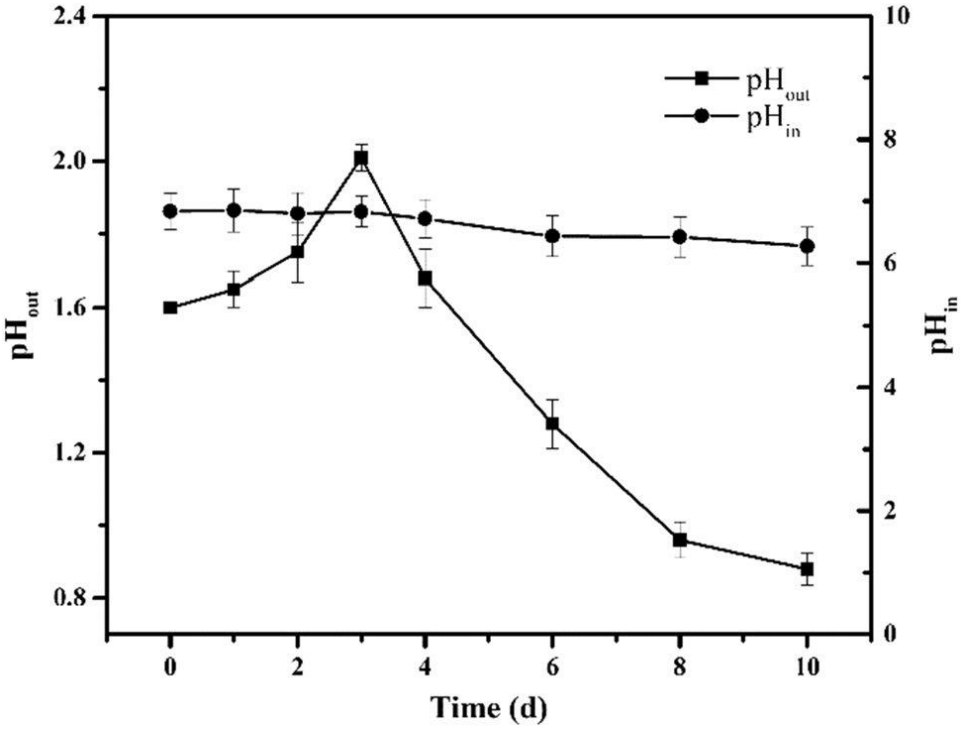

Figure 2. Changes in pH extracellular (out) and intracellular (in) in *At. thiooxidans* through the days, (From Yin et al., 2019).

In acidophiles, distinct mechanisms to thrive at low pH have been reported: potassium channels that generates an electrochemical gradient which enables the exit of H^+ at extracellular space or antiporters or pumps to export protons, alterations in membrane structure, reduction of the membrane permeability or high of alkaline amino acids to buffered the cytoplasm, to name a few (González-Rosales et al., 2022): all these mechanisms have been evolved in acidophiles (Boase et al., 2022). However, pilus of this bacteria is not necessarily "protected" against pH by the defense mechanisms cited above. Then, *At. thiooxidans* pilus should possessed an intrinsic mechanism to resist acidic conditions.

If we consider the fact that pili is formed by proteins, then these proteins are which really support the environment onslaught. Acidostable proteins exists in prokaryotes and eukaryotes cells and their study is a model to search for biotechnological applications (de Champodoré et al., 2007). The effects and resistance at low pH involved proteins changes in total charge, superficial charges, disordered regions or hydrophobicity (Thomas et al., 1977; Matzke et al., 1997; Dumetz et al., 2008). One pioneer work in flagellum of *At. thiooxidans* showed that this extracellular appendage formed by flagellin subunits tolerates pH of 1.0 and urea at 6 M maintains their function in live cells (Doetsch et al., 1967). Hence, pilus could tolerate similar conditions.

Electron transfer by the pili

Electron transfer through pili has been reported in non-acidophilic bacteria. The most studied is the T4P of *Geobacter sulfurreducens*. The T4P implication in extracellular electron transfer (EET) has been confirmed (Reguera et al., 2005; Malvankar et al., 2011; Sun et al., 2021). In addition, the T4P of *Flexistipes sinusarabici, Calditerrivibrio nitroreducens, Desulfurivibrio alkaliphilus, Aeromonas hydrophila* as well as *At. ferrooxidans* for citing some ones, have been described with EET capacity (Castro et al., 2014; Li and Li 2014; Walker at al., 2018). The applications possible of this conductive pili are promising; the most obvious is as nanowires (Sure at al., 2016) hence, tunable and high production performance protocols have been proposed (Malvankar et al., 2011; Ueki et al., 2019; Shu et al., 2020; Szmuc et al., 2023). However, the exact mechanism for electron transport through the pili filament remains unclear; some reports point to the presence of cytochromes along pili (Leang et al., 2010); the most accepted theory to explain the EET by pilus, are the presence of aromatics amino acids in pilins that facilitate the electron flow along pilins (Vargas et al., 2013; Shu et al., 2019; Liu et al., 2022). Nevertheless all this evidence, is not entirely clear whether all T4P of electrogenic bacteria conduct electrons and if they use the same mechanism or exists different ones accord the environmental conditions where bacteria live.

The PilY1 N-terminal domain role is more unclear than ever

PilY1 was related in functions with *N. gonorrhea* adhesin PilC since its C-terminal is sequentially and structurally similar. However, the “adhesin” PilY1 implication into the pili implies to promote the pili biogenesis or to acts as superficies and shear sensor (Kuchma et

al., 2010; Johnson et al., 2011; Siryaporn et al., 2014; Parker et al., 2015; Webster at al. 2021). Although the presence of PilY1 in T4aP is well documented in *P. aeruginosa* and *M. xanthus*, its tertiary structure has been solved only for its C-terminal domain (Orans et al., 2010), while its N-terminal domain and subdomains´ structures remain unresolved. For example, the N-terminal von Willebrand A (vWA) like domain had been described in the N-terminal PilY1 of *P. aeruginosa*, *At. thiooxidans* and other bacteria by homology using bioinformatics aproaches (Siryaporn et al., 2014, Alfaro et al., 2019, Webster et al., 2021, Xue et al., 2022), but its role in PilY1 and the vWA evolved through different bacteria species, is a mystery.

References Chapter I

Alfaro-Saldaña E, Hernández-Sánchez A, Patrón-Soberano OA, Astello-García M, Méndez-Cabañas JA, García-Meza JV. 2019. Sequence analysis and confirmation of the type IV pili-associated proteins PilY1, PilW and PilV in *Acidithiobacillus thiooxidans*. PLoS ONE. 14:e0199854. doi:10.1371/journal.pone.0199854

Alm RA, Hallinan JP, Watson AA, Mattick JS. 1996. Fimbrial biogenesis genes of *Pseudomonas aeruginosa*: *pilW* and *pilX* increase the similarity of type 4 fimbriae to the GSP protein-secretion systems and *pilY1* encodes a *gonococcal* PilC homologue. Mol Microbiol. 22:161–173. doi:10.1111/j.1365-2958.1996.tb02665.x

Averhoff B, Friedrich A. 2003. Type IV pili-related natural transformation systems: DNA transport in mesophilic and thermophilic bacteria. Arch Microbiol. 180:385–393. doi:10.1007/s00203-003-0616-6

Ayers M, Howell PL, Burrows LL. 2010. Architecture of the type II secretion and type IV pilus machineries. Future Microbiol. 5:1203–1218. doi:10.2217/fmb.10.76

Bardy SL, Ng SYM, Jarrell KF. 2003. Prokaryotic motility structures. Microbiology. 149:295–304. doi:10.1099/mic.0.25948-0

Barnier J-P, Meyer J, Kolappan S, Bouzinba-Ségard H, Gesbert G, Jamet A, Frapy E, Schönherr-Hellec S, Capel E, Virion Z, et al., 2021. The minor pilin PilV provides a conserved adhesion site throughout the antigenically variable *meningococcal* type IV pilus. Proc Natl Acad Sci U S A. 118. doi:10.1073/pnas.2109364118

Boase K, González C, Vergara E, Neira G, Holmes D, Watkin E. 2022. Prediction and inferred evolution of acid tolerance genes in the biotechnologically important *Acidihalobacter genus*. Front Microbiol. 13. doi:10.3389/fmicb.2022.848410

Burrows LL. 2012. *Pseudomonas aeruginosa* twitching motility: type IV pili in action. Annu Rev Microbiol. 66:493–520. doi:10.1146/annurev-micro-092611-150055

Castro L, Vera M, Muñoz JÁ, Blázquez ML, González F, Sand W, Ballester A. 2014. *Aeromonas hydrophila* produces conductive nanowires. Res Microbiol. 165(9):794–802. doi:10.1016/j.resmic.2014.09.005

Chi A, Valenzuela L, Beard S, Mackey AJ, Shabanowitz J, Hunt DF, Jerez CA. 2007. Periplasmic proteins of the extremophile *Acidithiobacillus ferrooxidans*: a high throughput proteomics analysis. Mol Cell Proteomics. 6:2239–2251. doi:10.1074/mcp.M700042-MCP200

Chlebek JL, Hughes HQ, Ratkiewicz AS, Rayyan R, Wang JC-Y, Herrin BE, Dalia TN, Biais N, Dalia AB. 2019. PilT and PilU are homohexameric ATPases that coordinate to retract type IVa pili. PLoS Genet. 15:e1008448. doi:10.1371/journal.pgen.1008448

Comolli JC, Hauser AR, Waite L, Whitchurch CB, Mattick JS, Engel JN. 1999. *Pseudomonas aeruginosa* gene products PilT and PilU are required for cytotoxicity in vitro and virulence in a mouse model of acute pneumonia. Infect Immun. 67:3625–3630. doi:10.1128/IAI.67.7.3625-3630.1999

Daum B, Gold V. 2018. Twitch or swim: towards the understanding of prokaryotic motion based on the type IV pilus blueprint. Biol Chem. 399:799–808. doi:10.1515/hsz-2018-0157

de Champdoré M, Staiano M, Rossi M, D'Auria S. 2007. Proteins from extremophiles as stable tools for advanced biotechnological applications of high social interest. J R Soc Interface. 4(13):183–191. doi:10.1098/rsif.2006.0174

Diao M, Nguyen TAH, Taran E, Mahler S, Nguyen AV. 2014. Differences in adhesion of *At. thiooxidans* and *At. ferrooxidans* on chalcopyrite as revealed by atomic force microscopy with bacterial probes. Miner Eng. 61:9–15. doi:10.1016/j.mineng.2014.03.002

Díaz M, Castro M, Copaja S, Guiliani N. 2018. Biofilm Formation by the Acidophile Bacterium *Acidithiobacillus thiooxidans* Involves c-di-GMP Pathway and Pel exopolysaccharide. Genes (Basel). 9:113. doi:10.3390/genes9020113

Doetsch RN, Cook TM, Vaituzis Z. 1967. On the uniqueness of the flagellum of *Thiobacillus thiooxidans*. Antonie Van Leeuwenhoek. 33(1):196–202. doi:10.1007/bf02045551

Dumetz AC, Chockla AM, Kaler EW, Lenhoff AM. 2008. Effects of pH on protein-protein interactions and implications for protein phase behavior. Biochim Biophys Acta. 1784(4):600–610. doi:10.1016/j.bbapap.2007.12.016

Fernández-Reyes JS, García-Meza JV. 2018. Bioelectrochemical system for the biooxidation of a chalcopyrite concentrate by acidophilic bacteria coupled to energy current generation and cathodic copper recovery. Biotechnol Lett. 40:63–73. doi:10.1007/s10529-017-2435-x

Fronzes R, Remaut H, Waksman G. 2008. Architectures and biogenesis of non-flagellar protein appendages in Gram-negative bacteria. EMBO J. 27:2271–2280. doi:10.1038/emboj.2008.155

García-Meza JV, Fernández JJ, Lara RH, González I. 2013. Changes in biofilm structure during the colonization of chalcopyrite by *Acidithiobacillus thiooxidans*. Appl Microbiol Biotechnol. 97:6065–6075. doi:10.1007/s00253-012-4420-6

Giltner CL, Habash M, Burrows LL. 2010. *Pseudomonas aeruginosa* minor pilins are incorporated into type IV pili. J Mol Biol. 398(3):444–461. doi:10.1016/j.jmb.2010.03.028

González DM, Lara RH, Alvarado KN, Valdez-Pérez D, Navarro-Contreras HR, Cruz R, García-Meza JV. 2012. Evolution of biofilms during the colonization process of pyrite by *Acidithiobacillus thiooxidans*. Appl Microbiol Biotechnol. 93:763–775. doi:10.1007/s00253-011-3465-2

González-Rosales C, Vergara E, Dopson M, Valdés JH, Holmes DS. 2022. Integrative genomics sheds light on evolutionary forces shaping the Acidithiobacillia class acidophilic lifestyle. Front Microbiol. 12. doi:10.3389/fmicb.2021.822229

Harneit K, Göksel A, Kock D, Klock J-H, Gehrke T, Sand W. 2006. Adhesion to metal sulfide surfaces by cells of *Acidithiobacillus ferrooxidans, Acidithiobacillus thiooxidans* and *Leptospirillum ferrooxidans*. Hydrometallurgy. 83:245–254. doi:10.1016/j.hydromet.2006.03.044

Hmelo LR, Borlee BR, Almblad H, Love ME, Randall TE, Tseng BS, Lin C, Irie Y, Storek KM, Yang JJ, et al., 2015. Precision-engineering the *Pseudomonas aeruginosa* genome with two-step allelic exchange. Nat Protoc. 10:1820–1841. doi:10.1038/nprot.2015.115

Jakovljevic V, Leonardy S, Hoppert M, Søgaard-Andersen L. 2008. PilB and PilT are ATPases acting antagonistically in type IV pilus function in *Myxococcus xanthus*. J Bacteriol.190:2411–2421.doi:10.1128/JB.01793-07

Jiménez-Paredes AE, Alfaro-Saldaña EF, Hernández-Sánchez A, García-Meza JV. 2021. An autochthonous *Acidithiobacillus ferrooxidans* metapopulation exploited for two-step pyrite biooxidation improves Au/Ag particle release from mining waste. Mining. 1:335–350. doi:10.3390/mining1030021

Johnson MDL, Garrett CK, Bond JE, Coggan KA, Wolfgang MC, Redinbo MR. 2011. *Pseudomonas aeruginosa* PilY1 binds integrin in an RGD- and calcium-dependent manner. PLoS One. 6(12):e29629. doi:10.1371/journal.pone.0029629

Koo J, Tammam S, Ku S-Y, Sampaleanu LM, Burrows LL, Howell PL. 2008. PilF is an outer membrane lipoprotein required for multimerization and localization of the *Pseudomonas aeruginosa* Type IV pilus secretin. J Bacteriol. 190:6961–6969. doi:10.1128/JB.00996-08

Koo J, Tang T, Harvey H, Tammam S, Sampaleanu L, Burrows LL, Howell PL. 2013. Functional mapping of PilF and PilQ in the *Pseudomonas aeruginosa* type IV pilus system. Biochemistry. 17:2914–2923. doi:10.1021/bi3015345

Kuchma SL, Ballok AE, Merritt JH, Hammond JH, Lu W, Rabinowitz JD, O'Toole GA. 2010. Cyclic-di-GMP-mediated repression of swarming motility by *Pseudomonas aeruginosa*: the *pilY1* gene and its impact on surface-associated behaviors. J Bacteriol. 192(12):2950–2964. doi:10.1128/JB.01642-09

Leang C, Qian X, Mester T, Lovley DR. 2010. Alignment of the c-type cytochrome OmcS along pili of *Geobacter sulfurreducens*. Appl Environ Microbiol. 76(12):4080–4084. doi:10.1128/AEM.00023-10

Li Y-Q, Wan D-S, Huang S-S, Leng F-F, Yan L, Ni Y-Q, Li H-Y. 2010. Type IV pili of *Acidithiobacillus ferrooxidans* are necessary for sliding, twitching motility, and adherence. Curr Microbiol. 60:17–24. doi:10.1007/s00284-009-9494-8

Li Y, Huang S, Zhang X, Huang T, Li H. 2013. Cloning, expression, and functional analysis of molecular motor *pilT* and *pilU* genes of type IV pili in *Acidithiobacillus ferrooxidans*. Appl Microbiol Biotechnol. 97:1251–1257. doi:10.1007/s00253-012-4271-1

Li Y, Li H. 2014. Type IV pili of *Acidithiobacillus ferrooxidans* can transfer electrons from extracellular electron donors. J Basic Microbiol. 54:226–231. doi:10.1002/jobm.201200300

Ligthart K, Belzer C, de Vos WM, Tytgat HLP. 2020. Bridging bacteria and the gut: Functional aspects of type IV Pili. Trends Microbiol. 28:340–348. doi:10.1016/j.tim.2020.02.003

Liu X, Holmes DE, Walker DJF, Li Y, Meier D, Pinches S, Woodard TL, Smith JA. 2022. Cytochrome OmcS is not essential for extracellular electron transport via conductive Pili in *Geobacter sulfurreducens* strain KN400. Appl Environ Microbiol. 88(1):e0162221

Lu S, Giuliani M, Harvey H, Burrows LL, Wickham RA, Dutcher JR. 2015. Nanoscale pulling of type IV Pili reveals their flexibility and adhesion to surfaces over extended lengths of the Pili. Biophys J. 108:2865–2875. doi:10.1016/j.bpj.2015.05.016

Macdonald DL, Pasloske BL, Paranchych W. 1993. Mutations in the fifth-position glutamate in *Pseudomonas aeruginosa* pilin affect the transmethylation of the N-terminal phenylalanine. Can J Microbiol. 39:500–505. doi:10.1139/m93-071

Mahoney RP, Edwards MR. 1966. Fine structure of *Thiobacillus thiooxidans*. J Bacteriol. 92:487–495. doi:10.1128/jb.92.2.487-495.1966

Maier B, Wong GCL. 2015. How bacteria use type IV Pili machinery on surfaces. Trends Microbiol. 23:775–788. doi:10.1016/j.tim.2015.09.002

Malvankar NS, Vargas M, Nevin KP, Franks AE, Leang C, Kim B-C, Inoue K, Mester T, Covalla SF, Johnson JP, et al., 2011. Tunable metallic-like conductivity in microbial nanowire networks. Nat Nanotechnol. 6(9):573–579. doi:10.1038/nnano.2011.119

Matzke J, Schwermann B, Bakker EP. 1997. Acidostable and acidophilic proteins: The example of the α-amylase from *Alicyclobacillus acidocaldarius*. Comp Biochem Physiol A Comp Physiol. 118(3):475–479. doi:10.1016/s0300-9629(97)00008-x

Melville S, Craig L. 2013. Type IV pili in Gram-positive bacteria. Microbiol Mol Biol Rev. 77:323–341. doi:10.1128/MMBR.00063-12

Nguyen Y, Sugiman-Marangos S, Harvey H, Bell SD, Charlton CL, Junop MS, Burrows LL. 2015. *Pseudomonas aeruginosa* minor pilins prime type IVa pilus assembly and promote surface display of the PilY1 adhesin. J Biol Chem. 290:601–611. doi:10.1074/jbc.M114.616904

Oki H, Kawahara K, Iimori M, Imoto Y, Nishiumi H, Maruno T, Uchiyama S, Muroga Y, Yoshida A, Yoshida T, et al., 2022. Structural basis for the toxin-coregulated pilus-dependent secretion of *Vibrio cholerae* colonization factor. Sci Adv. 8:eabo3013. doi:10.1126/sciadv.abo3013

Orans J, Johnson MDL, Coggan KA, Sperlazza JR, Heiniger RW, Wolfgang MC, Redinbo MR. 2010. Crystal structure analysis reveals *Pseudomonas* PilY1 as an essential calcium-dependent regulator of bacterial surface motility. Proc Natl Acad Sci U S A. 107(3):1065–1070. doi:10.1073/pnas.0911616107

Ossa Henao DM, Vicentini R, Rodrigues VD, Bevilaqua D, Ottoboni LMM. 2014. Differential gene expression in *Acidithiobacillus ferrooxidans* LR planktonic and attached cells in the presence of chalcopyrite. J Basic Microbiol. 54:650–657. doi:10.1002/jobm.201300871

Parker JK, Cruz LF, Evans MR, de la Fuente L. 2015. Presence of calcium-binding motifs in PilY1 homologs correlates with Ca-mediated twitching motility and evolutionary history across diverse bacteria. FEMS Microbiol Lett. 362(4):1–9. doi:10.1093/femsle/fnu063

Pelicic V. 2019. Monoderm bacteria: the new frontier for type IV pilus biology. Mol Microbiol. 112:1674–1683. doi:10.1111/mmi.14397

Pelicic V. 2023. Mechanism of assembly of type 4 filaments: everything you always wanted to know (but were afraid to ask). Microbiology. 169. doi:10.1099/mic.0.001311

Quatrini R, Escudero LV, Moya-Beltrán A, Galleguillos PA, Issotta F, Acosta M, Cárdenas JP, Nuñez H, Salinas K, Holmes DS, et al., 2017. Draft genome sequence of *Acidithiobacillus thiooxidans* CLST isolated from the acidic hypersaline Gorbea salt flat in northern Chile. Stand Genomic Sci. 12. doi:10.1186/s40793-017-0305-8

Reguera G, McCarthy KD, Mehta T, Nicoll JS, Tuominen MT, Lovley DR. 2005. Extracellular electron transfer via microbial nanowires. Nature. 435(7045):1098–1101. doi:10.1038/nature03661

Ronish LA, Sidner B, Yu Y, Piepenbrink KH. 2022. Recognition of extracellular DNA by type IV pili promotes biofilm formation by *Clostridioides difficile*. J Biol Chem. 298:102449. doi:10.1016/j.jbc.2022.102449

Rudel T, Scheurerpflug I, Meyer TF. 1995. *Neisseria* PilC protein identified as type-4 pilus tip-located adhesin. Nature. 373:357–359. doi:10.1038/373357a0

Rudel T, Facius D, Barten R, Scheuerpflug I, Nonnenmacher E, Meyer TF. 1995. Role of pili and the phase-variable PilC protein in natural competence for transformation of *Neisseria gonorrhoeae*. Proc Natl Acad Sci U S A. 92:7986–7990. doi:10.1073/pnas.92.17.7986

Shanmugasundarasamy T, Karaiyagowder Govindarajan D, Kandaswamy K. 2022. A review on pilus assembly mechanisms in Gram-positive and Gram-negative bacteria. Cell Surf. 8:100077. doi:10.1016/j.tcsw.2022.100077

Shu C, Xiao K, Sun X. 2020. Structural basis for the high conductivity of microbial Pili as potential nanowires. J Nanosci Nanotechnol. 20(1):64–80. doi:10.1166/jnn.2020.16883

Direct extracellular electron transfer of the Geobacter sulfurreducens Pili relevant to interaromatic distances. Biomed Res Int. 2019:6151587. doi:10.1155/2019/6151587

Siryaporn A, Kuchma SL, O'Toole GA, Gitai Z. 2014. Surface attachment induces *Pseudomonas aeruginosa* virulence. Proc Natl Acad Sci U S A. 111:16860–16865. doi:10.1073/pnas.1415712111

Sun Y-L, Montz BJ, Selhorst R, Tang H-Y, Zhu J, Nevin KP, Woodard TL, Ribbe AE, Russell TP, Nonnenmann SS, et al., 2021. Solvent-induced assembly of microbial protein nanowires into superstructured bundles. Biomacromolecules. 22(3):1305–1311. doi:10.1021/acs.biomac.0c01790

Sure S, Ackland ML, Torriero AAJ, Adholeya A, Kochar M. 2016. Microbial nanowires: an electrifying tale. Microbiology. 162(12):2017–2028. doi:10.1099/mic.0.000382

Szmuc E, Walker DJF, Kireev D, Akinwande D, Lovley DR, Keitz B, Ellington A. 2023. Engineering Geobacter pili to produce metal: organic filaments. Biosens Bioelectron. 222(114993):114993. doi:10.1016/j.bios.2022.114993

Tang D, Gao Q, Zhao Y, Li Y, Chen P, Zhou J, Xu R, Wu Z, Xu Y, Li H. 2018. Mg2+ reduces biofilm quantity in *Acidithiobacillus ferrooxidans* through inhibiting Type IV pili formation. FEMS Microbiol Lett. 365. doi:10.1093/femsle/fnx266

Thomas W-H, Weser U, Hempel K. 1977. Conformational changes induced by ionic strength and pH in two bovine myelin basic proteins. Hoppe Seylers Z Physiol Chem. 358(2):1345–1352. doi:10.1515/bchm2.1977.358.2.1345

Ueki T, Walker DJF, Tremblay P-L, Nevin KP, Ward JE, Woodard TL, Nonnenmann SS, Lovley DR. 2019. Decorating Microbially Produced Protein Nanowires with Peptide Ligands. bioRxiv. doi:10.1101/590224

Valdés JH, Pedroso I, Quatrini R, Hallberg KB, Valenzuela PDT, Holmes DS. 2007. Insights into the metabolism and ecophysiology of three *acidithiobacilli* by comparative genome analysis. Adv Mat Res. 20–21:439–442. doi:10.4028/www.scientific.net/amr.20-21.439

Valdés J, Ossandon F, Quatrini R, Dopson M, Holmes DS. 2011. Draft genome sequence of the extremely acidophilic biomining bacterium *Acidithiobacillus thiooxidans* ATCC 19377 provides insights into the evolution of the *Acidithiobacillus* genus. J Bacteriol. 193:7003–7004. doi:10.1128/JB.06281-11

Vargas M, Malvankar NS, Tremblay P-L, Leang C, Smith JA, Patel P, Snoeyenbos-West O, Nevin KP, Lovley DR. 2013. Aromatic amino acids required for Pili conductivity and long-range extracellular electron transport in *Geobacter sulfurreducens*. MBio. 4(2):e00210-13. doi:10.1128/mbio.00210-13

Waksman SA, Joffe JS. 1921. Acid production by a new sulfur-oxidizing bacterium. Science. 53:216–216. doi:10.1126/science.53.1366.216

Waksman SA, Joffe JS. 1922. Microorganisms concerned in the oxidation of sulfur in the soil ii. *Thiobacillus thiooxidans*, a new sulfur-oxidizing organism isolated from the soil1. J Bacteriol. 7:239–256. doi:10.1128/jb.7.2.239-256.1922

Walker DJ, Adhikari RY, Holmes DE, Ward JE, Woodard TL, Nevin KP, Lovley DR. 2018. Electrically conductive pili from pilin genes of phylogenetically diverse microorganisms. ISME J. 12(1):48–58. doi:10.1038/ismej.2017.141

Wang F, Baquero DP, Su Z, Beltran LC, Prangishvili D, Krupovic M, Egelman EH. 2020. The structures of two archaeal type IV pili illuminate evolutionary relationshiP. Nat Commun. 11:3424. doi:10.1038/s41467-020-17268-4

Webster SS, Lee CK, Schmidt WC, Wong GCL, O'Toole GA. 2021. Interaction between the type 4 pili machinery and a diguanylate cyclase fine-tune c-di-GMP levels during early biofilm formation. Proc Natl Acad Sci U S A. 118:e2105566118. doi:10.1073/pnas.2105566118

Webster SS, Mathelié-Guinlet M, Verissimo AF, Schultz D, Viljoen A, Lee CK, Schmidt WC, Wong GCL, Dufrêne YF, O'Toole GA. 2021. Force-induced changes of PilY1 drive surface sensing by *Pseudomonas aeruginosa*. MBio. 13(1):e0375421. doi:10.1128/mbio.03754-21

Xue S, Mercier R, Guiseppi A, Kosta A, De Cegli R, Gagnot S, Mignot T, Mauriello EMF. 2022. The differential expression of PilY1 proteins by the HsfBA phosphorelay allows twitching motility in the absence of exopolysaccharides. PLoS Genet. 18(4):e1010188. doi:10.1371/journal.pgen.1010188

Yang L, Zhao D, Yang J, Wang W, Chen P, Zhang S, Yan L. 2019. *Acidithiobacillus thiooxidans* and its potential application. Appl Microbiol Biotechnol. 103:7819–7833. doi:10.1007/s00253-019-10098-5

Yin Z, Feng S, Tong Y, Yang H. 2019. Adaptive mechanism of *Acidithiobacillus thiooxidans* CCTCC M 2012104 under stress during bioleaching of low-grade chalcopyrite based on physiological and comparative transcriptomic analysis. J Ind Microbiol Biotechnol. 46(12):1643–1656. doi:10.1007/s10295-019-02224-z

Significance

The *At. thiooxidans* T4aP offers the opportunity to understand the intricate equilibrium between functionality and resilience, which motivate us to found approaches to explore the biochemical and biophysical process as adaptive "skills" of a protein structure exposed to an extreme environment. Also, to contribute insights to know how this complex nanomachine works facing at low pH while transfer electrons.

The present work pretends to characterize the strategies against extreme pH changes in structural pili proteins, to elucidated if FimT, PilV, PilW, and PilX are minor or major pilins, to measure currents that could be pass through a pilin and finally, to inspect on PilY1 functions and its role in the T4aP of *At. thiooxidans*.

Objective

Structural and biophysical insights of the minor pilins and adhesin PilY1 of *At. thiooxidans* ATCC19377.

Specific objectives

- To employ bioinformatics approaches to search the *loci* of minor pilins and PilY1 genes of *At. thiooxidans*
- To utilize bioinformatics approaches to predict the secondary and tertiary structures of minor pilins and PilY1 of *At. thiooxidans*
- To apply bioinformatics methods to identify disorder, isoelectric point, amino acid composition, and pH effects in minor pilins and PilY1 of *At. thiooxidans*
- The heterologous expression and purification of minor PilV of *At. thiooxidans*
- To analyze the fluorescence spectrum to assess the tertiary structure before and after the exposure of PilV of *At. thiooxidans* to different pH
- To construct a device to determine the electric current through proteins in solution
- To evaluate the conductance of the minor pilin PilV of *At. thiooxidans*
- To perform *in silico* analyses of the adhesin PilY1 of *At. thiooxidans*, its differences and similarities with other bacteria

CHAPTER II

Extremophiles (2023) 27:31
https://doi.org/10.1007/s00792-023-01317-z

ORIGINAL PAPER

Disorder and amino acid composition in proteins: their potential role in the adaptation of extracellular pilins to the acidic media, where *Acidithiobacillus thiooxidans* grows

Edgar D. Páez-Pérez[1] · Araceli Hernández-Sánchez[1] · Elvia Alfaro-Saldaña[1] · J. Viridiana García-Meza[1]

Received: 8 March 2023 / Accepted: 26 September 2023

Abstract
There are few biophysical studies or structural characterizations of the type IV pilin system of extremophile bacteria, such as the acidophilic *Acidithiobacillus thiooxidans*. We set out to analyze their pili-comprising proteins, pilins, because these extracellular proteins are in constant interaction with protons of the acidic medium in which *At. thiooxidans* grows. We used the web server Operon Mapper to analyze and identify the cluster codified by the minor pilin of *At. thiooxidans*. In addition, we carried an in-silico characterization of such pilins using the VL-XT algorithm of PONDR® server. Our results showed that structural disorder prevails more in pilins of *At. thiooxidans* than in non-acidophilic bacteria. Further computational characterization showed that the pilins of *At. thiooxidans* are significantly enriched in hydroxy (serine and threonine) and amide (glutamine and asparagine) residues, and significantly reduced in charged residues (aspartic acid, glutamic acid, arginine and lysine). Similar results were obtained when comparing pilins from other *Acidithiobacillus* and other acidophilic bacteria from another genus versus neutrophilic bacteria, suggesting that these properties are intrinsic to pilins from acidic environments, most likely by maintaining solubility and stability in harsh conditions. These results give guidelines for the application of extracellular proteins of acidophiles in protein engineering.

Keywords Acidophiles · Protein disorder · Pilins · Biophysics · Isoelectric point · Protein stability

Disorder and amino acid composition in proteins: their potential role in the adaptation of extracellular pilins to the acidic media, where *Acidithiobacillus thiooxidans* grows

Abstract

There are few biophysical studies or structural characterizations of the type IV pilin system of extremophile bacteria such as the acidophilic *Acidithiobacillus thiooxidans*. We set out to analyze their pili-comprising proteins, pilins, because these extracellular proteins are in constant interaction with protons of the acidic medium in which *At. thiooxidans* grows. We used the web server Operon Mapper to analyze and identify the cluster codified by the minor pilin of *At. thiooxidans*. In addition, we carried an *in-silico* characterization of such pilins

using the VL-XT algorithm of PONDR® server. Our results showed that structural disorder prevails more in pilins of *At. thiooxidans* than in non-acidophilic bacteria. Further computational characterization showed that the pilins of *At. thiooxidans* are significantly enriched in hydroxy (serine and threonine) and amide (glutamine and asparagine) residues, and significantly reduced in charged residues (aspartic acid, glutamic acid, arginine and lysine). Similar results were obtained when comparing pilins from other *Acidithiobacillus* and other acidophilic bacteria from another genus *versus* neutrophilic bacteria, suggesting that these properties are intrinsic to pilins from acidic environments, most likely by maintaining solubility and stability in harsh conditions. These results give guidelines for the application of extracellular proteins of acidophilics in protein engineering.

Introduction

Bacteria and Archaea have filament-form appendages that serve important functions, such as adhesion, motility, and formation of microcolonies and colonization factors (Craig and Li 2008; Craig et al., 2019). The type IV filament superfamily (T4F) in particular has diversified into systems involved in surface sensing, adhesion to biotic or abiotic surfaces, protein secretion, DNA uptake during natural transformation, and twitching motility (Sauvonnet et al., 2000; Berry and Pelicic 2015; Denise et al., 2019). Their phylogeny suggests that "they may have been present in the last universal common ancestor" (Denise et al., 2019), as shown by the fact that bacteria and archaea possess T4F systems, such as type II secretion (T2SS), the pili type IVa (T4aP), type IVb (T4bP), type IVc or tight adherence (Tad) pili, mannosesensitive hemagglutinin (MSH), the archaeal–T4P and the competence pseudopili (Denise et al., 2019). These systems include core homologous components of similar architecture, including ATPases, an inner membrane platform, and a prepilin peptidase that matures the pilins (in pilus) or pseudopilins (in T2SS).

The pilus fiber of T4aP is composed of thousands of copies of the major pilin (PilA) and a smaller number of the so-called "minor pilins:" FimU or FimT, PilV, PilW, PilX and the adhesin PilY1 (in *Pseudomonas* spp. *Myxococcus* spp. and *Acidithiobacillus* spp. among other bacteria). Major and minor pilins are all evolutionarily related and show a similar tertiary structure; all share the same modular design, comprising of a lollipop-like shape with an N-terminus α-helix followed by a globular domain, but different molecular weights

(Pelicic 2008; Giltner et al., 2012; Denise et al., 2019). The α1-helix separates in turn into two segments, a transmembrane hydrophobic N-terminus region (α1-N), and a C-terminus part (α1-C), which extends towards the globular domain; this globular domain consists of the α1-C surrounded by one or two antiparallel β-sheets composed of four to seven strands (Jacobsen et al., 2020).

PilY1 and minor pilins are dependent on each other for incorporation into pili; their key role as a priming complex that is subsequently incorporated into the pilus was showed by Nguyen et al., (2015) in *Pseudomonas aeruginosa* and by Treuner-Lange et al., (2020), who proved that the lack of *fimTpilVWXY1* operon genes blocks pilus formation, extension and T4P-dependent motility in *Myxococcus xanthus*. In addition, the authors demonstrated that PilY1 and minor pilins provide a template for assembly of mature PilA and that this interaction results in a complex containing all five pilins for the pilus, concluding that FimT or FimU–PilVWXY1 functions as a priming complex for pilus extension and a tip complex in the extended pilus for adhesion. Thus, T4aP are sensing "sticky" filaments, including DNA binding.

Currently, there are few biophysical studies or structural characterizations of the T4aP system of bacteria of biotechnological interest, such as extremophile bacteria in the mining industry, one of which is *Acidithiobacillus thiooxidans* (optimal pH 1.6 to 2.5) (Hu et al., 2020). *At. thiooxidans* is a Gram-negative *Pseudomonadota* (synonym Proteobacteria; former, γ-Proteobacteria) of the class Acidithiobacillia, a class that includes chemolithoautotrophs capable of using Fe (II) and/or reduced sulfur compounds as an electron source (Williams and Kelly 2013). Like other Acidithiobacillaceae, *At. thiooxidans* grows in hostile environments, since it is able to oxidize sulfur compounds from mineral deposits to sulfuric acid. As a result, certain metals are dissolved, given that the pH is as low as 1.0 (Shukla et al., 2021). Their extremophilicity is due not only to the fact that they inhabit acidic environments with dissolved heavy metals among other ions, but also that the environments have high oxidation–reduction potential (oxidizing environments) and are subject to osmotic stress or K+ limitation (Travisany et al., 2014). In recent years, sequences of some pilins of this organism have been analyzed and confirmed, and it has also been suggested that the T4aP of *At. thiooxidans* may play an important role in bacterial adhesion to mineral surfaces,

causing an increased rate of dissolution of (poly)metallic sulfide minerals (Alfaro-Saldaña et al., 2019).

We are interested in the extracellular pilins of the acidophilic *At. thiooxidans*, since modifications in protein structures of organisms that have evolved under extreme environmental conditions differ in how they maintain optimal activity (Panja et al., 2020). For example, the molecular basis and physicochemical adaptive mechanisms of organisms that survive at very high temperatures have been extensively studied, showing that their proteins have a highly hydrophobic nucleus and a greater frequency of polar amino acids on their surfaces (England et al., 2003; Ma et al., 2010; Panja et al., 2020), while the majority of acidophilic microorganisms survive at low pH by modifying their proteins along their genome (Panja et al., 2020). However, little is known about the mechanisms that sustain the stability and function of these proteins, particularly the extracellular proteins exposed to these pHs, e.g., their intrinsic disorder. Intrinsically disorder proteins (IDPs) and IDP regions are those that lack a stable tertiary structure but carry out a wide range of biological functions (Bondos et al., 2021). It is known that this intrinsic disorder facilitates and regulates protein interactions (Galea et al., 2008; Tompa and Fersht 2009). In addition, greater intrinsic disorder has been described as being correlated with the proteins of aerobic bacteria adapted to live in many different environmental niches and with a variety of sources of nutrients, suggesting that disorder is an adaptation for survival in complex environments. This analysis also shows a greater content of intrinsic disorder in proteins found on the cell surface than those involved in metabolism (Pavlovic-Lazetic et al., 2011).

We compared differences in structural disorder and amino acid composition and conducted a set of studies *in silico* of the minor pilins FimT, PilV, PilW, PilX, PilY1 and the major pilin PilA in neutrophilic organisms with ortholog pilins from *At. thiooxidans*, enabling us to elucidate how functional stability of proteins exposed to a protonated environment, in extreme conditions, is maintained.

It is known that genes of minor pilins associated with T4aP are arranged as clusters in an operon in the same transcriptional direction; the existence of such a cluster reflects their crucial roles at the tip of the pili mediating specific functions, such as stabilizing the T4aP, participating in DNA binding, and cell aggregation (Sauvonnet et al., 2000; Yoshimura et al., 2009; Jacobsen et al., 2020). These clusters show some differences between upstream and

downstream genes but the arrangement, where *fimT/U–pilV–pilW–pilX–pilY1* genes are together and located in the same direction. Since no clusters or operons of minor pilins have been described in *At. thiooxidans*, we decided to search for them prior to characterizing the individual pilins.

Materials and methods

Analysis and identification of the cluster codified by the minor pilin of *At. thiooxidans*

Sequences of major and minor pilins of *At. thiooxidans* ATCC-19377 (NCBI ID: 930) were obtained from the GenBank BioProject PRJNA534527 (Locus SZUV01000001.1) described by Camacho et al., (2020). To identify the minor and major pilins, a cluster analysis was done using the Operon Mapper (https://biocomputo. ibt.unam.mx) (Taboada et al., 2018), which also provides information about clusters of orthologous genes (COG) and Kegg orthology (www.genome.jp/kegg). For comparison purposes, we also identified the operon of *P. aeruginosa* PAO1 (NCBI ID: 208964; BioProject: PRJNA57945; Locus NC002516.2) using the same bioinformatics resource; this operon was already described in the PAO1 strain (Belete et al., 2008). The major and minor pilins of other acidophilic and neutrophilic bacteria (Table S1) were obtained following a protein Basic Local Alignment Search Tool (BLAST) analysis (https://blast.ncbi.nlm.nih.gov/Blast.cgi).

The analyses of PilV, PilW, PilX and PilY1 of *At. thiooxidans* were done using their sequences previously confirmed by Alfaro-Saldaña et al., (2019), while for FimT we used the annotated sequence from Camacho et al., (2020). The accession numbers are summarized in ST1.

Computational characterization of the pilins

Structural disorder was predicted using the VL-XT algorithm on the PONDR® server (http://www.pondr.com/) (Xue et al., 2010). Composition Profiler (Vacic et al., 2007) (http://www.cprofiler.org/) was used to analyze the amino acid distribution. The server enabled the analysis of the enrichment or reduction of amino acids in relation to proteins found in nature to be carried out. This calculation was done using the amino acid composition of the proteins in the SWISS-PROT 51 data base (Bairoch et al., 2005) as a reference. The distribution obtained was combined with the distribution of the intrinsically disordered amino acids in the DisProt 3.4 data base (Sickmeier et al., 2007) and they were graphed together.

Molecular weight and isoelectric point were calculated with the Expasy Compute pI/MW tool (https://web.expasy.org/ compute_pi/). The charge distribution of pilins was calculated with the κ parameter using CIDER (Holehouse et al., 2017; https://pappulab.wustl.edu/CIDERinfo.html).

The structural analysis was carried out by submitting the pilin sequences into ColabFold (Mirdita et al., 2022). ColabFold is a fast, easy to use program that speeds up the prediction of protein structures by combining a rapid search of the MMseq2 homology with Alphafold2 (Jumper et al., 2021). The Protein-sol program (Hebditch and Warwicker 2019) (https://protein-sol.manchester.ac.uk/) was used to evaluate the stability of the pilins in an acid environment. In this program, the stability of the folded state and the charge on the proteins is calculated as a function of pH. The program uses the Debye-Hückel formula to calculate the pKas and, therefore, also the pH-dependent contribution to the stability of the folded state. All sequences used in this study were obtained from GenBank (ST1), after identifying the clusters/operons associated with the minor pilins. Notably, the sequences of PilV, PilW, PilX and PilY1 of *At. thiooxidans* ATCC-19377 are confirmed; that is, they are not annotated (Alfaro-Saldaña et al., 2019; this work).

Results and discussion

Minor pilin proteins encoded by gene cluster in *At. thiooxidans*

We identified two gene clusters in *At. thiooxidans* ATCC- 19377 that encode minor pilins (FimT, PilV, PilW, PilX) and the adhesin PilY1, as our further analysis reveals. We selected one of these clusters after performing COG, remaining orthologous groups (or ROG, since each ROG has at least three orthologous and conserved genes during evolution and are not shared by chance) (Taboada et al., 2010), Kegg orthology, and BLAST analyses of the reported genes in each cluster, e.g., the presence of conserved domain such as the von Willebrand factor A (vWFA) domain, the calcium-binding motif in PilY1, and other conserved regions found by multiple sequence alignments of pilins such the hydrophobic N-terminal region (Orans et al., 2010; Berry and Pelicic 2015; Alfaro-Saldaña et al., 2019; Treuner-Lange et al., 2020). *At. thiooxidans* and *P. aeruginosa* are Gram negative Proteobacteria of the classes Acidithiobacillia and γ-Proteobacteria, respectively. Williams and Kelly (2013) demonstrated that "Acidithiobacillia form a monophyletic clade that is sister to γ-Proteobacteria," after a multiprotein phylogenetic analysis. Our results showed

that the *fimUpilVWXY1* operon of *P. aeruginosa* that encodes for its core minor pilins is like *fimT-pilVWXY1* of *At. thiooxidans* (Fig. 3), as well as being like that of other species of the genus *Acidithiobacillus* and conserves the core structure, where four pilin genes and *pilY1* are consecutive.

Our results show that the minor pilin genes *fimT*, *pilV*, *pilW*, *pilX* and *pilY1* are clustered in a polycistronic manner similar to the operon for the minor pilins *fimU-pilVWXY1Y2E* of *P. aeruginosa* and the third cluster of *M. xanthus* (Treuner-Lange et al., 2020); however, downstream of the *pilY1*, the genes for *pilY2* and *pilE* of *P. aeruginosa* do not appear in *At. thiooxidans*. Differences between genes upstream or downstream of the minor pilins reflect differences between species and the different environments in which they are found. According to Pelicic (2008), the minor pilin gene cluster is conserved in species of various genera that possess T4aP, whether phylogenetically close or distant, and the homologous genes are often found at the same genomic location in more than 150 sequenced species of various phyla, mainly in β-, γ- and δ-proteobacteria, such as *Neisseria*, *Pseudomonas* and *Myxococcus*, respectively.

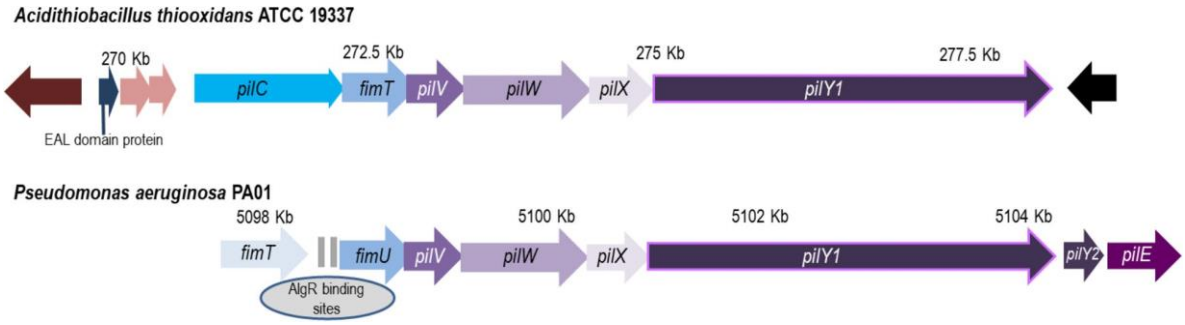

Figure 3. Putative organization of the *At. thiooxidans* minor pilin gene cluster. *At. thiooxidans* minor pilin gene cluster compared with the *P. aeruginosa* operon. Although there are marked differences in the upstream and downstream genes, it is notable that the four minor pilins of *At. thiooxidans* are in the same conformation with respect to the adhesin *pilY1* (darkest purple), while fimT (cyan) from *At. thiooxidans* seems to be the fimU homolog of *P. aeruginosa*. The *At. thiooxidans* cluster also contains the pilC (blue) upstream of fimT. The pilV (medium dark purple), pilW (medium purple) and pilX (light purple) genes have the same location and direction as their *P. aeruginosa* counterparts.

Special structural features of major and minor pilins from *At. thiooxidans*

The structural plasticity of the proteins results in molecular stability against stress induced by the pressure of natural selection (Panja et al., 2020). Several recent studies show that structural disorder is common in various proteomes, and that the content of this disorder is

usually an indicator both of their evolution and their adaptation to their environment (Uversky 2017). On the other hand, the role of structural disorder in adaptation to the environment can be illustrated by the fact that both extremophile Archaea and Bacteria contain more structural disorder than their neutrophilic counterparts (Uversky 2017). Taking this into account, we decided to undertake an analysis of intrinsic order of the major and minor pilins and of PilY1 from *At. thiooxidans*, and of their counterparts in *Pseudomonas aeruginosa* PAO1, although for *At. thiooxidans* it should be considered that only the expression of PilY1, PilW, PilV and PilX has been studied (unpublished data).

The predictions of structural disorder for each amino acid sequence were made using the VL-XT algorithm of the PONDR® predictor (Xue et al., 2010). The first minor pilin analyzed was FimT from *At. thiooxidans* compared to FimU from *P. aeruginosa*. The presence of disordered regions was predicted for both proteins, but for FimT, the disorder is found in the middle part of the protein (residues 89 to 115), while for FimU the disorder is predicted both for the N-terminus and for the C-terminus. The latter is a smaller portion of the sequence (Fig. 4a).

To better understand the nature of these disordered regions, we decided to calculate the composition of the amino acids (enrichment or reduction) using Composition Profiler (Vacic et al., 2007). In FimU, the most extensive disordered region is enriched in alanine and glutamine (A and Q), while the smallest region is enriched in glutamine and serine (Q and S). The FimT disordered region is enriched in Q and threonine (T) (data not shown). Only the amino acids A, Q, and S are considered to promote disorder, while the amino acid T is not considered to promote either order or disorder (Dunker et al., 2001). Knowing the predicted disordered regions did not clarify the significant differences between the two proteins, so we decided to analyze the amino acid composition of the complete proteins. This analysis showed that FimU is only enriched in A (Fig. 4b), while FimT, in addition to being enriched in A, is also enriched in Q, T, and tryptophan (W). Interestingly, there is a general reduction in amino acids with positive and negative charge, with a significant reduction in aspartic acid, lysine and histidine (D, K and H) (Fig. 4b).

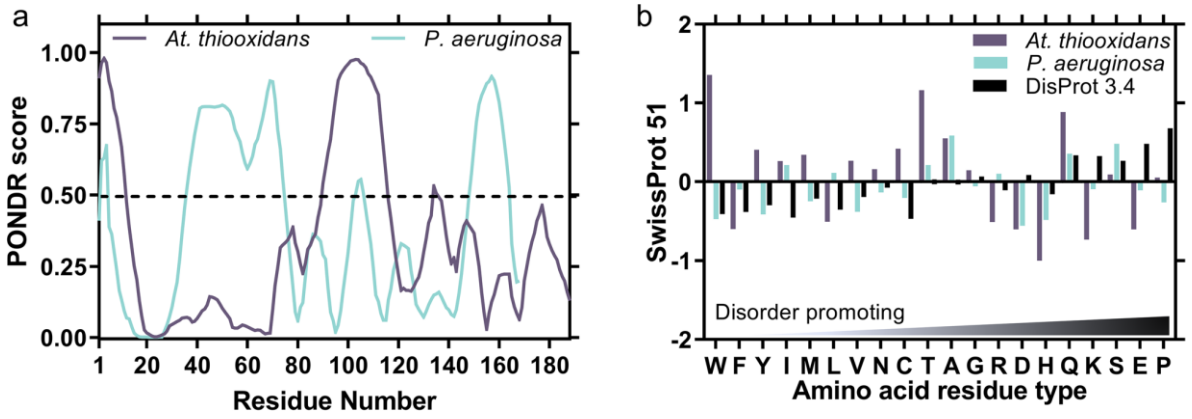

Figure 4. Prediction of intrinsic disorder and amino acid composition ogf FimT of *At. thiooxidans* and FimU of *P. aeruginosa.* **a** Intrinsic disorder profile of FimT (purple) and FimU (light blue) generated by the PONDR®predictor using the VL-XT algorithm. Values above 0.5 indicate a high probability of disorder. **b** Amino acid distribution of FimT (purple) and FimU (light blue) relative to the SWISS-PROT database; data are shown combined with the distribution of amino acids found in intrinsically disordered proteins (black). Enrichment (>0) or reduction (<0) in composition is also shown; amino acids are arranged in increasing order of disorder-promoting ability (light–dark gradient).

It is known that FimU is not essential for the formation or incorporation of the PilVWXY1E complex in the pili of *P. aeruginosa*, but rather that it has a role as a stabilizing subunit, since it can interact with the major pilin PilA and the minor pilin PilV and with PilE (Nguyen et al., 2015). In the case of the PilVWX and PilY1 proteins, however, each one depends on the other for incorporation into the pili, since it is suggested that these minor pilins could form a complex with PilY1, since no pilins are present if PilY1 is absent (Nguyen et al., 2015).

The analyses of disorder in the minor pilins PilV, PilW and PilX show a similar trend to FimT and FimU except that now the pilins of *At. thiooxidans* have more regions that tend towards disorder than the pilins of *P. aeruginosa* (Fig. 5).

The PilV of both bacteria seem to conserve the tendency to be disordered at their respective N-terminus; however, the *At. thiooxidans* protein has a long segment in the middle of its sequence of about 56 residues that is more likely to be disordered, probably because it is proline-enriched (P) according to the Composition Profiler analysis (Fig. 5a). This segment is characterized by PONDR® as a region that may transition from disorder to order in the event of some change, such as binding to a partner (Xue et al., 2010). We then decided to analyze the amino acid composition of the complete proteins, finding that the PilV from *At. thiooxidans* is significantly enriched with the amino acids T and glycine (G), and substantially enriched with the amino acids S, Q and asparagine (N) (Fig. 5b). Interestingly, we observed the same pattern of reduction in charged amino acids as in FimT, except that

the reduction is significant for arginine (R), K, D, and glutamic acid (E). PilV from *P. aeruginosa* is only significantly enriched in S and substantially enriched in cysteine (C) and methionine (M), and charged amino acids are reduced in H and E (Fig. 5b).

The next pilin evaluated was PilW from *At. thiooxidans*. We found that it has six regions that tend to be disordered, and it is the latter that has the greatest number of amino acids (58 residues). In contrast, PilW from *P. aeruginosa* has only three regions with a slight tendency to disorder (Fig. 5c). The amino acid composition analysis showed that PilW from *At. thiooxidans* is significantly enriched in the amino acids N, Q, S, and T, and again significantly reduced in K, E, and D, and substantially reduced in R. PilW from *P. aeruginosa* is only significantly enriched in Q and reduced in H (Fig. 5d).

In general, the tendency in amino acid composition was also maintained in PilX from *At. thiooxidans*. The analysis indicated that it is significantly enriched in T and, interestingly, in the non-polar amino acid valine (V), substantially increased in Q and N, and significantly reduced in K and D and substantially in R and E (Fig. 5f). A similar result was found for PilX from *P. aeruginosa*, which is also enriched in T but differs in also being enriched in N. Charged amino acids show a significant reduction in K and D and a substantial reduction in H (Fig. 5f). Interestingly, the disorder analysis did not show any region that might be a potential transition from disorder to order for either of the two proteins (Fig. 5e).

It was mentioned above that PilVWX and PilY1 depend on each other for incorporation into the pili. Unlike the minor pilins, PilY1 is a soluble protein with a type I peptide signal followed by a poorly conserved N-terminus region and a well-conserved C-terminus PilY1 domain with a modified beta propeller-type structure (Orans et al., 2010). It is known that PilY1 is important in *Pseudomonas* spp. for the formation of T4aP, since it is suggested that it stimulates the formation of this system in addition to promoting adhesion to host cells during infection (Treuner-Lange et al., 2020).

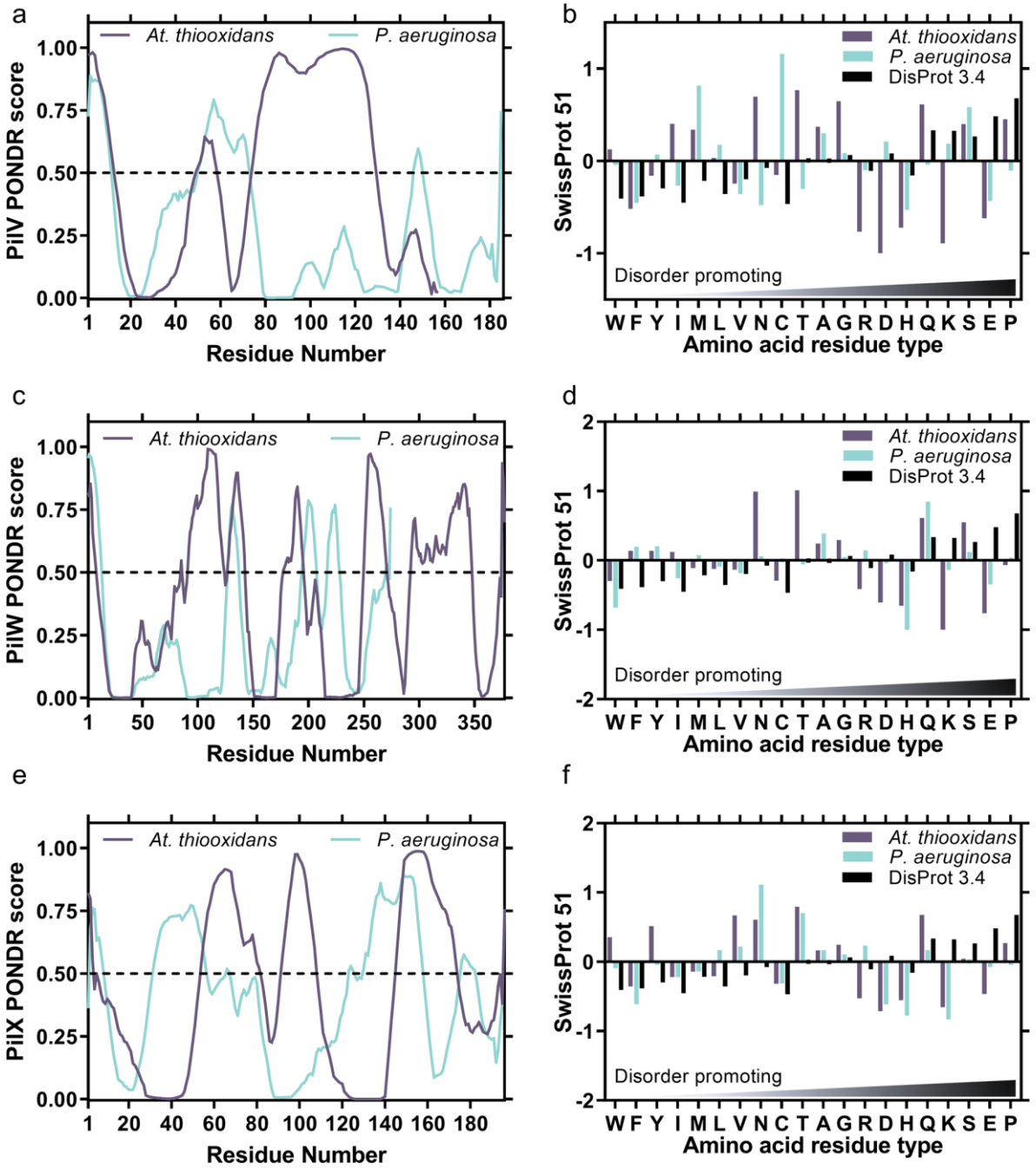

Figure 5. Prediction of intrinsic disorder and amino acid composition of PilV, PilW and PilX. Intrinsic disorder profile of PilV (**a**), PilW (**c**) and PilX (**e**) of *At. thiooxidans* (purple) and *P. aeruginosa* (light blue) generated by the PONDR® predictor. Amino acid distribution of PilV (**b**), PilW (**d**) and PilX (**f**) from *At. thiooxidans* (purple) and *P. aeruginosa* (light blue) relative to SWISS-PROT database; data are shown combined with the distribution of amino acids found in intrinsically disordered proteins (black).

The analysis of structural disorder of PilY1 from *At. thiooxidans* shows many segments with a tendency to disorder, although only three of these are predicted to have regions with transitions from disorder to order (Fig. 6a). The first consists of 132 amino acids which

include residues 41–172, the second contains 89 amino acids that correspond to residues 640–729 and the third consists of 44 amino acids that go from residue 1042 to 1176. In the case of PilY1 from *P. aeruginosa*, it also contains some segments with a tendency to disorder, but none are predicted to have transitions from disorder to order (Fig. 6a). PilY1 from *At. thiooxidans* is significantly enriched in the amino acids A, N, G, S, T, and in tyrosine (Y) (Fig. 6b). PilY1 from *P. aeruginosa* is also significantly enriched in the same amino acids, as well as in D, Q, and W. Significantly reduced amino acids in PilY1 from *At. thiooxidans* are R, D, C, E, H, K, L, and isoleucine (I), and in PilY1 from *P. aeruginosa* only C, E, H, L, K, M, and V (Fig. 6b).

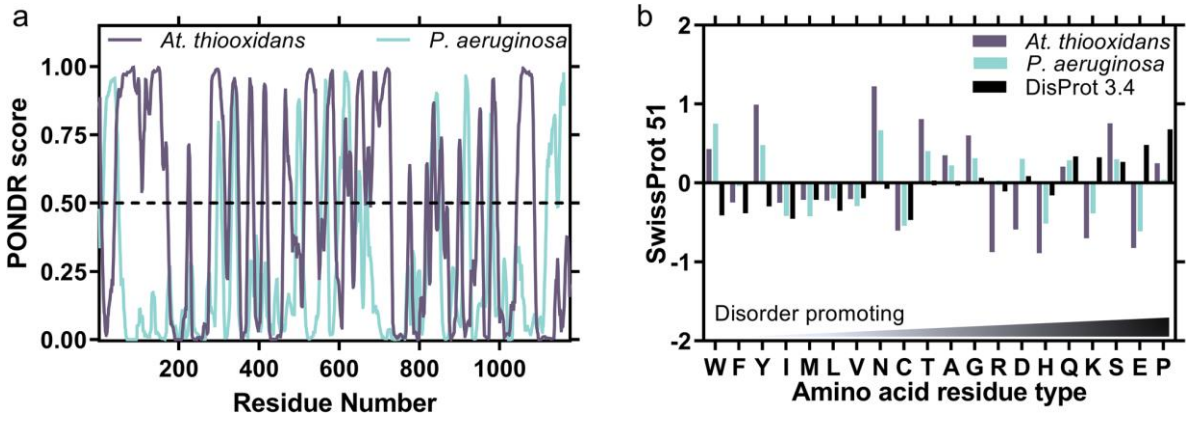

Figure 6. Prediction of intrinsic disorder and amino acid composition of PilY1. **a** Intrinsic disorder profile of PilY1 of *At. thiooxidans* (purple) and PilY1 of *P. aeruginosa* (light blue) generated by the PONDR® predictor. **b** Amino acid distribution of PilY1 of *At. thiooxidans* (purple) and PilY1 of *P. aeruginosa* (light blue) relative to the SWISSPROT database; data are shown combined with the distribution of amino acids found in intrinsically disordered proteins (black).

In *At. thiooxidans*, both the enriched polar amino acids (S, T, N, and Q) and reduced charged amino acids (K, R, D, and E) seem to be a distinctive characteristic of the minor pilins of this organism. The analysis of structural disorder is similar to that of FimU and FimT, since the profile of PilA from *At. thiooxidans* is more ordered in the N-terminus region than that of PilA from *P. aeruginosa*. Apart from this, the profile is similar in the two proteins, with that of *At. thiooxidans* tending more to disorder. In general, this behavior was observed in the majority of the proteins analyzed (Fig. 7a). The amino acid composition of PilA from *At. thiooxidans* was significantly enriched only in A and T, and significantly reduced in R and D, and substantially reduced in H, while there were no marked differences in K or E as in the

minor pilins. For PilA from *P. aeruginosa*, significant enrichment was only found in A, I, and T, but a substantial reduction only in the charged amino acids (Fig. 7b).

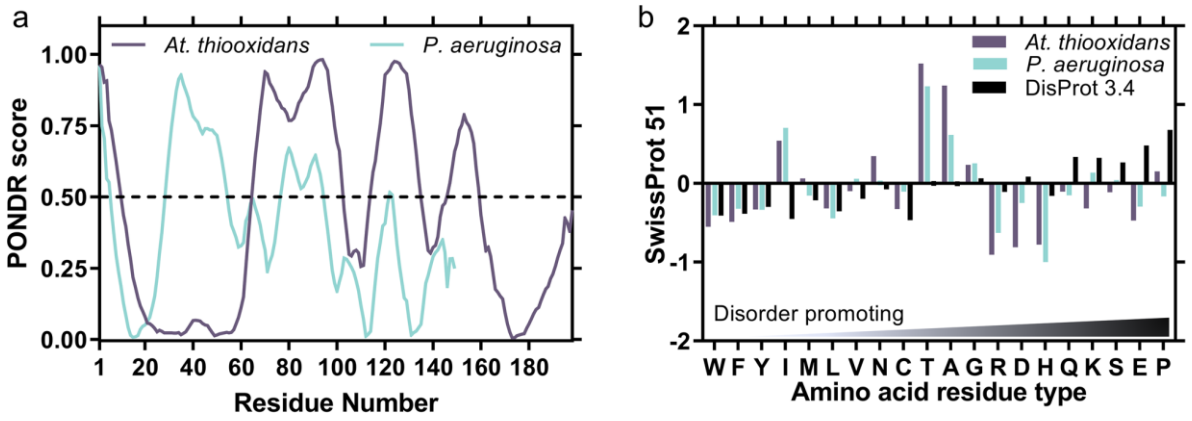

Figure 7. Prediction of intrinsic disorder and amino acid composition of PilA. **a** Intrinsic disorder profile of PilA of *At. thiooxidans* (purple) and of *P. aeruginosa* (light blue) generated by the PONDR® predictor. **b** Amino acid distribution of PilA of *At. thiooxidans* (purple) and of *P. aeruginosa* (light blue) relative to the SWISSPROT database; data are shown combined with the distribution of amino acids found in intrinsically disordered proteins (black).

When compared to folded counterparts, IDPs and IDP regions have a biased sequence composition, being enriched in charged and disorder-promoting amino acids and depleted in order-promoting ones. It has been described that the conformational ensembles of IDPs are influenced by the net charge per residue (Mao et al., 2010). Moreover, the distribution of charged residues affects the average size and shape of these proteins, since charge clustering induces remodeling of the conformational ensemble, promoting compaction (Bianchi et al., 2022). To determine whether there is a difference in charge distribution in addition to the decrease in charged amino acids in the major and minor pilins, we calculated the κ parameter with the CIDER webserver (Fig. 8).

The κ values of the pilins from *At. thiooxidans* are slightly higher than the pilins of *P. aeruginosa*, except for PilA (Fig. 8). Therefore, opposite charges of the pilins from *P. aeruginosa* are more evenly distributed along the sequence, while only PilV from *At. thiooxidans* show a greater charge segregation. Therefore, we can conclude that although the pilins of *At. thiooxidans* have fewer charged residues, these are not segregated.

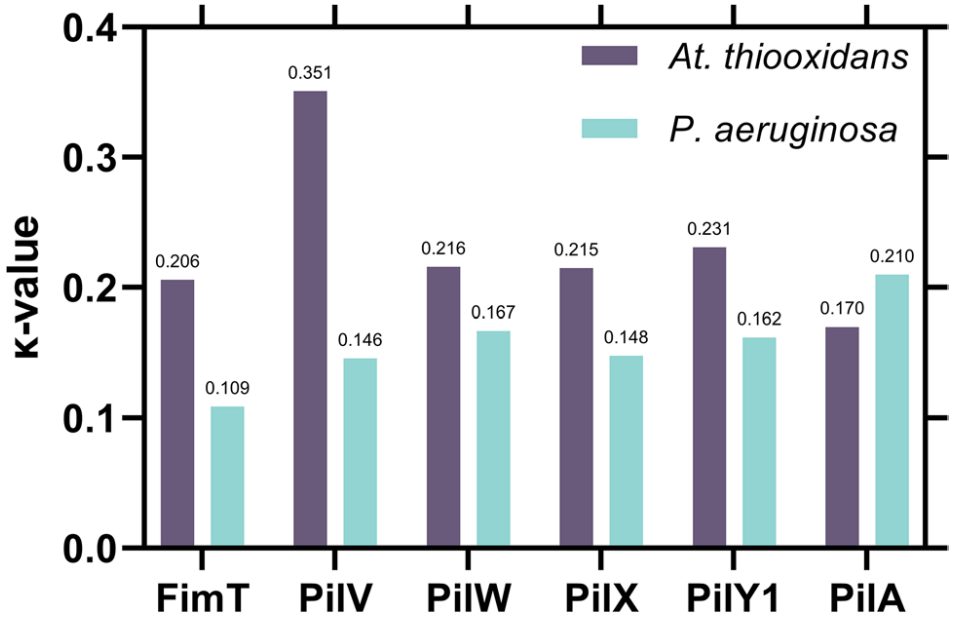

Figure 8. Comparative analysis of the κ parameter of the major and minor pilins of *At. thiooxidans* and *P. aeruginosa*. The values of κ range between 0 and 1. A κ value of 0 represents an evenly mixed distribution of positive and negative charges within a long linear sequence. On the other hand, a κ value of 1 signifies the complete segregation of oppositely charged residues in the sequence.

The majority of known globular structures in pilins share the same folding (C-terminus domain), even though the amino acid sequences of these pilins are so diverse that even structurally similar proteins have few identical sequences (Cehovin et al., 2010).

Taking this into account, we decided to explore the possibility that the enrichment of polar amino acids and reduction in charged amino acids as well as structural disorder, may be a characteristic of the pilins of bacteria that grow in acid environments, and to carry out the same comparison with non-acidophilic bacteria. An analysis was carried out of the amino acid composition and predictions of structural disorder of all the minor pilins from some bacteria of genus *Acidithiobacillus* and some acidophilic bacteria of *Acidiferrobacter* and *Acidobacteria*. These were compared with the pilins of non-acidophilic mesophilic bacteria *Acidovorax* sp., *P. aeruginosa* and *Escherichia coli* EDL933, *E. coli* K-12 and a non-acidophilic (thermophile) extremophile, *Thermus thermophilus*. It should be noted that like *At. thiooxidans*, the amino acid sequences of the minor pilins analyzed were of genes from the same cluster in all these organisms (Table S1). Using 19 sequences of PilY1, Alfaro-Saldaña et al., (2019) obtained a phylogenetic tree that showed that the *Acidithiobacillus* genus forms a cohesive cluster with other bacteria from acid mine drainage or mine tailings

(e.g., *Th. bhubaneswarensis*, *Ac. thiooxidans*, *Ga. acididurans*, *Sulfuriferula* sp.); this cohesive group was clearly separated from neutrophiles as *P. aeruginosa*. Now, in this work, we have provided data that shed light on why the primary structure of certain PilY1 differs in relation to their environment. Similar results were obtained with other pilins (data not shown).

The results of the comparison of amino acid composition were comparable to the previous set of comparisons described above. In general, significant enrichment in amino acids S, T, N, and Q and a significant reduction in K, R, E, and D were conserved in the pilins from the bacteria that grow in acid environments compared to their nonacidophilic counterparts (Fig. S1). A direct consequence of the amino acid composition of a protein sequence is that it determines its isoelectric point (pI) as a function of the combination of values of the disassociation constant (pKa) of its constituent amino acids. Two amino acids, D and E, have a negative charge, and three amino acids, K, R, and H, have a positive charge at a neutral pH, and are determined by their pKa values. Therefore, an integral property of proteins, such as their pI, is a result of the discrete acidic and basic pKa values of the lateral chains of their amino acids (Tokmakov et al., 2021). We, therefore, decided to calculate the pI of the minor pilins and compare it to their acidophilic and neutrophilic counterparts. We found that the majority ($\geq$ 70%) of the pilins of acidophilic organisms have a low pI, while approximately 60% of pilins of neutrophilic organisms have a higher pI (Fig. S2). This interesting correlation (acid environment and low pI of minor pilins) is consistent with previous reports that acid-stable proteins generally have low pI (Sharma et al., 2012; Reed et al., 2013). It has recently been reported that distributions of protein pI values (complete proteome) are multimodal in different species, and the hypothesis has been proposed that this multimodality is associated with various different subcellular environments and local distributions of pI. As a consequence, in a low pH (acid) environment, pI would tend to be acid (low) (Tokmakov et al., 2021).

Regarding the analysis of structural disorder (represented as mean disorder scores), the previously observed trend persists, indicating that pilins from acidophilic organisms tend to exhibit more structural disorder compared to their non-acidophilic counterparts (Fig. S1).

Physicochemical factors of the amino acid composition of the pilins of *At. thiooxidans*

As a next step, we decided to investigate the implications of the special amino acid composition of the pilins of this extremophile bacteria. We recall that this organism lives in an extremely low-pH environment; that is, essentially a highly protonated environment.

It is known that it is the surfaces of the proteins that are responsible for their stability in extreme environmental conditions; keeping this in mind, we observed that the enriched amino acids (S, T, N, and Q) in the pilins from *At. thiooxidans* have the characteristic of being preferentially located on the surfaces of proteins in general (Sillerud and Larson 2005). In addition, it has been reported that enrichment of the amino acids S and T is characteristic of acid-stable proteins, since these amino acids contain a hydroxyl group on their lateral chains (Michaux et al., 2010; Højgaard et al., 2016). Another important characteristic that we found was the reduction in charged amino acids, previously described for acid-stable proteins, such as the α-amylase of the acidophilic bacteria *Alicyclobacillus acidocaldarius* (Matzke et al., 1997). It is suggested that having fewer charged residues decreases the probability that the protein will become unstable due to elimination of the ion bridges from protonation/deprotonation at extreme pH values (Jelesarov and Karshikoff 2009). It is, therefore, suggested that enrichment of amide residues such as N and Q will enable acid-stable proteins to maintain stability and structure in spite of lacking charged residues (Højgaard et al., 2016).

To visualize and contrast these characteristics lent by the amino acid composition of *At. thiooxidans* pilins, we decided to obtain the three-dimensional structure of its PilV (AQP39907.1) and compare it with its counterpart PilV of *P. aeruginosa* (NP_253241.1) (Fig. 9). Even though PilV of *At. thiooxidans* is predicted to have a largely disordered region, this protein appears to share the same 3D structure as PilV from *P. aeruginosa*. This has been previously observed with *Dichelobacter nodosus* FimA, which has a largely unstructured α/β loop (region that links the conserved N-terminal α-helix with the globular domain in pilins) and still shares the same overall structure with its equivalents *Neisseria gonorrhoeae* GC pilin and *P. aeruginosa* PilA (Hartung et al., 2011; Giltner et al., 2012). It is important to note the difference between the charged residues of the two pilins: PilV from *At. thiooxidans* has four E but no D, as well as two R and one K in its sequence, which indicates a reduced

surface charge (Fig. 9a). In contrast, PilV from *P. aeruginosa* contains 12 D, 7 E, 9 R and 13 K in its sequence, most of which are distributed on its surface (Fig. 9b).

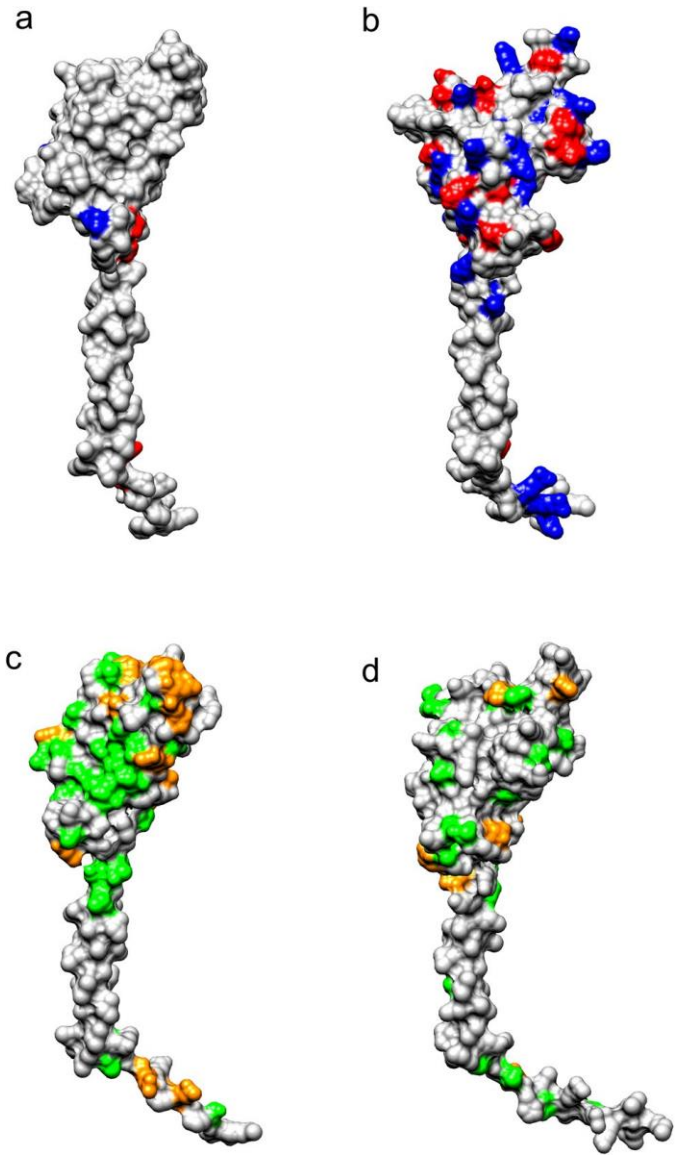

Figure 9. Composition of the surface of acidophilic and non-acidophilic PilV. Representation of surface charged residues of PilV of **a** *At. thiooxidans* and **b** *P. aeruginosa*, showing arginine R and lysine K residues in blue, and aspartic and glutamic acid residues in red; also shown are hydroxyl (serine and threonine) residues in green and amide (glutamine and asparagine) in orange from the PilV of **c** *At. thiooxidans* and **d** *P. aeruginosa*.

The hydroxyl residues (S and T) and amide residues (N and Q) of PilV from *P. aeruginosa* (numbers of residues: 20 S; 7 T; 4 N; and 7 Q) are generally located in isolation along the length of the surface (Fig. 9d), while for the PilV from *At. thiooxidans* (number of residues: 15 S; 15 T; 11 N; and 10 Q), these residues form patches that cover a large part of the surface

of the protein (Fig. 9c). It is interesting to note that the ratio T:S is 1.0 in the globular part of the PilV from *At. thiooxidans*, which is larger than the same ratio calculated for the PilV from *P. aeruginosa* (0.4). A larger ratio suggests a better formation of β-sheet, which leads to a more rigid folding (Hakulinen et al., 2003; Kellock et al., 2022). We suggest that it is due to these properties that the pilins of *At. thiooxidans*, and probably those of other acidophilic bacteria, have the ability to maintain their structure and function in hostile environments. These properties of enrichment in hydroxyl and amide residues and low surface charge density have been previously described for the cellulose of a xylanase B of *Cellulomonas fimi* (PDB code 1EXG), where it was shown that this protein has resilience in a broad range of pH values (2 to 11).

We also have this pH resilience in the context of these pilins: acidophiles can grow at pH < 3 maintaining their intracellular pH at around 6.5 (Fig. 10) (Cox et al., 1979; Hu et al., 2020). The synthesis of T4aP implies that the pilins of the filament (PilA and FimTPilVWXY1) transit from a circumneutral to an acidic environment (Fig. 10). Major PilA and minor FimTPilVWX are synthesized as prepilin with a signal peptide in cytoplasm, a circumneutral region; the transferred prepilin has a negative charge that attracts "the positively charged alignment protein subunits in the growing pilus length" (Proft and Baker 2009). The signal peptide is predicted to be fully unstructured, and is cleaved between G and F1, and methylated at its new N-terminus by a prepilin peptidase (PilD). Assembly of the mature pilins is carried out by the action of the ATPase pilin (PilB). PilD and PilB are on the cytoplasmic side of the inner membrane; the mature pilins line up and the filament grows in the alignment complex (PilMNOP) present in periplasmic region with a pH of 2.5–3.0 (Chi et al., 2007; Hu et al., 2020), to the outer membrane secretion system (PilQ) (McCallum et al., 2019). Then, the filament emerges from the cell, where it is exposed to an acid environment, pH < 3.

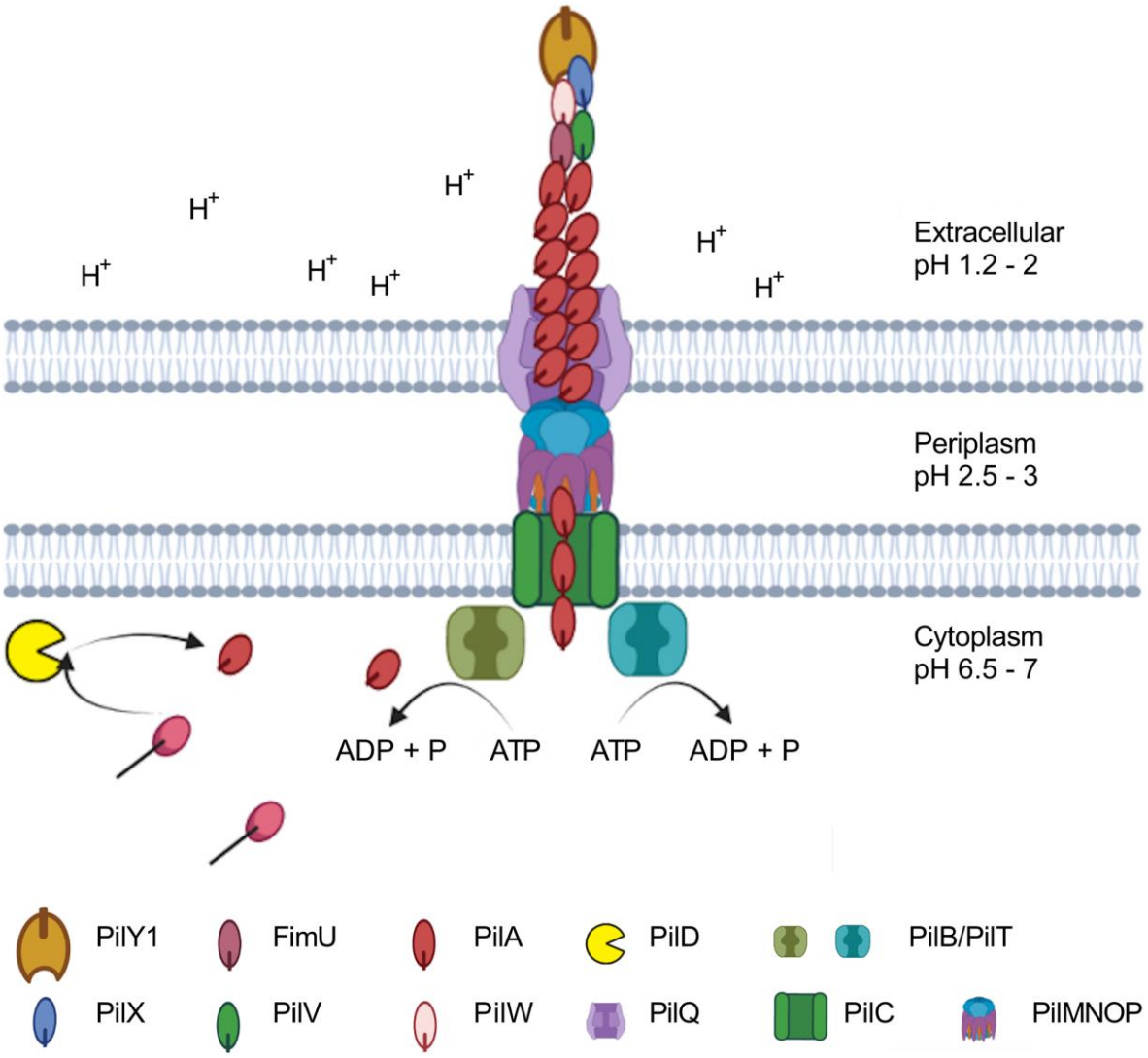

Figure 10. Representation of general organization of T4aP proteins in *At. thiooxidans.* The proteins that make up the pili structure mature in the cytoplasm (neutral pH); however, the T4aP of *At. thiooxidans* must maintain its structure and function even in a highly protonated environment (extracellular pH below 2 and periplasmic pH *ca*. 3). Our results suggest that this resilience occurs due to surface characteristics in its major pilin (PilA in red), minor pilins (FimT in magenta, PilV in green, PilW in pink and PilX in blue), and the adhesine PilY1 (orange).

Having the qualities described (acid-stable, resilient proteins) could be important for the pilins in biotechnology and/ or biotherapeutic applications due to surface or interface properties. We, therefore, set out to analyze the stability of the folded state and net charge of the cellulose binding domain of xylanase B, and found that it is very similar to that predicted for PilV from *At. thiooxidans*. The stability values of the folded state of these two proteins are almost equal in a broad pH range (2–8) and range of ionic strengths (0.0005 to 0.3 M) (Fig. S4). This can also be seen in the graphs of pH against energy (Fig. S5) and against

charge (Fig. S6), which show that these proteins maintain their stability and maintain little net charge, since their transitions from the midpoint are difficult to distinguish. In contrast, the same analysis for PilV from *P. aeruginosa* shows greater protonation (Fig. S7b) and less stability in its folded state (Fig. S6a) at acid pH levels, and stability transitions (Fig. S7c) and charge transitions (Fig. S7d) more similar to those of the FAB (fragment antigen-binding) domains. Although neutral stability values may be maintained for the cellulosebinding domain, these results are sufficient to show that this protein maintains its stability and function (Højgaard et al., 2016), suggesting that PilV may have a similar behavior, and that the same holds for the remaining pilins (data not shown). A more detailed analysis enabled us to find another example of resilience to pH, which is the case of the CH1 domain of the FAB segments. These have the distinctive feature of having the same amino acid composition (enrichment and reduction) as the pilins of *At. thiooxidan*s, as well as a tendency to structural disorder (Hebditch et al., 2017, 2020), which adds to the robustness of our study.

Conclusion

In summary, bioinformatic analysis of the genes associated with the T4aP tip of *At. thiooxidans* confirms that as in other prokaryotic species, they are in the same cluster and probably form an operon, indicating their importance. Regarding the proteins, we have found remarkable characteristics in the major (PilA) and minor pilins (FimTPilVWX) as well as in the adhesin (PilY1) of *At. thiooxidans*, which are conserved in the same proteins in the genus *Acidithiobacillus*, in other genera and possibly in other pilins of acidophilic bacteria. The most important characteristics associated with its functional stability can be summarized as: (1) the enrichment of hydroxyl and amide residues on its surface, and (2) the reduction of charged residues. These two characteristics suggest a high resilience to extreme pH (experimental validation pending), which give us guidelines for its application in protein engineering.

References Chapter II

Alfaro-Saldaña E, Hernández-Sánchez A, Patrón-Soberano OA et al (2019) Sequence analysis and confirmation of the type IV piliassociated proteins PilY1, PilW and PilV in *Acidithiobacillus thiooxidans*. PLoS ONE 14:e0199854. doi.org/10.1371/ journal.pone.0199854

Bairoch A, Apweiler R, Wu CH et al (2005) The Universal Protein Resource (UniProt). Nucleic Acids Res 33:D154–D159. doi.org/10.1093/nar/gki070

Belete B, Lu H, Wozniak DJ (2008) *Pseudomonas aeruginosa* AlgR regulates type IV pilus biosynthesis by activating transcription of the *fimU-pilVWXY1Y2E* operon. J Bacteriol 190:2023–2030. doi.org/10.1128/jb.01623-07

Berry J-L, Pelicic V (2015) Exceptionally widespread nanomachines composed of type IV pilins: the prokaryotic Swiss Army knives. FEMS Microbiol Rev 39:134–154. doi.org/10.1093/femsre/fuu001

Bianchi G, Mangiagalli M, Barbiroli A et al (2022) Distribution of charged residues affects the average size and shape of intrinsically disordered proteins. Biomolecules 12:561. doi.org/ 10.3390/biom12040561

Bondos SE, Dunker AK, Uversky VN (2021) On the roles of intrinsically disordered proteins and regions in cell communication and signaling. Cell Commun Signal 19:1–9. doi.org/10.1186/ s12964-021-00774-3

Camacho D, Frazao R, Fouillen A et al (2020) New insights into *Acidithiobacillus thiooxidans* sulfur metabolism through coupled gene expression, solution chemistry, microscopy, and spectroscopy analyses. Front Microbiol 11:411. doi.org/10.3389/ fmicb.2020.00411

Cehovin A, Winterbotham M, Lucidarme J et al (2010) Sequence conservation of pilus subunits in *Neisseria meningitidis*. Vaccine 28:4817–4826

Chi A, Valenzuela L, Beard S et al (2007) Periplasmic proteins of the extremophile *Acidithiobacillus ferrooxidans*: a high throughput proteomics analysis. Mol Cell Proteomics 6:2239–2251. doi.org/10.1074/mcp.m700042-mcp200

Cox JC, Nicholls DG, Ingledew WJ (1979) Transmembrane electrical potential and transmembrane pH gradient in the acidophile *Thiobacillus ferrooxidans*. Biochem J 178:195–200. doi. org/10.1042/bj1780195

Craig L, Li J (2008) Type IV pili: paradoxes in form and function. Curr Opin Struc Biol 18:267–277. doi.org/10.1016/j.sbi. 2007.12.009

Craig L, Forest KT, Maier B (2019) Type IV pili: dynamics, biophysics and functional consequences. Nat Rev Microbiol 17:429–440. doi.org/10.1038/s41579-019-0195-4

Denise R, Abby SS, Rocha EPC (2019) Diversification of the type IV filament superfamily into machines for adhesion, protein secretion, DNA uptake, and motility. PLoS Biol 17:e3000390. doi.org/10.1371/journal.pbio.3000390

Dunker AK, Lawson JD, Brown CJ et al (2001) Intrinsically disordered protein. J Mol Graph Model 19:26–59. doi.org/10.1016/ S1093-3263(00)00138-8

England JL, Shakhnovich BE, Shakhnovich EI (2003) Natural selection of more designable folds: a mechanism for thermophilic adaptation. Proc Natl Acad Sci USA 100:8727–8731. doi.org/10. 1073/pnas.1530713100

Galea CA, Wang Y, Sivakolundu SG, Kriwacki RW (2008) Regulation of cell division by intrinsically unstructured proteins: Intrinsic flexibility, modularity, and signaling conduits. Biochemistry 47:7598–7609. doi.org/10.1021/bi8006803

Giltner CL, Nguyen Y, Burrows LL (2012) Type IV Pilin proteins: versatile molecular modules. Microbiol Mol Biol Rev 76:740–772. doi.org/10.1128/mmbr.00035-12

Hakulinen N, Turunen O, Jänis J et al (2003) Three-dimensional structures of thermophilic β-1,4-xylanases from *Chaetomium thermophilum* and *Nonomuraea flexuosa*. Eur J Biochem 270:1399–1412. doi.org/10.1046/j.1432-1033.2003.03496.x

Hartung S, Arvai AS, Wood T et al (2011) Ultrahigh resolution and full-length pilin structures with insights for filament assembly, pathogenic functions, and vaccine potential. J Biol Chem 286:44254–44265. doi.org/10.1074/jbc.M111.297242

Hebditch M, Warwicker J (2019) Web-based display of protein surface and pH-dependent properties for assessing the developability of biotherapeutics. Sci Rep 91(9):1–9. doi.org/10.1038/ s41598-018-36950-8

Hebditch M, Curtis R, Warwicker J (2017) Sequence composition predicts immunoglobulin superfamily members that could share the intrinsically disordered properties of antibody CH1 domains. Sci Rep 71(7):1–9. doi.org/10.1038/s41598-017-12616-9

Hebditch M, Kean R, Warwicker J (2020) Modelling of pH-dependence to develop a strategy for stabilising mAbs at acidic steps in production. Comput Struct Biotechnol J 18:897–905. doi.org/ 10.1016/j.csbj.2020.03.002

Højgaard C, Kofoed C, Espersen R et al (2016) A soluble, folded Protein without charged amino acid residues. Biochemistry 55:3949– 3956. doi.org/10.1021/acs.biochem.6b00269

Holehouse AS, Das RK, Ahad JN et al (2017) CIDER: resources to analyze sequence-ensemble relationships of intrinsically disordered proteins. Biophys J 112:16–21. doi.org/10.1016/j. bpj.2016.11.3200

Hu W, Feng S, Tong Y et al (2020) Adaptive defensive mechanism of bioleaching microorganisms under extremely environmental acid stress: advances and perspectives. Biotechnol Adv 42:107580. doi.org/10.1016/j.biotechadv.2020.107580

Jacobsen T, Bardiaux B, Francetic O et al (2020) Structure and function of minor pilins of type IV pili. Med Microbiol Immunol 209:301– 308. doi.org/10.1007/S00430-019-00642-5

Jelesarov I, Karshikoff A (2009) Defining the role of salt bridges in protein stability. Methods Mol Biol 490:227–260. doi.org/ 10.1007/978-1-59745-367-7_10

Jumper J, Evans R, Pritzel A et al (2021) Highly accurate protein structure prediction with AlphaFold. Nature 596:583–589. doi. org/10.1038/s41586-021-03819-2

Kellock M, Rahikainen J, Borisova AS et al (2022) Inhibitory effect of lignin on the hydrolysis of xylan by thermophilic and thermolabile GH11 xylanases. Biotechnol Biofuels Bioprod 15:1–18. doi.org/10.1186/s13068-022-02148-4

Ma BG, Goncearenco A, Berezovsky IN (2010) Thermophilic adaptation of protein complexes inferred from proteomic homology modeling. Structure 18:819–828. doi.org/10.1016/j.str. 2010.04.004

Mao AH, Crick SL, Vitalis A et al (2010) Net charge per residue modulates conformational ensembles of intrinsically disordered proteins. Proc Natl Acad Sci USA 107:8183–8188. doi.org/ 10.1073/pnas.0911107107

Matzke J, Schwermann B, Bakker EP (1997) Acidostable and acidophilic proteins: the example of the alpha-amylase from *Alicyclobacillus acidocaldarius*. Comp Biochem Physiol A Physiol 118:475–479. doi.org/10.1016/s0300-9629(97)00008-x

McCallum M, Burrows LL, Howell PL (2019) The dynamic structures of the Type IV pilus. Microbiol Spectr 7:1–12. doi.org/10. 1128/microbiolspec.psib-0006-2018

Michaux C, Pouyez J, Mayard A et al (2010) Structural insights into the acidophilic pH adaptation of a novel endo-1,4-β-xylanase from *Scytalidium acidophilum*. Biochimie 92:1407–1415. doi. org/10.1016/j.biochi.2010.07.003

Mirdita M, Schütze K, Moriwaki Y et al (2022) ColabFold: making protein folding accessible to all. Nat Methods 19:679–682. doi.org/10.1038/s41592-022-01488-1

Nguyen Y, Sugiman-Marangos S, Harvey H et al (2015) *Pseudomonas aeruginosa* minor pilins prime type IVa pilus assembly and promote surface display of the PilY1 adhesin. J Biol Chem 290:601– 611. doi.org/10.1074/jbc.m114.616904

Orans J, Johnson MDL, Coggan KA et al (2010) Crystal structure analysis reveals *Pseudomonas* PilY1 as an essential calcium-dependent regulator of bacterial surface motility. Proc Natl Acad Sci USA 107:1065–1070. doi.org/10.1073/pnas.0911616107

Panja AS, Maiti S, Bandyopadhyay B (2020) Protein stability governed by its structural plasticity is inferred by physicochemical factors and salt bridges. Sci Rep 10:1–9. doi.org/10.1038/ s41598-020-58825-7

Pavlovic-Lazetic GM, Mitić NS, Kovačević JJ et al (2011) Bioinformatics analysis of disordered proteins in prokaryotes. BMC Bioinform 12:1–22. doi.org/10.1186/1471-2105-12-66

Pelicic V (2008) Type IV pili: *e pluribus unum*? Mol Microbiol 68:827–837. doi.org/10.1111/j.1365-2958.2008.06197.x

Proft T, Baker EN (2009) Pili in Gram-negative and Gram-positive bacteria - structure, assembly and their role in disease. Cell Mol Life Sci 66:613–635. doi.org/10.1007/S00018-008-8477-4

Reed CJ, Lewis H, Trejo E et al (2013) Protein adaptations in archaeal extremophiles. Archaea 2013:1–14. doi.org/10.1155/2013/ 373275

Sauvonnet N, Vignon G, Pugsley AP, Gounon P (2000) Pilus formation and protein secretion by the same machinery in *Escherichia coli*. EMBO J 19:2221–2228. doi.org/10.1093/emboj/19. 10.2221

Sharma A, Kawarabayasi Y, Satyanarayana T (2012) Acidophilic bacteria and archaea: acid stable biocatalysts and their potential applications. Extremophiles 16:1–19. doi.org/10.1007/ s00792-011-0402-3

Shukla SK, Khan A, Rao TS (2021) Microbial fouling in water treatment plants. Microb Nat Macromol. doi.org/10.1016/b978- 0-12-820084-1.00023-5

Sickmeier M, Hamilton JA, LeGall T et al (2007) DisProt: the database of disordered proteins. Nucleic Acids Res 35:D786–D793. doi.org/10.1093/nar/gkl893

Sillerud L, Larson R (2005) Design and structure of peptide and peptidomimetic antagonists of protein-protein interaction. Curr Protein Pept Sci 6:151–169. doi.org/10.2174/1389203053545462

Taboada B, Verde C, Merino E (2010) High accuracy operon prediction method based on STRING database scores. Nucleic Acids Res 38:e130. doi.org/10.1093/nar/gkq254

Taboada B, Estrada K, Ciria R, Merino E (2018) Operon-mapper: a web server for precise operon identification in bacterial and archaeal genomes. Bioinformatics 34:4118–4120. doi.org/ 10.1093/bioinformatics/bty496

Tokmakov AA, Kurotani A, Sato K-I (2021) Protein pI and intracellular localization. Front Mol Biosci 8:775736. doi.org/10.3389/ fmolb.2021.775736

Tompa P, Fersht A (2009) Structure and function of intrinsically disordered proteins. CRC Press

Travisany D, Cortés MP, Latorre M et al (2014) A new genome of *Acidithiobacillus thiooxidans* provides insights into adaptation to a bioleaching environment. Res Microbiol 165:743–752. doi.org/10.1016/j.resmic.2014.08.004

Treuner-Lange A, Chang YW, Glatter T et al (2020) PilY1 and minor pilins form a complex priming the type IVa pilus in *Myxococcus xanthus*. Nat Commun 11:1–14. doi.org/10.1038/ s41467-020-18803-z

Uversky VN (2017) Paradoxes and wonders of intrinsic disorder: stability of instability. Intrinsically Disord Proteins 5:e1327757. doi.org/10.1080/21690707.2017.1327757

Vacic V, Uversky VN, Dunker AK, Lonardi S (2007) Composition profiler: a tool for discovery and visualization of amino acid composition differences. BMC Bioinform 8:211. doi.org/10. 1186/1471-2105-8-211

Williams KP, Kelly DP (2013) Proposal for a new class within the phylum Proteobacteria, *Acidithiobacillia* classis nov., with the type order *Acidithiobacillales*, and emended description of the class *Gammaproteobacteria*. Int J Syst Evol Microbiol 63:2901–2906. doi.org/10.1099/ijs.0.049270-0

Xue B, Dunbrack RL, Williams RW et al (2010) PONDR-FIT: a metapredictor of intrinsically disordered amino acids. Biochim Biophys Acta Proteins Proteomics 1804:996–1010. doi.org/ 10.1016/j.bbapap.2010.01.011

Yoshimura F, Murakami Y, Nishikawa K et al (2009) Surface components of *Porphyromonas gingivalis*. J Periodontal Res 44:1–12. doi.org/10.1111/j.1600-0765.2008.01135.x

Supplementary information of Chapter II

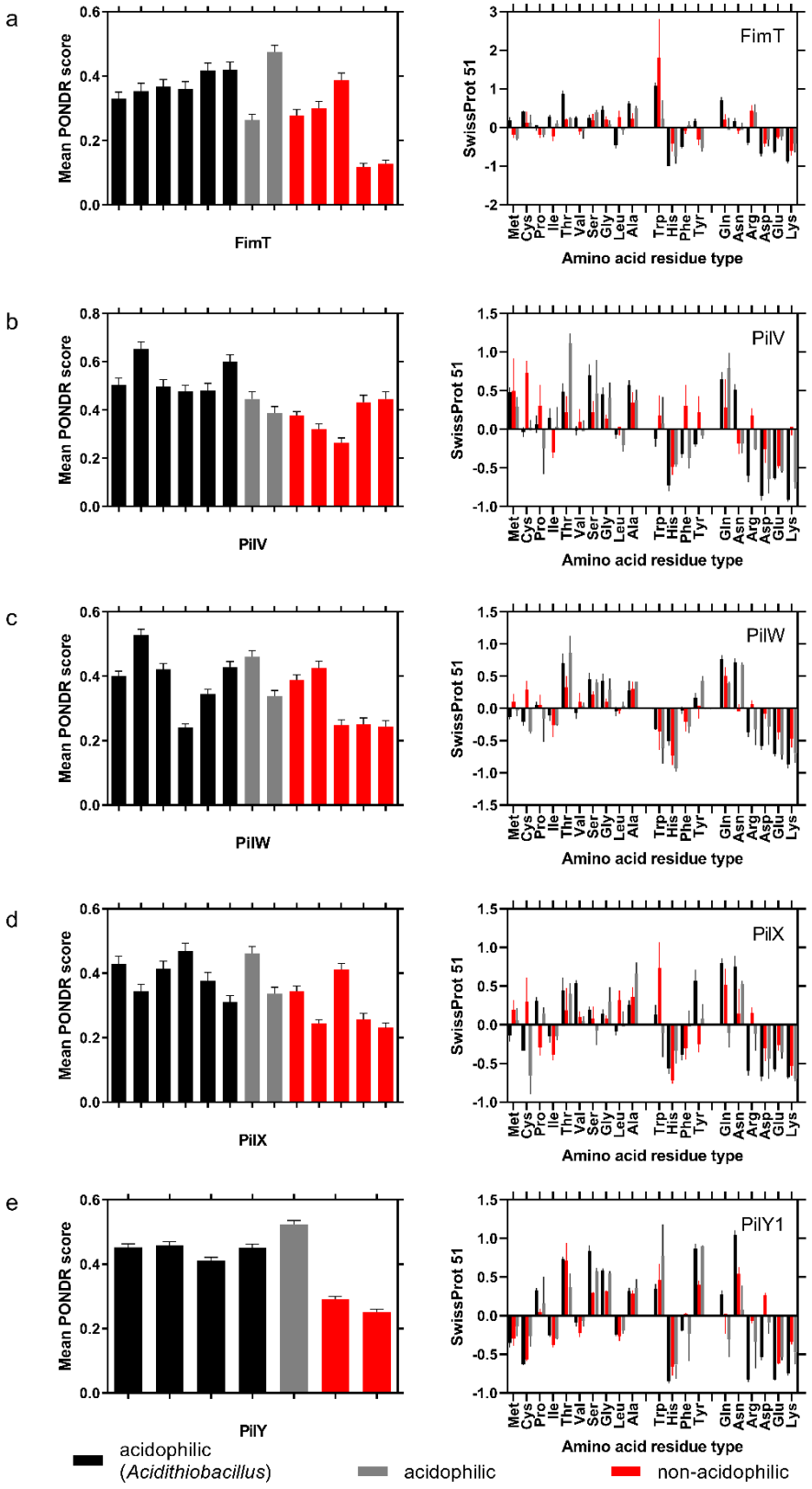

Fig. S1 Mean disorder scores and amino acid composition profile of the minor pilins of acidophilic and non-acidophilic bacteria. A comparison of mean disorder (left panels) and amino acid composition (right panels) was done using the minor pilins (a) FimT/U, (b) PilV, (c) PilW, (d) PilX and (e) PilY of acidophilic (black and gray) and non-acidophilic bacteria (red), according to the SWISS-PROT database. Amino acid residues are classified into three groups: aliphatic, aromatic and charged. Error bars represent the corresponding standard error in mean disorder scores.

Table S1 Accession numbers of minor pilins used in this work

Organism	***FimT****	***PilV****	***PilW****	***PilX****	***PilY1****
At. thiooxidans	TQN50488.1	AWP39907.1	AWP39906.1	OQ410719	AWP39905.1
At. ferrooxidans	WP_257482162.1	WP_257482161.1	WP_257482160.1	WP_257482159.1	WP_257482158.1
At. ferrivorans	CDQ09111.1	CDQ09112.1	CDQ09113.1	CDQ09114.1	
At. ferridurans	WP_215877965.1	WP_226828902.1	WP_226828945.1	WP_215878555.1	
At. albertensis	WP_075322774.1	WP_077218455.1	WP_075322775.1	WP_242947738.1	WP_075322776.1
At. caldus	WP_215865398.1	WP_215865399.1	MBU2763193.1	WP_215870274.1	WP_215874089.1
Acidiferrobacter spp. SP3/III	WP_110136415.1	WP_168185556.1	WP_168185557.1	WP_110136416.1	WP_110136417.1
Acidobacteria bacterium	MCA1591324.1	MCA1591323.1	MCA1591322.1	MCC7295874.1	
Acidovorax sp.	MBP7545800.1_	MBP7545799.1	MBP7545798.1	MBP7545797.1	PJI95759.1
Thermus thermophilus HB27	AAM55482.1	AAM55483.1	AAM55484.1	AAM55485.1	
Pseudomonas aeruginosa PAO1	NP_253240.1	NP_253241.1	NP_253242.1	NP_253243.1	NP_253244.1
Escherichia coli EDL933	WP_000857037.1	WP_001276465.1	WP_001144311.1	WP_001078379.1	
Escherichia coli K-12	NP_417303.1	NP_417300.1	NP_417302.1	NP_417301.4	

* Equivalent minor pilin in *P. aeruginosa* PA01

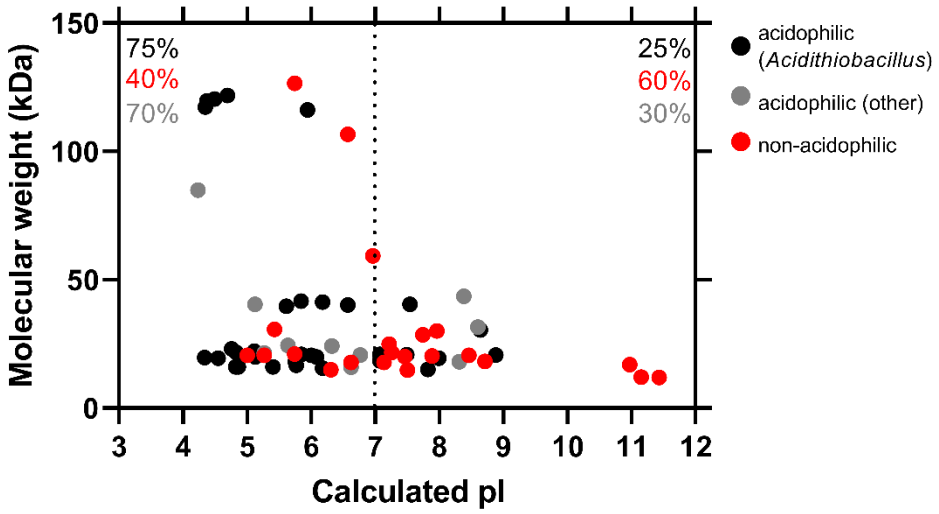

Fig. S2 The pI distribution of minor pilins. Scatter plot of minor pilins based on calculated pI and molecular weight from *Acidithiobacillus* (black), other acidophilic bacteria (gray) and non-acidophilic bacteria (red) reported in Table S1. *Acidithiobacillus* species show the lower values of pI (up to 75%) followed by other acidophilic bacteria (up to 70%), while non-acidophilic bacteria have the highest values of pI (60%).

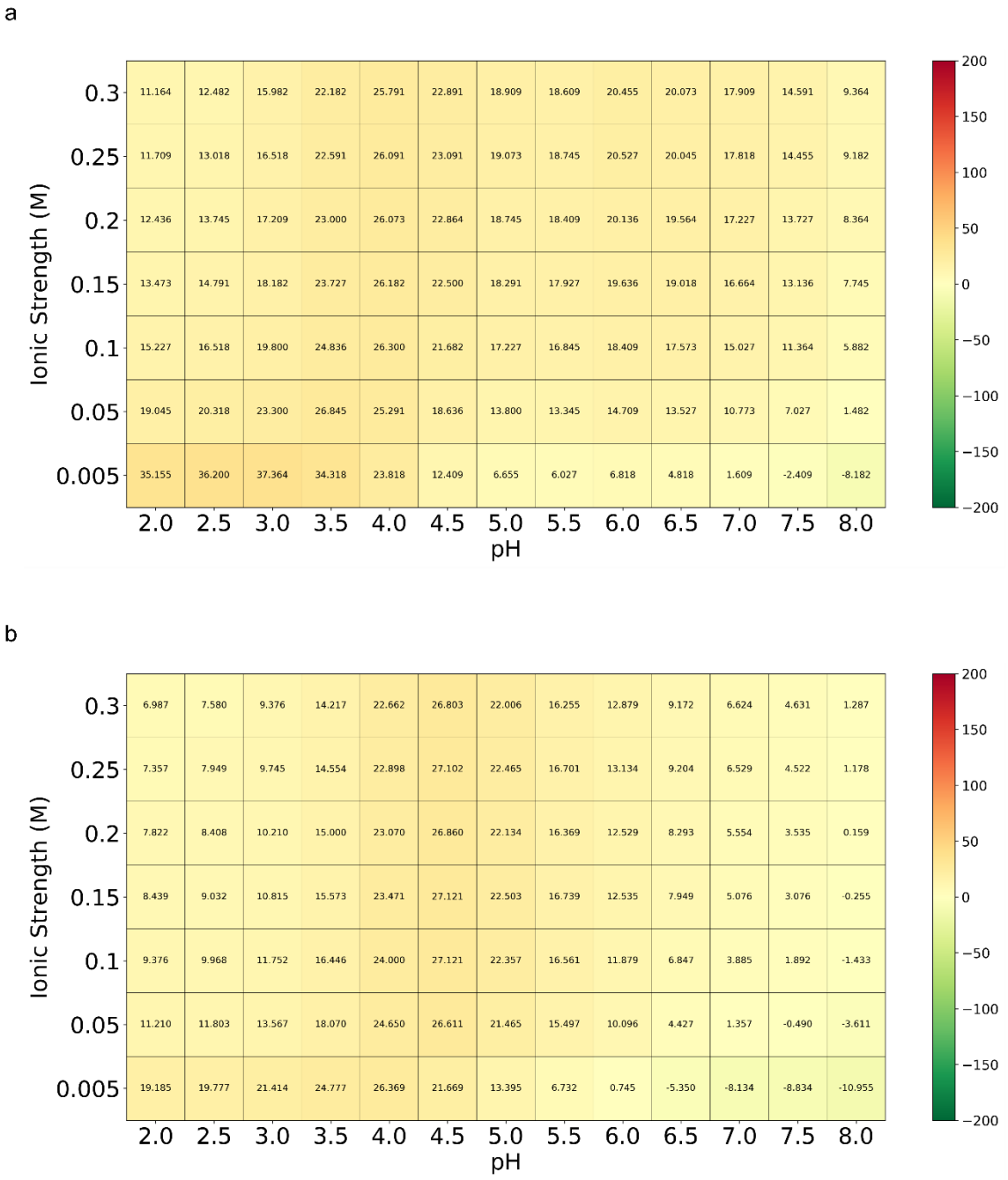

Fig. S3 Stability heat maps obtained with the protein-sol server (https://protein-sol.manchester.ac.uk/). Calculated fold state stability for (a) cellulose-binding domain from xylanase B of *Cellulomonas fimi*, and (b) PilV of *At. thiooxidans*

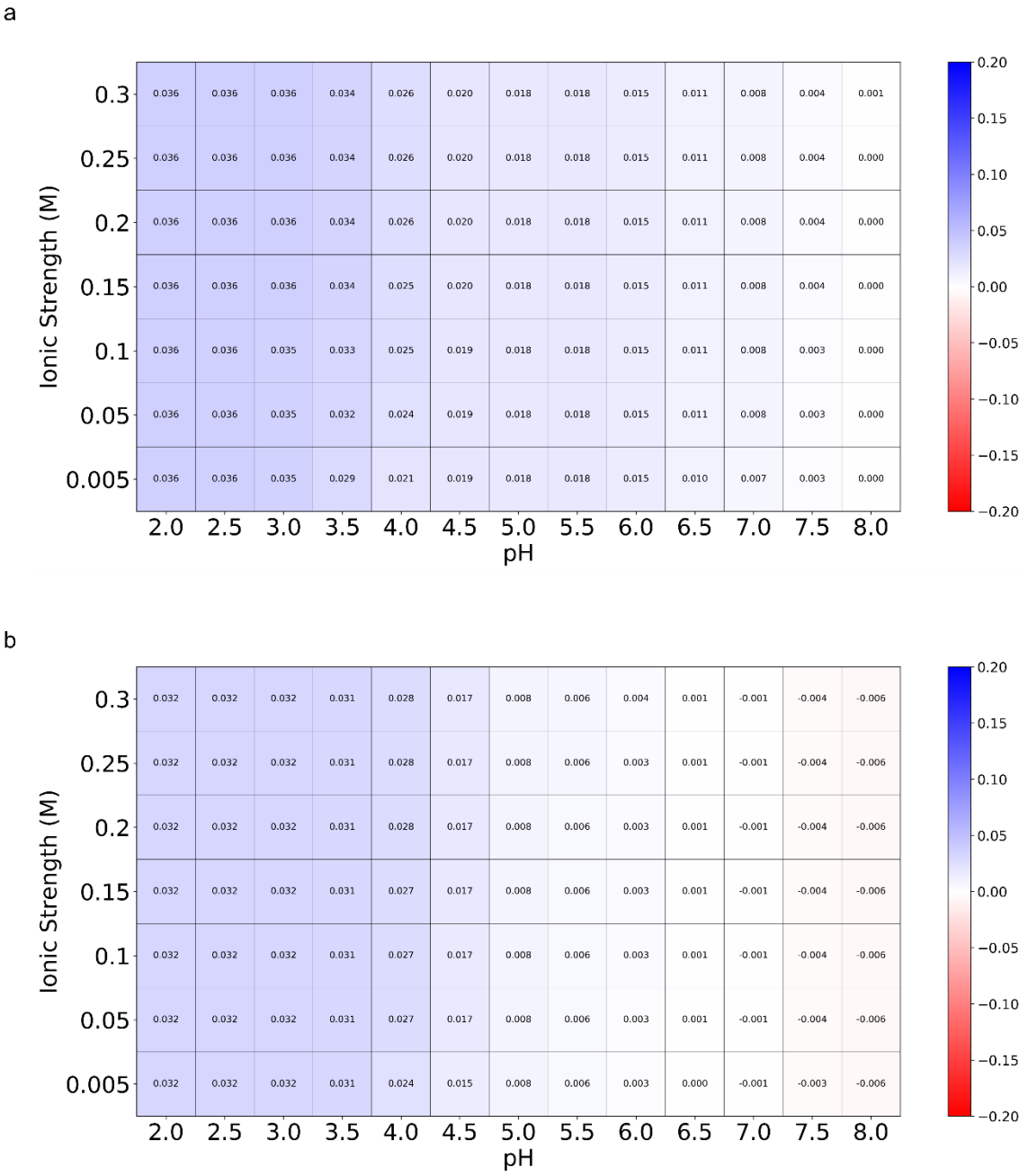

Fig. S4 Charge heat maps obtained with the protein-sol server (https://protein-sol.manchester.ac.uk/). Charge heatmap calculated for (a) cellulose-binding domain from xylanase B of *Cellulomonas fimi*, and (b) PilV of *At. thiooxidans*

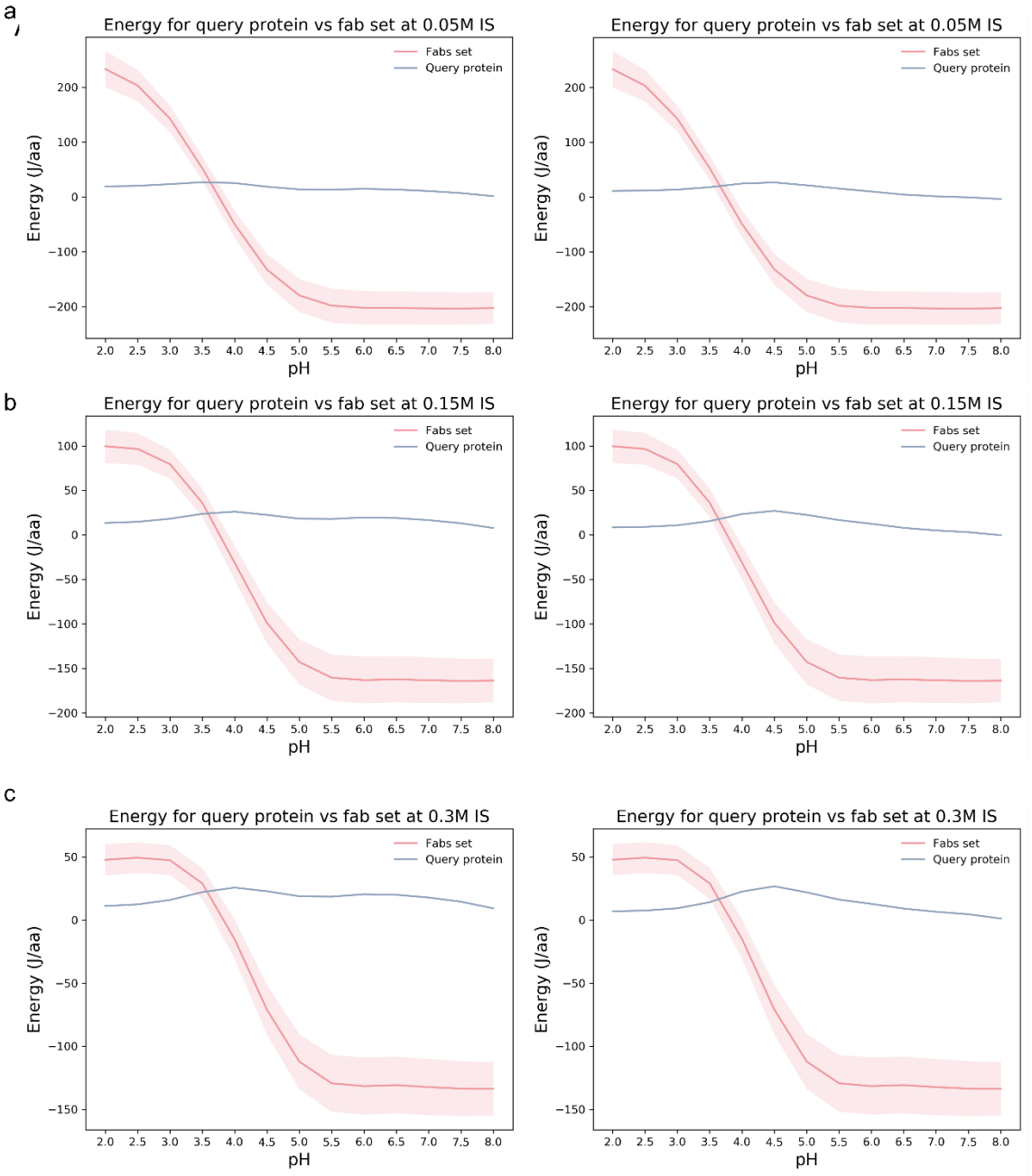

Fig. S5 Protein stability plot obtained with the protein-sol server (https://protein-sol.manchester.ac.uk/). Calculated fold state stability for cellulose-binding domain from xylanase B of *Cellulomonas fimi* (left panel), and PilV of *At. thiooxidans* (right panel) at different pH (2–8) and ionic strengths (a) 0.05, (b) 0.15, and (c) 0.3 M. FAB dataset corresponds to structures in the PDB with fragment antigen-binding regions.

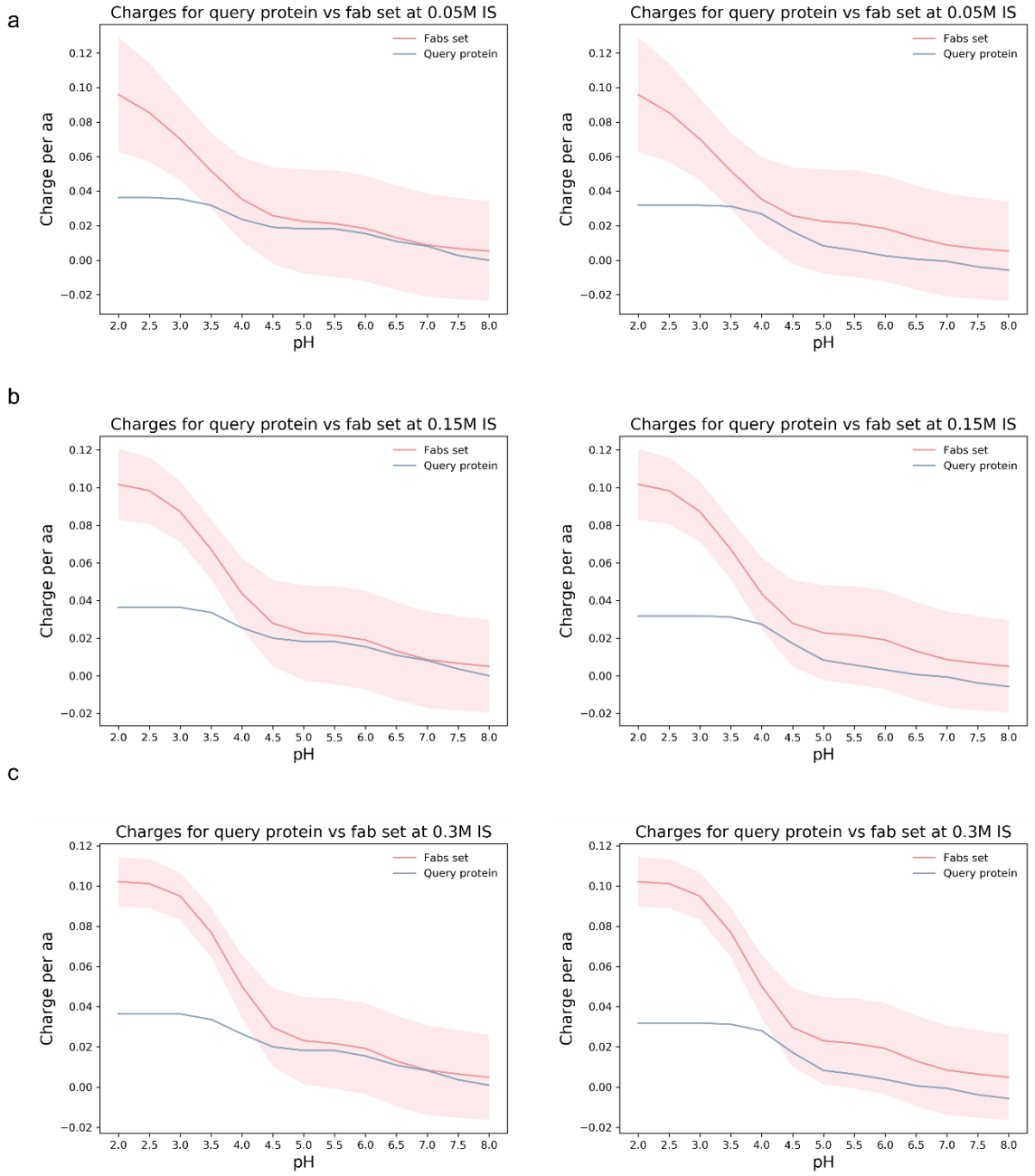

Fig. S6 Calculated charge plot obtained with the protein-sol server (https://protein-sol.manchester.ac.uk/). Charge calculated for cellulose-binding domain from xylanase B of *Cellulomonas fimi* (left panel), and PilV of *At. thiooxidans* (right panel) at different pH (2–8) and ionic strengths (a) 0.05, (v) 0.15, and (c) 0.3 M. FAB dataset corresponds to structures in the PDB with fragment antigen-binding regions.

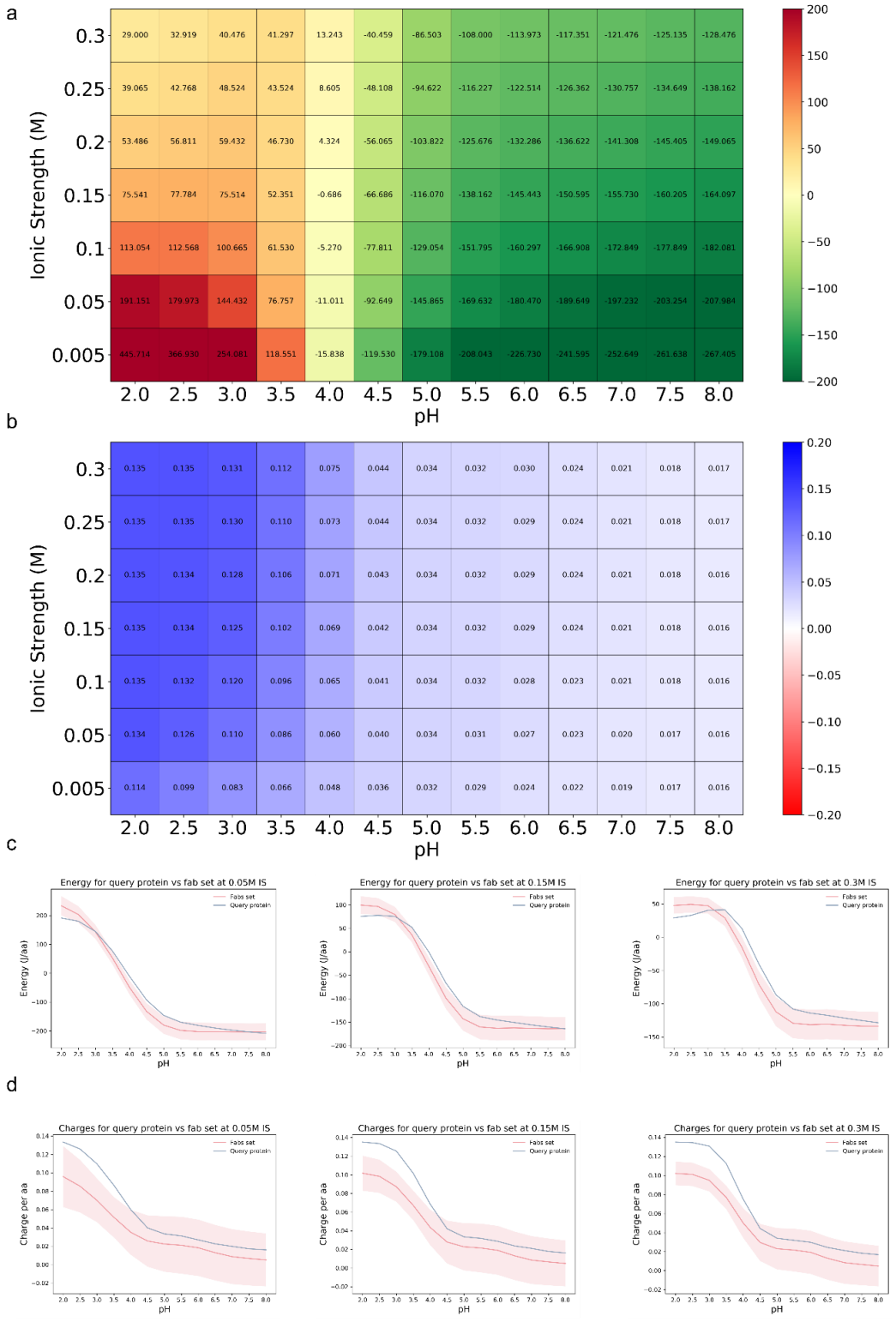

Fig. S7 *Pseudomonas aeruginosa* PilV protein stability and calculated charge obtained with the protein-sol server (https://protein-sol.manchester.ac.uk/). Stability and charge heatmaps (a and b) and plot (c and d) calculated for PilV of *P. aeruginosa.*

CHAPTER III

J. Microbiol. Biotechnol. 2024. 34(3): 525–537
https://doi.org/10.4014/jmb.2310.10033

Understanding a Core Pilin of the Type IVa Pili of *Acidithiobacillus thiooxidans*, PilV

Araceli Hernández-Sánchez[1], Edgar D. Páez-Pérez[1*], Elvia Alfaro-Saldaña[1], Vanesa Olivares-Illana[2], and J. Viridiana García-Meza[1*]

[1]*Geomicrobiología, Metalurgia, Universidad Autónoma de San Luis Potosí, Sierra Leona 550, San Luis Potosí, 78210, SLP, México*
[2]*Laboratorio de Interacciones Biomoleculares y Cáncer. Instituto de Física, Universidad Autónoma de San Luis Potosí, Av. Parque Chapultepec 1570, Privadas del Pedregal, San Luis Potosí, 78210, SLP, México*

Pilins are protein subunits of pili. The pilins of type IV pili (T4P) in pathogenic bacteria are well characterized, but anything is known about the T4P proteins in acidophilic chemolithoautotrophic microorganisms such as the genus *Acidithiobacillus*. The interest in T4P of *A. thiooxidans* is because of their possible role in cell recruitment and bacterial aggregation on the surface of minerals during biooxidation of sulfide minerals. In this study we present a successful *ad hoc* methodology for the heterologous expression and purification of extracellular proteins such as the minor pilin PilV of the T4P of *A. thiooxidans*, a pilin exposed to extreme conditions of acidity and high oxidation-reduction potentials, and that interact with metal sulfides in an environment rich in dissolved minerals. Once obtained, the model structure of *A. thiooxidans* PilV revealed the core basic architecture of T4P pilins. Because of the acidophilic condition, we carried out *in silico* characterization of the protonation status of acidic and basic residues of PilV in order to calculate the ionization state at specific pH values and evaluated their pH stability. Further biophysical characterization was done using UV-visible and fluorescence spectroscopy and the results showed that PilV remains soluble and stable even after exposure to significant changes of pH. PilV has a unique amino acid composition that exhibits acid stability, with significant biotechnology implications such as biooxidation of sulfide minerals. The biophysics profiles of PilV open new paradigms about resilient proteins and stimulate the study of other pilins from extremophiles.

Keywords: PilV, protein expression, protein purification, protein structure, protein disorder, *A. thiooxidans*

Received: October 25, 2023
Accepted: December 29, 2023

Understanding a core pilin of the type IVa pili of *Acidithiobacillus thiooxidans*, PilV

Abstract

Pilins are protein subunits of pili. The pilins of type IV pili (T4P) in pathogenic bacteria are well characterized, but anything is known about the T4P proteins in acidophilic chemolithoautotrophic microorganisms such as the genus *Acidithiobacillus*. The interest in T4P of *At. thiooxidans* is because of their possible role in cell recruitment and bacterial aggregation on the surface of minerals during biooxidation of sulfide minerals. In this study we present a successful *ad hoc* methodology for the heterologous expression and purification of extracellular proteins such as the minor pilin PilV of the T4P of *At. thiooxidans*, a pilin exposed to extreme conditions of acidity and high oxidation-reduction potentials, and that

interact with metal sulfides in an environment rich in dissolved minerals. Once obtained, the model structure of *At. thiooxidans* PilV revealed the core basic architecture of T4P pilins. Because of the acidophilic condition, we carried out *in silico* characterization of the protonation status of acidic and basic residues of PilV in order to calculate the ionization state at specific pH values and evaluated their pH stability. Further biophysical characterization was done using UV-visible and fluorescence spectroscopy and the results showed that PilV remains soluble and stable even after exposure to significant changes of pH. PilV has a unique amino acid composition that exhibits acid stability, with significant biotechnology implications such as biooxidation of sulfide minerals. The biophysics profiles of PilV open new paradigms about resilient proteins and stimulate the study of other pilins from extremophiles.

Introduction

Pili are polymers of pilins, dynamic semiflexible filaments anchored to and extending from the cellular membrane of most Bacteria and Archaea. They are about 4-9 nm in diameter and 4-5 μm long but can be extended by up to several more micrometers by adding additional units (polymerize) and retracted (depolymerize) by removing units. These units are generically named pilins [1–4]. Extension or retraction can occur at a rate of >1000 subunits/s [5]. The complex pilin assembly process employs a proteinaceous machinery that uses the energy required for assembly and disassembly provided by two cytoplasmic ATPases associated with the transmembrane complex of the pilus[1,6]. Thus, the basic pilins are: a major pilin, adhesion pilin, minor pilins, and assembly and retraction ATPases [5,7]. Pili play a number of different roles in cells, such as motility, chemotactic migration, surface sensing, surficial twitching motility, detection of neighboring cells, microcolony and biofilm formation, secretion of colonization factors, resistance to mechanical stresses >100 pN [8,9], cell aggregation, stabilization of extracellular polymeric substances (EPS), adhesion to surfaces or to host cells [10], and enabling extracellular electron transport [11–14] and DNA uptake and lateral gene transfer [9], among other functions.

Various types of pili have been described according to their mechanisms of assembly, pilin structure, and morphology [1]. The type IV pili (T4P) are the most common filaments or fimbriae [15] and have been grouped based on the aminoacidic homology of the pilins, which

are relatively conserved in Gram-negative bacteria [16,17], including chemolithoautotrophic acidophiles such as *Acidithiobacillus ferrooxidans* and *At. thiooxidans* [11,18–20]. All T4P share domain structures and preserved sequences such as the conserved N-terminal motif in major and minor pilins, which is a type III signal peptide [1,6,21]. This motif is cleaved off by one peptidase before the mature protein is incorporated into the pilus structure [22] and it has become the landmark for pilus structure proteins [23,24].

The structure of T4P and their pilins in pathogenic bacteria are well characterized; however, little is known about the T4P proteins or pilins in acidophilic microorganisms such as the genus *Acidithiobacillus*. The interest in *At. ferrooxidans* and *At. thiooxidans* is because of their role in bioleaching during metal removal in landfills and mining. To access the free electrons from sulfide minerals such as pyrite (FeS_2), chalcopyrite ($CuFeS_2$) or sphalerite (ZnS), both acidithiobacilli require contact with the mineral surface, which allows individuals to begin to form biofilms. Previous research has shown that the pili of *At. ferrooxidans* are involved with recruitment of cells and bacterial aggregation to the surface of pyrite, and a significant up-expression of pilins involved in cell adhesion and pili biogenesis has been detected [12,18]. Also, for *At. ferrooxidans*, T4P enable electron transference in addition to their adhesion properties [11,13]. Like *At. ferrooxidans*, surface colonization and adhesion by *At. thiooxidans* should be mediated by pili and enhanced by EP. Thus, a better understanding of the role of pilins during the colonization of mineral surfaces can improve the mineral bioleaching processes employed to recover Cu, Ni, Zn, Co and/or Au, or to improve sulfur removal from solid sources, and even energy generation in microbial fuel cells [25,26]. It is important to note that all of these bioleaching processes occur at low pH values (0.5-2.5) and under high oxidant conditions.

In some proteobacteria such as *Pseudomonas spp*. and *Geobacter spp*., PilV is a minor pilin or outer membrane protein necessary for pilus biogenesis and stabilization [27,28]. PilV acts after pilus assembly along with other minor pilins (e.g., PilW, PilX, PilY1), forming a core assembly initiation subcomplex that primes pilus assembly by lowering the energy barrier necessary for major pilins to emerge from the membrane, in which PilV interacts with FimU, which then interacts with major PilA [28,29]. PilV includes the consensus motif or signal peptide sequence GXXXXE, as well as a highly conserved N-terminal domain in bacterial

T4P pilins, whose functions are inner membrane insertion, signal processing, and pilin polymerization to form a central helical core of the pilus filament [27,30]. PilV has been described in *At. ferrooxidans* as a "prepilin-type N-terminal cleavage/methylation domain-containing protein", domain that belongs to the PilV superfamily. An extracellular structure, the T4P pilus assembly protein involved in cell motility, e.g., lower expression PilV mRNA in *At. ferrooxidans*, affects motility and attachment to the substrate [31]. What is interesting is that the PilV of *Acidithiobacillus* species has been little described and analyzed. PilV of *At. thiooxidans* shares up to 93% homology with PilV of *At. ferrooxidans* in its mature form [20]. Recently we found that PilV is in a cluster *fimT-pilW-pilV-pilX-pilY1* similar to the minor-pilins cluster of *P. aeruginosa* [32]. It is clear that pathogenic and acidophilic bacteria have type IV pili (T4P); therefore, their pili are in contact with different external environments. It is possible that among all types of pili in different microorganisms, the pilins share shape and size properties. However, at the same time, they should present differences at the surface level that enable them to adapt to thousands of different external conditions.

In the realm of acidophilic prokaryotic organisms, maintaining homeostasis assumes paramount importance for their survival. Numerous studies have concentrated on elucidating intracellular and extracellular mechanisms of resistance to low pH, with references to recent work by Feng *et al.,* [33], Boase *et al.,* [34], and González-Rosales *et al.,* [35]. However, scant attention has been paid to the adaptations of extracellular protein structures, such as T4P, which remain vulnerable to low pH due to their exposure outside the cell. Recent studies have hinted at potential mechanisms for acid protection in T4P. In acidophilic thermophilic Archaea, the prevalence of amino acids like serine and threonine is thought to provide acid protection, potentially via O-glycosylation sites, as proposed by Wang *et al.,* [36]. On the other hand, bacterial T4P also exhibit features that suggest acid stability, characterized by a composition rich in polar amino acids and a low proportion of charged amino acids, as discussed in a recent study by Páez-Pérez *et al.,* [32]. Similar trends in amino acid composition have been observed in pili-like structures in *At. ferrooxidans*, most likely reflecting a responsive variation linked to the protein stabilization at low pH [37]. These findings shed light on the fascinating adaptations of extracellular protein structures in acidophilic microorganisms, offering insights into their ability to thrive in challenging acidic environments.

Currently there are no reports regarding cloning and heterologous expression of major or minor pilins from species of *Acidithiobacillus* despite their being acidophiles, nor are any reports of *in silico* or experimental analysis pilins from acidophiles, e.g., the acid stability of their pilins. Here we introduce such analyses with the premise that the pilin PilV is due to a particular amino acid composition indicating a reduction in charged amino acids. This was computationally evaluated using molecular dynamics and stability predictions, which showed acid stability, likely due to low surface charge. Also, in this work, PilV of *At. thiooxidans* was expressed and purified for the first time. Through molecular cloning techniques, recombinant proteins were obtained by *in vitro* expression systems. Cloning was done using the TOPO-TA system (vector pGEM-T Easy), and its insertion into *E. coli* JM109; the *pilV* obtained from the pGEM-*pilV* construct was ligated into the expression vector pET-32b(+), then expressed in *E. coli* BL21-CodonPlus (DE3) and purified with nickel affinity and anion exchange chromatography. The stability of the protein at different pH was then evaluated by monitoring its solubility using UV-Vis and fluorescence spectroscopy.

Material and Methods

Culture of *Acidithiobacillus thiooxidans* and synthesis of cDNA pilin

Cells of type strain *At. thiooxidans* ATCC 19377 were aerobically cultured at 29±1°C in ATCC-125 medium (with g/L: 0.4 $(NH_4)_2SO_4$, 0.5 $MgSO_4 \cdot 7H_2O$, 0.25 $CaCl_2$, 3 KH_2PO_4, 0.005 $FeSO_4 \cdot 7H_2O$; 10 of sterilized S^0; pH 2.0 adjusted with concentrated H_2SO_4). The cultures were incubated for 28 days to obtain *ca*. 1×10^8 cells/mL. At this cellular density, the cells were concentrated and washed at 800 ×g for 1 min to remove the S^0, and at 21100 ×g for 1 min using saline phosphate buffer PBS; in g/L: 8 NaCl, 1.44 Na_2HPO_4, 0.24 KH_2PO_4 (J.T. Baker, USA), and 0.2 KCl (Sigma, USA; pH 7.4). The bacterial pellet was preserved until its use. mRNA was extracted by the TRIzol® (Invitrogen, USA) method following the protocol provided by the manufacturer and the cDNA was obtained using M-MLV retrotranscriptase (RT, Invitrogen).

Design of primers and PCR

Primers were designed based on the sequence of a non-redundant PilV protein (AWP39907.1; GenBank, ncbi.nlm.nih.gov/genbank) of *At. thiooxidans* ATCC 19377

(NZ_SZUV01000001.1:273124-274257; GenBank), using Vector NTI Express (Thermo Fisher Scientific). The primers were then synthesized by T4 Oligo (México) as follows: *pilV* forward*:* 5′-CTCACTCTCATTGACTATGATCG-3′; *pilV* reverse, 5′-TCAGTATCCCACGATGGTTTG-3′. We obtained the PCR-amplified region of 444 bp of *pilV*.

The *pilV* mRNA was amplified using GoTaq DNA Polymerase (Promega, USA) according to the protocol provided by the manufacturer. The PCR cycling conditions were: Initial denaturation (95°C, 1 min), 35 cycles consisting of denaturation (95°C, 1 min), primer annealing (55°C, 1 min), and extension (72°C, 1:20 min); followed by a final extension step (72°C, 5 min). PCR products were analyzed by electrophoresis in 1% (w/v) agarose gels (Sigma, USA) and purified by gel extraction with the Wizard SV Gel kit and PCR Clean-Up system (Promega, USA).

Cloning of *pilV*

The purified *pilV* product of PCR was ligated into the pGEM-T Easy cloning vector (Promega, USA) at the following proportions: 5 µL of buffer ligation 2X, 1 µL of pGEM-T Easy vector, 1-3 µL of PCR product, 1 µL of T4 DNA ligase (Promega, USA), and DNAse-free water, incubated 1 h at room temperature. After ligation, the *E. coli* JM109 competent cells (Promega, USA) were transformed according to the protocol provided by the manufacturer. *E. coli* strains were inoculated at 37°C into Luria-Bertani (LB) medium supplemented with ampicillin (100 µg/mL; Sigma-Aldrich, USA), IPTG (Isopropylthio-β-D-galactoside) (0.5 mM; Invitrogen, USA) and X-Gal (5-bromo-4-chloro-3-indolyl-β-d-galactopyranoside) (50 µg/mL; Roche, Germany).

Minipreps of transformed cells were carried out using the QIAprep Spin Miniprep Kit (Qiagen, Germany), followed by sequencing analyses using the universal M13 primers of the pGEM-T Easy vector, to confirm the correct direction of *pilV* insertion. The sequences of the inserts were analyzed at LANBAMA (National Biotechnology Laboratory, IPICYT, México). The recombinant plasmid was named pGEM-*pilV*.

The pGEM-*pilV* and the pET-32b(+) vector (Novagen, USA) were digested with EcoRI (Invitrogen) at 37°C for 1 h and the enzyme was then inactivated by incubating at 65°C for

15 min; the resulting fragments were separated by electrophoresis in 1% (w/v) agarose gels and purified by gel extraction (Wizard SV Gel and PCR clean-up system; Promega, USA).

Subcloning the *pilV* fragment into pET-32b(+) expression vector

We chose pET-32b(+) as the expression vector because it provides a higher level of expression than other systems and because the proteins are fused with a thioredoxin (Trx) that favors protein solubility, avoiding the formation of inclusion bodies [38]. The *pilV* fragment was subcloned into the pET-32b(+) vector (Novagen, Germany) using T4 DNA ligase (Promega, USA) with an insert:vector ratio of 3:1; the reaction was carried out at room temperature for 1 h. The resulting pET32-*pilV* construct was sequenced for verification, and then transformed into *E. coli* Top10 (Invitrogen, USA) according to the manufacturer's protocol. The cells were incubated on ice for 30 min followed by a thermal shock in a water bath at 42°C for 30 s. The cells were then incubated at 37°C for 24 h in LB medium. The transformed cells were then collected and cultured in solid LB medium supplemented with ampicillin (50 µg/mL; Sigma-Aldrich, USA), at 37°C for 16 h. The pET32-*pilV* construct was extracted from the transformed cells by means of minipreps and digested with EcoRI as previously described. The presence, integrity, and orientation of the inserts were verified by PCR using the universal T7 primers and sequencing (LANBAMA, IPICYT, México). The correctly oriented clones were stored at -20°C until use.

PilV expression and purification

The fusion protein was expressed in *E. coli* BL21-CodonPlus (DE3) cells (Agilent Technologies, Inc. 2015) as follows: first, fresh bacterial colony harboring the recombinant vector was inoculated into 500 mL of LB medium with 100 µg/mL ampicillin, 75 µg/mL streptomycin and 34 µg/mL chloramphenicol and incubated at 37°C until it reached an absorbance of 0.8 at 600 nm (OD_{600}). Then the inductor (IPTG) was added to a final concentration of 1.0 mM; the culture was orbitally incubated at 16°C overnight, and lastly, the cells were harvested by centrifugation at 4200 ×g for 10 min [39] and the pellet was stored at -20°C until use.

Bacteria were resuspended in 30 mL of buffer A (50 mM HEPES pH 7.0, 100 mM NaCl and 0.1 mg/mL lysozyme) and disrupted by sonication (amplitude 50%; pulse on 15 s; pulse off 45 s). Soluble and insoluble fractions were separated by centrifugation at 15000 ×g for 30

min at 4°C and aliquots from the supernatant and pellet were used to determine recombinant protein expression by sodium dodecyl sulfate polyacrylamide gel electrophoresis (SDS-PAGE) using Coomassie brilliant blue (BioRad, Switzerland) for staining. The recombinant fusion protein was found in the insoluble fraction.

The insoluble fraction was resuspended in buffer B (20 mM Tris-HCl pH 8.0, 2% (v/v) Triton X-100 and 1 M urea) and stirred for 30 min, then centrifuged at 15000 ×g for 30 min at 4°C, recovering the fusion protein from the supernatant.

The His6 tagged fusion protein was purified by a one-step procedure. The supernatant was loaded onto a column with His60 Ni-Superflow resin (Takara, USA) equilibrated with buffer B. The column was washed with three column volumes (CVs) of buffer C (20 mM Tris-HCl pH 8.0, 2% Triton X-100 and 100 mM NaCl). Subsequently the column was washed extensively with buffer C supplemented with 20 mM imidazole. Elution of the recombinant protein was carried out in one step with three CVs of buffer C supplemented with 300 mM imidazole.

To verify protein expression and purification, SDS-PAGE was carried out with 12% acrylamide gels using established procedures [40].

Gels for western blot (WB) were transferred to 0.45 μm nitro-cellulose membrane (Bio-Rad, Switzerland) at 300 mA for 1 h. The membranes were blocked for 1 h in PBS 1× with 5% (w/v) non-fat milk and 0.01% Tween 20, and then incubated at 4°C overnight with mouse 6x-His Tag (1:1000; Invitrogen, USA). After this, the membrane was washed (three times, each time for 10 min in agitation) with TBS 1× with 0.01% Tween 20, incubated with mouse Anti-His-HRP secondary antibody (1:5000; Invitrogen, USA) for 1 h, at room temperature and washed as previously described.

In order to obtain free PilV in solution, digestion was carried out with thrombin protease, for which we used recombinant thrombin from Sigma-Aldrich according to the manufacturer's instructions.

After digestion, the sample was desalted in 25 mM Tris pH 8.0, 150 mM NaCl, 2% Triton X-100, and applied to an anion exchange column (Pierce™ Strong Anion Exchange Spin Columns), which was extensively washed with the same buffer. Subsequently, the protein

was eluted with a buffer containing 25 mM Tris-HCl pH 8.0, 300 mM NaCl, and 2% CHAP. The protein was quantified by measuring absorbance at 280 nm, and it was stored at 4°C until further use.

Structure prediction and structure alignment analysis

For prediction of the PilV structures of *At. thiooxidans* ATCC 19377 and other bacteria (*Thermus thermophilus* HB27, *Pseudomonas aeruginosa* PAO1 and *Geobacter sulfurreducens* PCA), the AlphaFold2 program ColabFold V1.5.2 was used (https://alphafold.ebi.ac.uk/) following the instructions recommended by Jumper *et al.*, [41]. The complete amino acid sequence of pilins, including the propeptide, were submitted and analyzed with default parameters to run in each prediction. Using PilV structures obtained in PDB format generated by AlphaFold2, its structures as well as structure alignment analyses and the percent of similarity (two by two) were visualized and computed using UCSF Chimera 1.16 (www.cgl.ucsf.edu/chimera/) [42].

Disorder, secondary structure, and transmembrane topology prediction

Structural disorder was predicted using the PONDR® server (http://www.pondr.com/) [43], employing the VL-XT algorithm, PSIPRED (http://bioinf.cs.ucl.ac.uk/psipred/) [44], and DeepTMHMM (https://dtu.biolib.com/DeepTMHMM/) [45].

Protonation and deprotonation of PilV at different pH

The protonation status of acidic and basic residues in the PilV protein was analyzed using the PDB2PQR web server (https://server.poissonboltzmann.org/pdb2pqr). The PDB2PQR uses the PROPKA algorithm together with the PARSE force field to calculate the ionization state of the protein at specific pH values. So, the submitted PilV structure was modified by incorporating protons, which were added according to the ionization states of the titratable groups at pH 2, 3, 4, 5, 6, 7 and 8. The Protein-sol program [46] (https://protein-sol.manchester.ac.uk/) was used to evaluate the pH stability of PilV. This program computes the stability of the folded conformation and the charge characteristics of the proteins as pH varies. It employs the Debye-Hückel formula to determine the pKa, thus accounting for the pH-dependent impact on the stability of the folded state.

Molecular dynamics simulation

Molecular dynamics (MD) simulations of the different protonation states of PilV that had been generated were carried out using the WebGRO program, based on GROMACS (https://simlab.uams.edu/index.php). To assess the stability of PilV, four main parameters were evaluated: RMSD (root mean square deviation), RMSF (root mean square fluctuation), Rg (radius of gyration) and total number of hydrogen bonds. The force field used was GROMOS96 43a1. Simple Point Charge (SPC) was selected as the solvent model (triclinic water box). This system was neutralized by adding sodium or chlorine ions depending on the total charges. Protein energy minimizations were performed using the steepest descent method in the presence of solvent, with a maximum of 5000 steP. MD simulations were carried out in the presence of 0.15 M NaCl using a constant temperature (300 K) and pressure (1.0 bar). Approximately 1000 frames were generated each simulation. The simulation time was set to 50 ns.

pH-dependent PilV aggregation

To measure precipitation propensity, PilV was suspended in 10 mM sodium phosphate buffer at the specified pH. After centrifugation for 20 min at 20000 ×g, the absorbance at 280 nm was measured using a Nanodrop spectrophotometer. Samples were kept at room temperature between measurements. Extinction coefficients obtained from ExPASy ProtParam (https://web.expasy.org/protparam/) [47] were employed to convert absorbance into protein concentration.

Exposure of PilV to different pHs and denaturing conditions

The PilV protein was diluted to 5 μM using different buffers at various pH values (2.0, 3.6, 5.0, and 8.0) and equilibrated at room temperature. The following buffers (100 mM each) were used: glycine-HCl (pH 2.0), acetate (pH 3.6 and 5.0) and sodium phosphate buffer (pH 8.0).

A 5 μM PilV sample was diluted in 8 M urea and incubated at room temperature for 60 min. For heat denaturation, another 5 μM PilV sample was diluted in water and incubated at 90°C for 15 min.

Fluorescence spectroscopy

The fluorescence emission spectra of PilV (5 μM) at various pH levels and denaturing conditions were measured using a Cary Eclipse Fluorescence Spectrophotometer from Agilent Technologies in a quartz cuvette with a 1 cm path length. The samples were excited at 280 nm, and the fluorescence spectra were recorded within the range of 300–400 nm. Both the excitation and emission slit widths were fixed at 5 nm. The samples were incubated in the dark at room temperature for 5 min before recording the fluorescence emission spectra. All values are the mean of three independent measurements.

Results

Inserts obtained after cloning protocol

After cloning, the pGEM-*pilV* construct was transformed in *E. coli* JM109 cells. The recombinant plasmid was then extracted and analyzed, and the electrophoretic analysis showed fragments of 400 bp of pGEM-*pilV* (Fig. 11). The presence of the recombinant plasmid was confirmed a second time by PCR using M13 primers, amplifying the pGEM-*pilV*; we obtained a fragment of 800 bp (Fig. 11). Thus, cloning was successful and the construct was independently subcloned into the recombinant plasmid pET-32b(+).

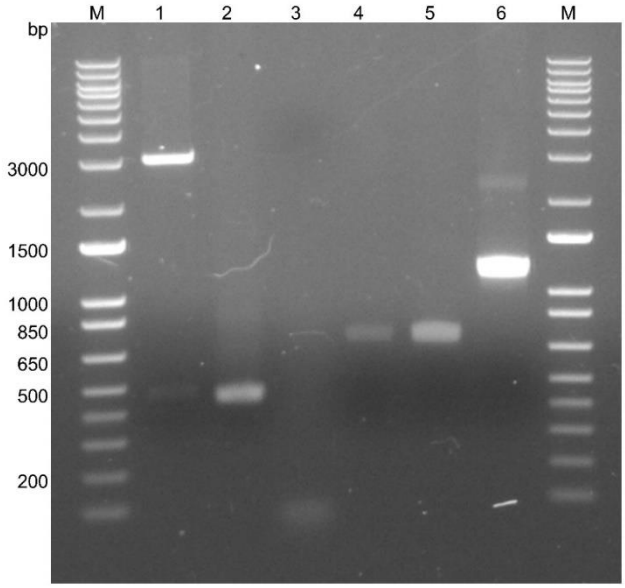

Figure 11. Gene cloning and expression construct. Lane 1: detection of pGEM-pilV of about 400 bp after digestion. Lane 2: pilV PCR as positive control (400 bp). Lane 3: Negative control. Lane 4: amplicon of pilV after PCR using M13 primers. Lane 5: amplicon of empty vector pET32b(+) (*ca.* 700 bp). Lane 6: amplicon of vector pET32b-pilV (ca. 1100 bp). M: molecular weight marker.

Subcloning *pilV* into pET-32b(+) expression vector

The *pilV* insert was subcloned into the expression vector pET-32b(+). Then the plasmid DNAs were extracted and purified (miniprep) and PCR were done using T7 primers. The gel analysis showed the corresponding bands of the plasmids with the pilins and of pET-32b(+) without any pilin insert (Fig. 11). Then the inserts were sequenced, and the obtained sequences were translated. Comparing the translated sequences of *pilV* from the corresponding plasmids with the reported GenBank sequence of PilV (AWP39907.1) confirmed that the mature proteins are identical (data not shown).

Expression and purification of PilV

Initially, attempts were made to express the PilV protein as a fusion protein together with the Trx protein in *E. coli* BL21 (DE3) strain; however, there was no correct expression of this despite changing different parameters (e.g., expression time, temperature, and inducer concentration; data not shown). So, we decided to analyze whether *pilV* had a "bias codon". This analysis showed us that *pilV* has 6 low-use codons that correspond to 3 prolines (CCC), 2 isoleucines (AUA), and one arginine (CGA). Considering this, we decided to use the *E. coli* BL21-CodonPlus (DE3)-RIPL cells, obtaining a correct expression of the fusion protein with an expected theoretical weight of 33 kDa (Fig. 12A).

The solubility tests indicated that the fusion protein is in the insoluble fraction, probably due to an interaction of the α-helix of the N-terminal region of PilV with the cell membrane since this α-helix is transmembranal according to the MEMSAT-SVM analysis from PSIPRED and DeepTMHMM. Therefore, we decided to use the Triton-X100 detergent at a percentage of 2% v/v, managing to solubilize the fusion protein (Fig. 12B), to then perform a nickel affinity chromatography, since the fusion protein has a 6x-His tag before the thrombin cleavage site between the Trx protein and PilV (Fig. 12C). The results show that in fractions 6-9, the fusion protein elutes at the expected molecular weight, which is confirmed by WB (Fig. 12D). These fractions were combined and desalted to be digested with thrombin protease and to have PilV without the Trx tag (Fig. 12E).

Using the thrombin assay at a concentration of at least 1 U/mL of sample, a good quantity of PilV can be obtained for its later purification.

A screening was conducted to determine the NaCl concentrations at which Trx does not bind but PilV does, resulting in 150 mM NaCl. Consequently, the protein sample was desalted into buffer (25 mM Tris-HCl pH 8.0, 150 mM NaCl, 2% Triton X-100) before washing the column with 25 mM Tris-HCl, 150 mM NaCl, 2% CHAPS, and finally the protein was eluted using the same buffer supplemented with 300 mM NaCl (Fig. 12F).

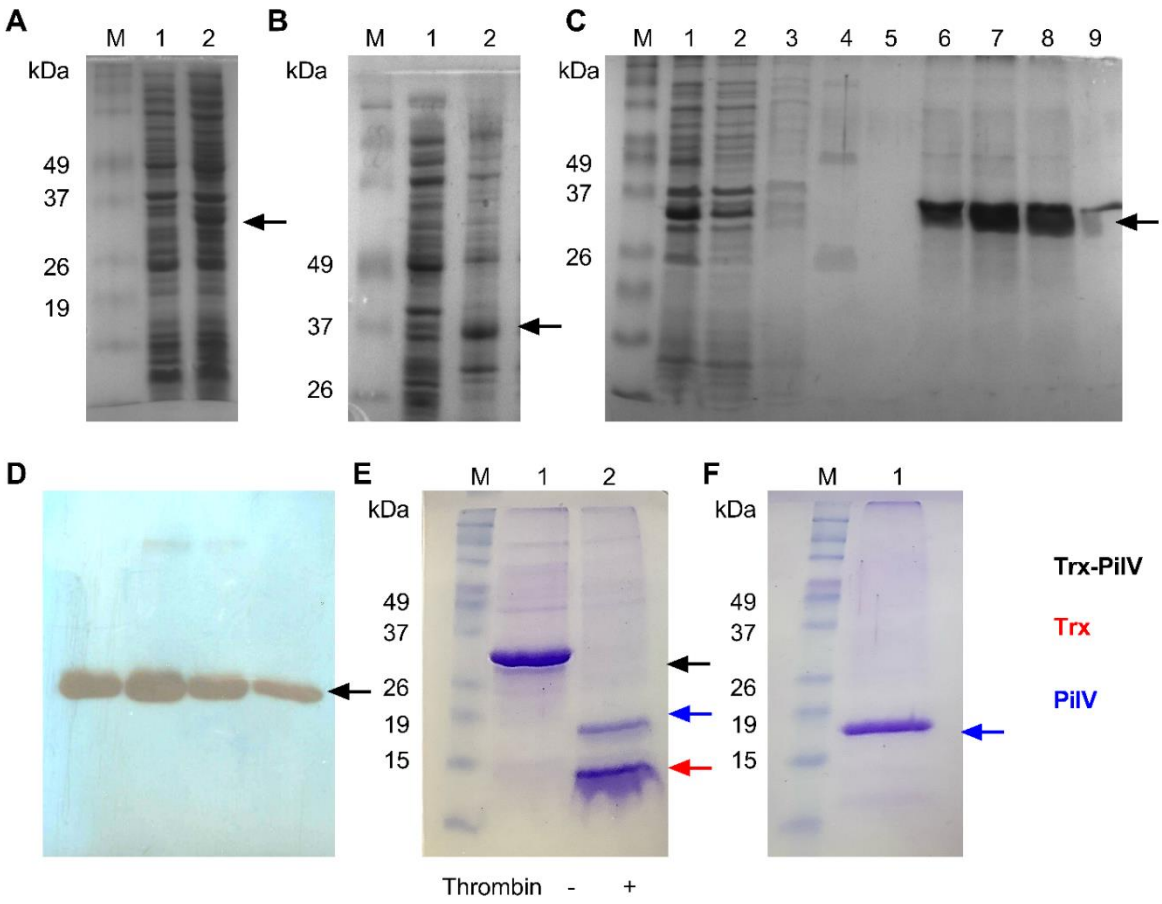

Figure 12. Expression and purification of PilV of *At. thiooxidans.* (**A**) Heterologous expression of PilV in *E. coli* BL21-CodonPlus (DE3)-RIPL with the pET32-*pilV* vector. M: molecular weight. Lane 1: protein profile before induction. Lane 2: protein profile after induction. (**B**) Solubilization of PilV with detergent. Lane 1: soluble fraction. Lane 2: fraction solubilized with detergent. (**C**) Purification of PilV by nickel affinity chromatography. Lane 1: solubilized fraction. Lane 2: unbound fraction. Lane 3: proteins eluted with buffer C. Lanes 4 and 5: protein eluted with buffer C supplemented with 10 mM imidazole. Lanes 6 to 9: proteins eluted with buffer C supplemented with 300 mM imidazole. (**D**) WB detection of fractions eluted with 300 mM imidazole. (**E**) Cleavage of the Trx-PilV fusion protein with thrombin protease. M: molecular weight. Lane 1: fusion protein without protease (-). Lanes 2: cleaved fusion protein after incubation with thrombin protease (+). Trx: 13.9 kDa and PilV: 19.2 kDa. (**F**) PilV protein obtained after purification by anion exchange chromatography. M: molecular weight. Lane 1: purified PilV.

Structural model of PilV of *At. thiooxidans*

The predicted structure of PilV of *At. thiooxidans* obtained using AlphaFolfd2 shows the typical characteristics of pilin: a hydrophobic α-helix of stick-like shape in its α1-N (Leu-13 to Gly-44), a less hydrophobic α1-C (Asn-45 to Phe-71), and β-sheets joined with head-like loops and two terminal cysteines (Cys-130 and Cys-132) flanking a putative D-region; these two Cys are very close (Figs. 13A and 13A') and hinder the formation of the typical C-terminal disulfide bond (Figs. 13B and 13C'). The C-terminal head-like structure includes the characteristic short αβ-loop (between α1-C and the first β-sheet) of amino acids (Asn-72 to Ala-115) (Fig. S1)**.**

Once the PilV model of *At. thiooxidans* was selected, we aligned the structure against the corresponding structures of *Th. thermophilus* HB27, *P. aeruginosa* PAO1 and *Ge. sulfurreducens*. The PilV of *At. thiooxidans* overlaps PilV of *P. aeruginosa* (Fig. 13C) and of *Ge. sulfurreducens* better, with which it has 15.92% identity (RMSD between 61 pruned atom pairs of 1.030 Å across all 153 pairs: 9.067) and 16.67% identity (RMSD between 78 pruned atom pairs of 0.889 Å; across all 130 pairs: 5.471) respectively. Interestingly, the alignment of PilV of *Ge. sulfurreducens* and *At. thiooxidans* shows a major identity and superposition in both the stick-like and head-like shape structures (Fig. 13D). The PilV of *At. thiooxidans* and *Th. thermophilus* showed the lowest identity and superposition, 7.64% (RMSD of 34 pruned atom pairs is 0.831 Å; across all 137 pairs: 18.501).

PilV behavior at different pH

To investigate the behavior of the protein at different pH values, it is necessary to evaluate the protonation state of the titratable groups under conditions in which the electrostatic environment changes. After obtaining the different states of protonation of PilV at pH 2, 3, 4, 5, 6, 7 and 8, molecular dynamics simulations were carried out for each pH at 300 K temperature (26.8°C).

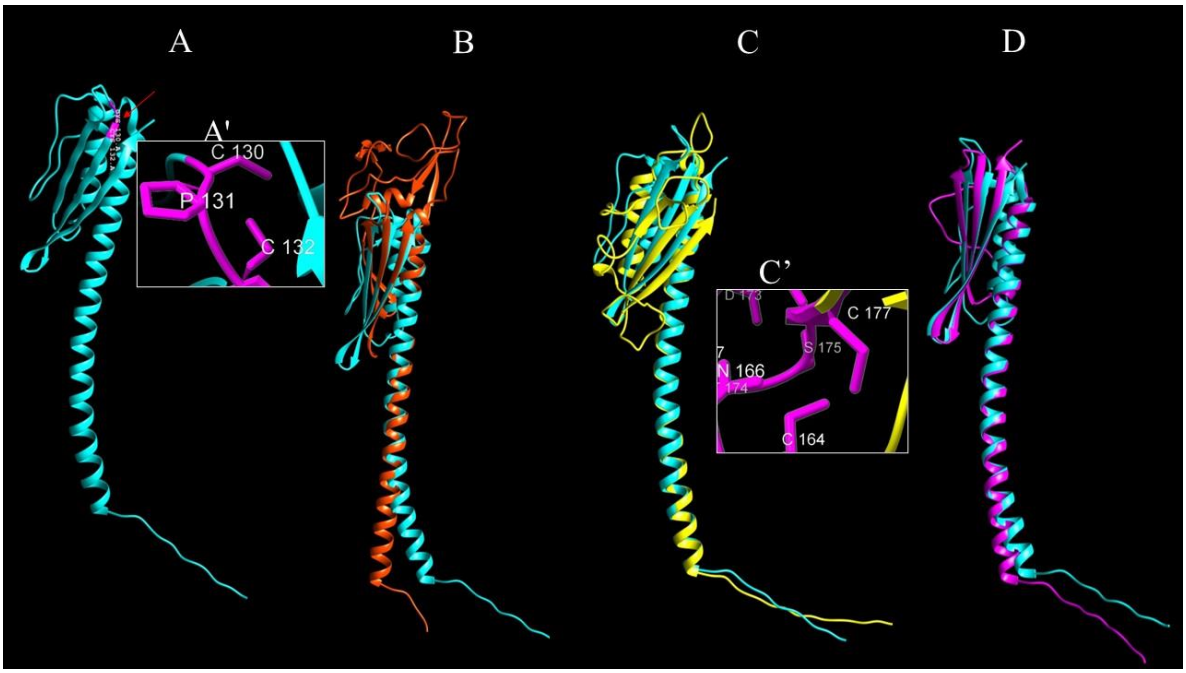

Figure 13. Predicted structure of PilV. (**A**) PilV of *At. thiooxidans* (cyan color) obtained by AlphaFold2 and compared through superposition with: (**B**) "prepilin-like protein" of *Th. thermophilus* HB27 (orange; GenBank: AAM55483.1); (**C**) "type 4 fimbrial biogenesis protein PilV" of *P. aeruginosa* PAO1 (yellow; NP_253241.1); (**C'**) shows its D-region, and (**D**) "type IV pilus minor pilin PilV" of *Ge. sulfurreducens* PCA (magenta; AAR34389.2). PilV structures were overlain (two by two) using UCSF Chimera. Red arrow in (**A**) indicates the putative D-region, amplified in (**A'**) to show the two Cys residues separated by Pro-131.

The RMSD for PilV indicates a deviation of 1 to 1.5 nm at all modeled pH, after 45 ns. These changes in the initial structure may be due to the fact that the hydrophobic N-terminal of PilV is exposed to the solvent, causing self-folding to decrease the contact area and exposure to the polar medium (Fig. 14A). This is verified in the RMSF graphs: the first 40 residues outside the globular domain of PilV have higher RMSF than the rest of the protein, due to the rate of fluctuations comparable at all the pH tested (Fig. 14B). In addition, it is observed that the region of residues 65-120, predicted as disordered, has a greater fluctuation rate.

The Rg analysis shows that PilV at different pH tends to compact (lower Rg), except at pH 5.0, where a small portion of the N-terminal folds in on itself. This analysis leads us to infer that PilV remains stable at different pH and shows resilience to pH changes (Fig. 14C). The number of intra-protein H-bonds, and therefore the stability of the protein in PilV, is maintained at the different pH, except for pH 5 (Fig. 14D).

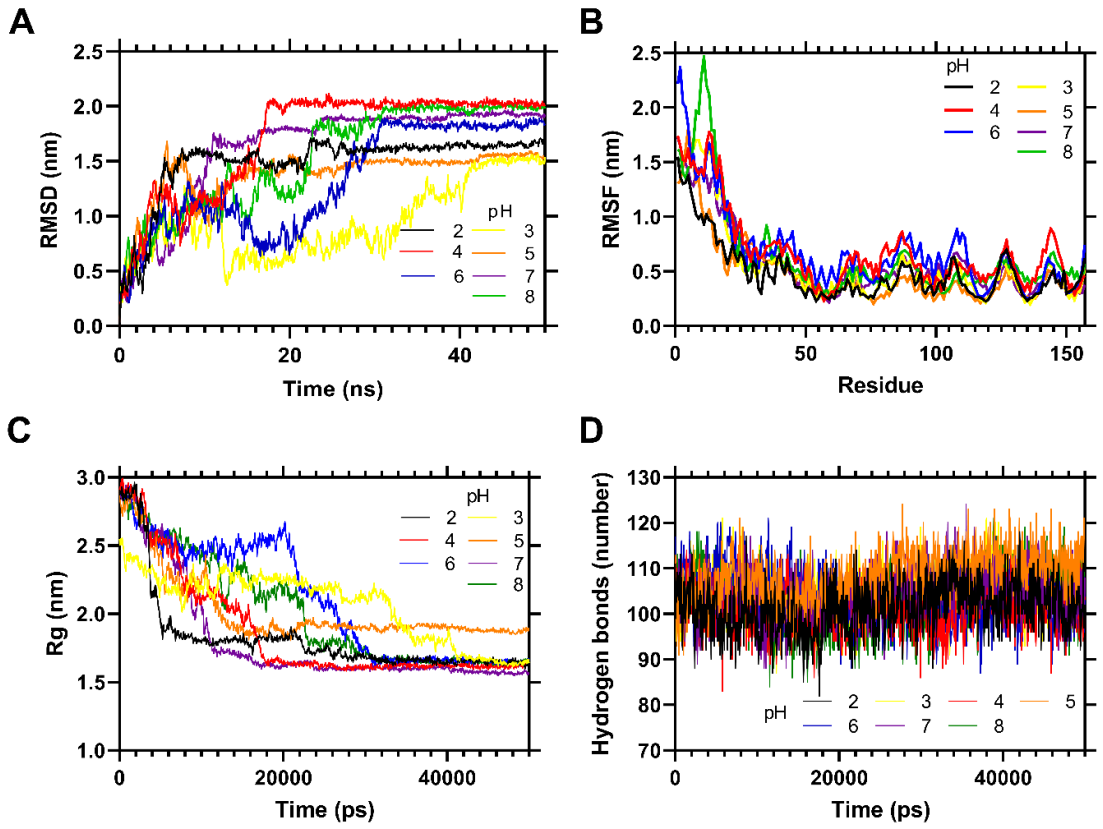

Figure 14. pH-MD simulations of PilV of *At. thiooxidans*. (**A**) RMSD. (**B**) RMSF. (**C**) Rg. (**D**) Hydrogen bond plot of PilV at different pH.

For a deeper understanding of the stability of PilV at different pH, surface electrostatics were analyzed *in silico*; the data were obtained with the APBS-PDB2PQR program. The surface charge of PilV remains homogeneous at different pH (Fig. 15A); it is observed with few regions that indicate ionizable groups, probably because this protein has 4 glutamic acid, 2 arginine and one lysine. The protein acquires little surface charge at pH <4.0 and remains neutral at pH >4.0 (Fig. 15B). Therefore, having low surface charge, it maintains structural integrity, even with different values of ionic strength (Fig. 15C). The pH that gives stability of the folded state show homogeneity.

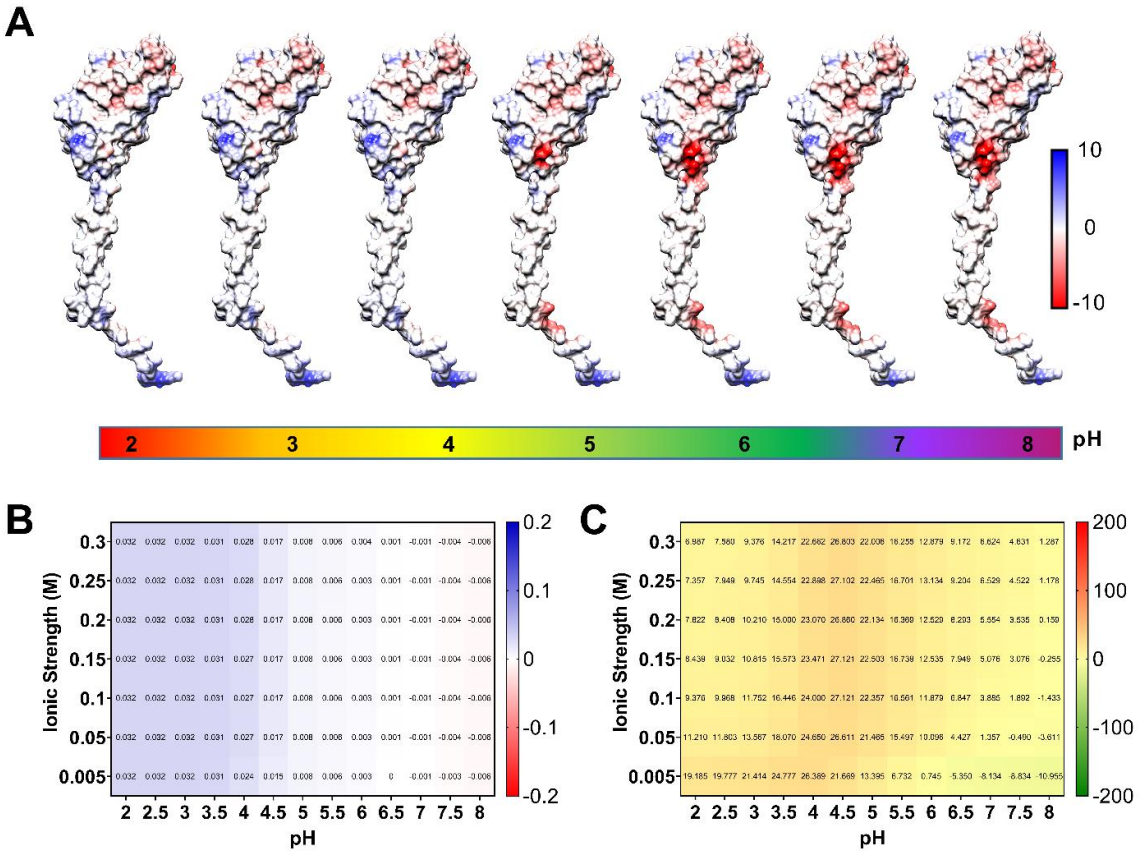

Figure 15. Computational characterization of PilV. (**A**) Visualization of the surface charge of PilV is achieved by incorporating amino acid protonation states calculated based on pH using PDB2PQR and APBS. (**B**) Heatmap of predicted average charge for PilV at different pH and ionic strengths. (**C**) Heatmap of predicted protein stability in the folded state, considering the interactions between ionizable head groups in J/residue for PilV at different pH and ionic strength values.

Considering that the results from molecular dynamics and folded state stability analyses demonstrate resilience to a range of pH values, we decided to experimentally assess these conditions. To do so, we evaluated the solubility of PilV at pH 2, 5, and 8 by monitoring the protein concentration over time through UV-Vis spectroscopy, measuring the absorbance at 280 nm. Following incubation of the recombinant PilV at a concentration of 1 mg/mL for a period of up to 24 h, we did not observe any precipitation, and the protein remained stable at pH 2, 5 and 8 (Fig. 16).

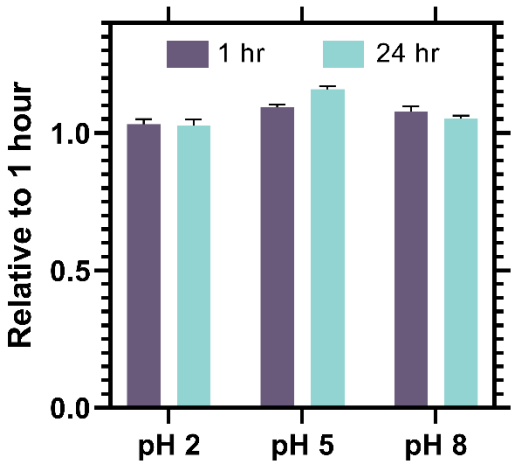

Figure 16. The precipitation behavior of PilV. The precipitation was examined by assessing its likelihood to form precipitates under three distinct pH conditions. The measurements were carried out in triplicate and then normalized to the average value obtained at the 1-hour mark. The initial protein concentration used was 1 mg/mL.

In conditions of extreme pH, the primary factor causing the protein to unfold is the repulsion between charged groups within the protein molecule, modifying salt bridges and hydrogen bonding formed between the side chains, leading to denaturation and subsequent aggregation and precipitation due to exposure of the hydrophobic core. For some proteins, the equilibrium between these internal repulsive forces and hydrophobic interactions (and potentially electrostatic disulfide cross-links and metal-protein interactions) is delicate enough that the protein may undergo partial unfolding or, in the most extreme scenarios, retain its folded structure [48]. So, if protein lacks charged amino acids, it may have fewer charged groups available for electrostatic interactions. As a result, the electrostatic repulsion within the protein may be reduced in extreme pH conditions. This reduction in charged groups could result in the equilibrium between repulsive and stabilizing forces shifting in favor of the latter.

Using intrinsic fluorescence to measure PilV stability upon different pH and denaturing conditions

Tryptophan fluorescence is commonly used to measure the stability of proteins by monitoring conformational changes. The fluorescence intensity and the maximum wavelength of tryptophan emission are used as signals to measure the stability of proteins. This method is particularly useful for monitoring the unfolding of proteins and can be employed to study the effect of pH and temperature on protein conformational changes [49].

Changes in the tertiary structure of PilV were monitored by analyzing changes in the intrinsic fluorescence emission. Intrinsic fluorescence spectra of PilV at different pH are shown in Fig. 17A. Regarding the maximum fluorescence intensity of PilV at different pH values, it was 330 nm for pH 3.6, 5, 8, and 333 nm for pH 2 indicating a characteristic feature of folded proteins (Fig. 17B). It's worth mentioning that the fluorescence intensity is very similar across the range of pH values, except for pH 5, which exhibits a slight decrease, but probably the microenvironment around aromatic residues was relative unchanged in different pH levels (Fig. 17A). To gain more insight into the structural stability of PilV, we denatured the protein with high concentration of urea (8 M) firstly, and then we incubated it at high temperature (90°C). For both conditions, the fluorescence spectrum shows a red shift with maximum intensities of 335 and 340 for urea and temperature, respectively (Fig. 17B), indicating that the tertiary structure of PilV destabilized due to unfolding (Fig. 17A). Remarkable, during denaturation with urea, there is an increase in fluorescence intensity, a phenomenon that has already been observed in other proteins, most likely due to the removal of other tryptophan quenching as the protein unfolds [50]. Finally, it is important to say that PilV has 2 tryptophan residues in its sequence [32].

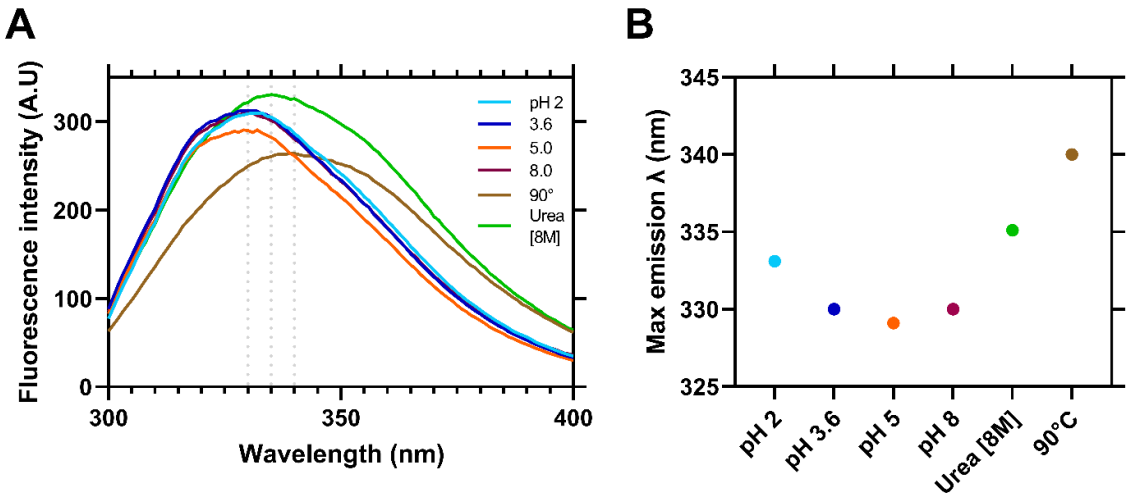

Figure 17. Intrinsic fluorescence spectra of PilV. (A) Emission spectra pf PilV at different pH and denaturing condition (chaotropic agent and high temperature, separately). An excitation wavelength of 280 nm was used and monitored emission in the range of 300-400 nm. (B) Max emission λ plotted with respect to pH and denaturing conditions.

Discussion

Seminal reports about T4P have been based on studies only in mesophile and pathogenic bacteria such as *P. aeruginosa*, by studying the homolog expression of the pilins. Although the homologous expression has many technical complications and flats. It is easier to analyze than heterologous T4P of bacteria from extreme natural environments. Understanding of the latter remains poor because it is more difficult to find culture media and suitable conditions. Heterologous expression is therefore the best option for characterizing extremophiles. However, it is crucial to be mindful of the inherent challenges associated with this approach, including protein stability, folding, and functional assays in non-native hosts.

In this work we present the methodology developed to achieve heterologous expression and acquire pure PilV, as well as the results obtained. Various methodologies were followed and some vector expression systems were assayed, namely the two-step cloning that enables the construct pGEM-*pilV* to be independently subcloned into the recombinant plasmid pET-32b(+).

Improving yields is an important issue in the production of recombinant proteins. One of the determining factors is the incubation temperature; we observed that low temperature yields certain advantages such as obtaining a soluble recombinant protein, avoiding the formation of inclusion bodies. This significantly improves protein quality, as was previously observed by Mühlmann *et al.,* [51] and Bartolo-Aguilar *et al.,* [52]. Our results show that PilV is better expressed at 16°C; despite also being expressed at 37°C, we chose to express PilV at the lower temperature to obtain a well-folded protein.

We succeeded in standardizing the appropriate purification technique for PilV protein, obtaining a yield of 2.0 mg of solubilized protein in a liter of culture after 2 purification steP. Pilin PilV was expressed mainly in the insoluble fraction and recovery after detergent solubilization, likely because an interaction between the hydrophobic α-helix of the N-terminal of PilV and the bacterial membrane is broken: PilV can be considered a transiently peripheral protein, as pilus assembly involves the transport of pilins through the membrane; first, pilin precursors present in the cytoplasm are transported to the outer membrane through the SecA translocon [53], then peripheral membrane protein can associate with the membrane in a variety of ways. For example, the mitochondrial enzyme dihydroorotate dehydrogenase

(DHODH) has an N-terminal transmembrane helix to ensure correct orientation of the substrate binding site towards the membrane; of these, DHODH requires detergent micelles to stabilize it before further experimental characterization such as native mass spectrometry [54].

The expression and purification of PilV of *At. thiooxidans* enables techniques such as protein crystallization to be developed, to expand knowledge about this pilin; e.g., to elucidate its structure and function. However, currently the use of simulations is transforming molecular research through modeling systems for the initial approach. Thanks to this, it is possible to advance in molecular characterization and subsequently recreate experiments to validate the predicted characteristics. Consequently, and since our cloning was successful (Fig. 11), we decided to model the PilV sequence using a structure approach to seek homology between the PilV of *At. thiooxidans* and three other distant taxa, taking advantage of the powerful tool AlphaFold2 to make predictions of protein structure [41] since pilins share a similar basic modular structure (Figs. 13A and 13D). Our predicted model of PilV of *At. thiooxidans* resulted in such a "lollipop-like" structure, confirming that the predicted structure is like other pilins (Fig. 13).

We aligned the structure of *At. thiooxidans* PilV with the corresponding PilV of two classes of Proteobacteria, the Gammaproteobacteria *P. aeruginosa* and the Deltaproteobacteria *Ge. sulfurreducens*; we also compared it with PilV of the extremophile *Th. thermophilus*, phylum Deinococcus-Thermus. The selected species have the PilV domains known as extracellular T4P pilus assembly proteins involved in cell motility [55] as minor pilins [56]. Despite the existence of variable regions, the PilV model of *At. thiooxidans* and the selected species confirm the canonical basic architecture of T4P pilins. The primary structure of the compared PilV proteins have low similarity, $\leq$16.67%; nevertheless, the results of superimposed PilV structures or tertiary structure (Fig. 13) exhibit a greater overlap along the N-terminal α-helix, with the lowest identity because of the variable regions beyond the first 25 amino acids, commonly observed in evolutionarily distant species [5].

It is known that the greatest structural difference in the minor pilins is the versatile αβ-loop region that connects the α1-C helix to the β-sheet, as well as the D-region or the disulfide-bonded loop enclosed by the C-terminal disulfide bond that is found in some species [7] (Fig.

13C'). Disorder analysis shows that the entire αβ-loop region is located precisely at the peak of the most disordered region of PilV of *At. thiooxidans*, but it could transition into an ordered state [32]. Additionally, it has been observed that the αβ-loop is involved in the proper assembly of pilins and exhibits a slow structural dynamic (μs to ms) [57], suggesting its role in protein-protein interactions. In both major and minor pilins, the D-region typically consists of 10 to 20 amino acids forming a loop (Fig. 13) [6]. It is proposed that this contributes to the structural stability of the globular domain, and it is often found connected to the last β-sheet of the tail [58], stabilizing the interactions between structural pilins [59] or exposed for surface binding and pilus assembly [60]. It should be noted that these disulfide bridges are disrupted under reducing conditions, leading to the rapid disintegration of the pilus structure [61].

Surprisingly, although PilV of *At. thiooxidans* possesses two Cys in its C-terminal, they do not form a disulfide bond with each other due to their close position (130 and 132) and the presence of a Pro residue between them (Pro131; Fig. 13A'). When two consecutive Cys residues are separated by a Pro residue, it can lead to the formation of a small disulfide loop, but the formation of a disulfide in Cys-Cys requires prior formation of an unfavorable *cis* peptide bond between the cysteines, and prolines have only limited ability to adopt the *cis* configuration [62]. Like PilV of *At. thiooxidans*, the PilV of *Ge. sulfurreducens* do not show a D-region, while the PilV of *P. aeruginosa* and *Th. thermophilus* do have D-region (Cys164 to Cys177 and Cys170 to Cys185, respectively), forming a disulfide bond. These results confirm that the D-region in minor pilins is variable and not always present [6]. Similar to FimA of *D. nodosus*, in our PilV model we found two hydrogen bonds joined to the last β-sheet with Cys 130 (data not shown) [63]. This could imply that hydrogen bonds are responsible for the intermolecular interactions.

Considering this information, we can assume that disulfide bonds are not formed in D-region between the two cysteines of PilV of *At. thiooxidans* but rather with the cysteines of another minor pilin (PilW, PilX or PilY1) or that they serve as a surface sensor or complex because D-region is exposed to the surface; e.g., a divalent metal of metal sulfide such as pyrite (FeS_2) forming a Cys-S-Fe complex as suggested by Rojas-Chapana and Tributsch [64]. Moreover,

according to Ye *et al.,* [65] the electron transferred is through the disulfide bridges, promoting the transfer of S species to the sulfur-oxidant bacteria.

Previously we reported that the pili of *At. thiooxidans* exhibit characteristics that would make them resilient to changes in pH and reducing environments [32]. Here, specifically for the PilV pilin, we evaluated specific regions of the tertiary structure that are known to be in contact with the external environment. In the case of the segment corresponding to the αβ-loop (from Asn-72 to Ala-115), we found that compared to the same region of PilV in *P. aeruginosa*, the degree of intrinsic disorder has opposite values. The αβ-loop of *At. thiooxidans* shows a high tendency towards disorder, whereas that of *P. aeruginosa* shows a strong tendency towards order. For the case of the same region of PilV in *Th. thermophilus*, something very similar occurs in the central structure of the loop; however, at the ends, a pronounced tendency toward disorder is observed. In the case of PilV of *Ge. sulfurreducens*, due to the size of their αβ-loop (24 amino acids) it is not possible to determine a disorder region, however the middle αβ-loop region shows a tendency to disorder (Fig. S2). For the αβ-loop segments in particular, these results confirm our previously reported data [32].

We have proposed a model by which the extracellular pilins of *At. thiooxidans* can maintain their stability and functionality at different pH to which pilins are exposed (from their synthesis in the cytoplasm to their incorporation into the pili and coming into contact with the extracellular medium). Until the present study, the effect of pH on the minor pilins had not been investigated nor, to the best of our knowledge, has any previous computational study investigated the behavior of PilV at different pH. Here, the computational characterization was performed using molecular dynamics, and the analysis revealed the stability of PilV at different pH. Other proteins become unstable to changes of pH due to ionizable side chains and Coulomb repulsion between the polar groups of the charged heads of amino acids (e.g., Asp, Glu, His, Lys, and Arg) [66–68]. Analysis of the amino acid composition of PilV of *At. thiooxidans* indicates a significant decrease in charged amino acids, which most likely confers acid stability. Indeed, the electrostatic repulsion between residues with the same charge is one of the main factors affecting protein structure, stability, and function [69–71].

If we observe the surface charge at different pH values, we notice that overall PilV maintains a low net charge and very similar values for the stability of the folded state. We did not carry

out further analyses under more basic pH. These predictions were initially confirmed by measuring the protein's tendency to precipitate, which indicated that it remains soluble even with significant changes of pH (Fig. 16). Further biophysical characterization using intrinsic tryptophan fluorescence provides information about the local microenvironment of the tryptophan residue, which responds very sensitively to any change in the protein's tertiary structure. The maximum fluorescent intensity of PilV at different pH values is around 330 nm, suggesting that this residue stays in a hydrophobic environment. There is only a red shift when the protein is exposed to a high concentration of urea or when it is incubated at a high temperature, indicating that the tryptophan residues' microenvironment changes from a non-polar to a solvent-exposed environment during the unfolding of the protein.

In summary, despite the existence of various methods of protein cloning and purification, few reports have been published on acidophilic chemolithoautotrophs, which are of interest due to their extracellular protein present in protonated microenvironments that do not resemble heterologous organism such as *E. coli*. We proposed such method for cloning and heterologous expression. To date, there have been very few reports in the literature reporting the study of pilins from non-pathogenic bacteria. It is crucial to begin characterizing pilins from different organisms, as they can provide us with guidance for applying their key adaptability characteristics in various conditions. As demonstrated by our study of pilin PilV, we suggest that due to its unique amino acid composition, it exhibits acid stability, which could have significant implications in medicine and in biotechnology such as bioleaching of sulfide mineral. For instance, identifying stabilizing substitutions; some proteins may find stabilizing amino acid substitutions by comparing their sequences with homologs from acidophilic microorganisms. A bioinformatics approach makes it possible to explore experimental conditions that close the gap and guide the characterization toward realistic achievements.

References Chapter III

1. Pelicic V. 2008. Type IV pili: *e pluribus unum*? *Mol. Microbiol.* 68: 827–837. doi:10.1111/j.1365-2958.2008.06197.x
2. Gerven N, Waksman G, Remaut H. 2011. Pili and flagella: biology, structure, and biotechnological applications. *Prog. Mol. Biol. Transl. Sci* 103: 21-72. doi:10.1016/B978-0-12-415906-8.00005-4.
3. Conrad JC. 2012. Physics of bacterial near-surface motility using flagella and type IV pili: implications for biofilm formation. *Res. Microbiol.* 163: 619–629. doi:10.1016/j.resmic.2012.10.016
4. Craig L, Forest KT, Maier B. 2019. Type IV pili: dynamics, biophysics and functional consequences. *Nat. Rev. Microbiol.* 17: 429–440. doi:10.1038/s41579-019-0195-4
5. Craig L, Li J. 2008. Type IV pili: paradoxes in form and function. *Curr. Opin. Struct. Biol.* 18: 267–277. doi:10.1016/j.sbi.2007.12.009
6. Jacobsen T, Bardiaux B, Francetic O, Izadi-Pruneyre N, Nilges M. 2020. Structure and function of minor pilins of type IV pili. *Med. Microbiol. Immunol.* 209: 301–308. doi:10.1007/s00430-019-00642-5
7. Helaine S, Dyer DH, Nassif X, Pelicic V, Forest KT. 2007. 3D structure/function analysis of PilX reveals how minor pilins can modulate the virulence properties of type IV pili. *Proc. Natl. Acad. Sci. USA* 104: 15888–15893. doi:10.1073/pnas.0707581104
8. Maier B, Potter L, So M, Seifert HS, Sheetz MP. 2002. Single pilus motor forces exceed 100 pN. *Proc. Natl. Acad. Sci. USA* 99: 16012–16017. doi:10.1073/pnas.242523299
9. Berry JL, Pelicic V. 2015. Exceptionally widespread nanomachines composed of type IV pilins: the prokaryotic Swiss Army knives. *FEMS Microbiol. Rev.* 39: 134-154. doi: 10.1093/femsre/fuu001
10. Singhi D, Srivastava P. 2020. Role of bacterial cytoskeleton and other apparatuses in cell communication. *Front. Mol. Biosci.* 7: 158. doi:10.3389/fmolb.2020.00158
11. Li Y, Huang S, Zhang X, Huang T, Li H. 2013. Cloning, expression, and functional analysis of molecular motor pilT and pilU genes of type IV pili in *Acidithiobacillus*

ferrooxidans. *Appl. Microbiol. Biotechnol.* 97: 1251–1257. doi:10.1007/s00253-012-4271-1

12. Tu B, Wang F, Li J, Sha J, Lu X, Han X. 2013. Analysis of genes and proteins in *Acidithiobacillus ferrooxidans* during growth and attachment on pyrite under different conditions. *Geomicrobiol. J.* 30: 255–267. doi:10.1080/01490451.2012.668608
13. Li Y, Li H. 2014. Type IV pili of *Acidithiobacillus ferrooxidans* can transfer electrons from extracellular electron donors. *J. Basic Microbiol.* 54: 226–231. doi:10.1002/jobm.201200300
14. Malvankar NS, Lovley DR. 2014. Microbial nanowires for bioenergy applications. *Curr. Opin. Biotechnol.* 27: 88–95. doi:10.1016/j.copbio.2013.12.003
15. Piepenbrink KH. 2019. DNA uptake by type IV filaments. *Front. Mol. Biosci.* 6: 1. doi:10.3389/fmolb.2019.00001
16. Lukaszczyk M, Pradhan B, Remaut H. 2019. The biosynthesis and structures of bacterial pili, pp 369–413. In Kuhn A (ed.), *Bacterial Cell Walls and Membranes*. Springer, Cham. doi:10.1007/978-3-030-18768-2_12
17. Raynaud C. 2021. Understanding type IV pili mediated adhesion in *Streptococcus sanguinis*. PhD Dissertation. Imperial College, London. doi:10.25560/92922
18. Valdés J, Pedroso I, Quatrini R, Dodson RJ, Tettelin H, Blake R, Eisen JA, Holmes DS. 2008. *Acidithiobacillus ferrooxidans* metabolism: From genome sequence to industrial applications. *BMC Genomics* 9: 597. doi:10.1186/1471-2164-9-597
19. Díaz- Beneventi M, Castro M, Copaja-Castillo S, Guiliani-Guerin N. 2018. Biofilm formation by the acidophile bacterium *Acidithiobacillus thiooxidans* Involves c-di-GMP Pathway and Pel exopolysaccharide. *Genes* 9: 113. doi:10.3390/genes9020113
20. Alfaro-Saldaña E, Hernández-Sánchez A, Araceli Patrón-Soberano OA, Astello-García M, Méndez-Cabañas JA, García-Meza JV. 2019. Sequence analysis and confirmation of the type IV pili-associated proteins PilY1, PilW and PilV in *Acidithiobacillus thiooxidans*. *PLoS ONE* 14(1): e.0199854. doi:10.1371/journal.pone.0199854

21. Giltner CL, Habash M, Burrows LL. 2010. *Pseudomonas aeruginosa* minor pilins are incorporated into type iv pili. *J. Mol. Biol.* 398: 444–461. doi:10.1016/j.jmb.2010.03.028
22. Hospenthal MK, Costa TRD, Waksman G. 2017. A comprehensive guide to pilus biogenesis in Gram-negative bacteria. *Nat. Rev. Microbiol.* 15: 365–379. doi:10.1038/nrmicro.2017.40
23. Bardy SL, Ng SYM, Jarrell KF. 2003. Prokaryotic motility structures. *Microbiol.* 149: 295–304. doi:10.1099/mic.0.25948-0
24. Linhartová M, Skotnicová P, Hakkila K, Tichý M, Komenda J, Knoppová J, Gilabert JF, Guallar V, Tyystjärvi T, Sobotka R. 2021. Mutations suppressing the lack of prepilin peptidase provide insights into the maturation of the major pilin protein in cyanobacteria. *Front. Microbiol.* 12: 756912. doi:10.3389/fmicb.2021.756912
25. García-Meza JV, Fernández JJ, Lara RH, González I. 2013. Changes in biofilm structure during the colonization of chalcopyrite by *Acidithiobacillus thiooxidans*. *Appl. Microbiol. Biotechnol.* 97: 6065–6075. doi:10.1007/s00253-012-4420-6
26. Yang L, Zhao D, Yang J, Wang W, Chen P, Zhang S, Yan L. 2019. *Acidithiobacillus thiooxidans* and its potential application. *Appl. Microbiol. Biotechnol. 2019 10319* 103: 7819–7833. doi:10.1007/s00253-019-10098-5
27. Alm RA, Mattick JS. 1997. Genes involved in the biogenesis and function of type-4 fimbriae in *Pseudomonas aeruginosa*. *Gene* 192: 89–98. doi:10.1016/S0378-1119(96)00805-0
28. Nguyen Y, Sugiman-Marangos S, Harvey H, Bell SD, Charlton CL, Junop MS, Burrows LL. 2015. *Pseudomonas aeruginosa* minor pilins prime type iva pilus assembly and promote surface display of the PilY1 adhesin. *J. Biol. Chem.* 290: 601–611. doi:10.1074/jbc.M114.616904
29. McCallum M, Burrows LL, Howell PL. 2019. The dynamic structures of the type iv pilus. *Microbiol. Spectr.* 7: 10-1128. doi:10.1128/microbiolspec.PSIB-0006-2018
30. Craig L, Pique ME, Tainer JA. 2004. Type IV pilus structure and bacterial pathogenicity. *Nat. Rev. Microbiol.* 2: 363–378. doi:10.1038/nrmicro885

31. Tang D, Gao Q, Zhao Y, Li Y, Chen P, Zhou J, Xu R, Wu Z, Xu Y, Li H. 2018. Mg^{2+} reduces biofilm quantity in *Acidithiobacillus ferrooxidans* through inhibiting Type IV pili formation. *FEMS Microbiol. Lett.* 365: fnx266. doi:10.1093/femsle/fnx266
32. Páez-Pérez ED, Hernández-Sánchez A, Alfaro-Saldaña E, García-Meza JV. 2023. Disorder and amino acid composition in proteins: their potential role in the adaptation of extracellular pilins to the acidic media, where *Acidithiobacillus thiooxidans* grows. *Extremophiles* 27: 31. doi: 10.1007/s00792-023-01317-z
33. Feng S, Li K, Huang Z, Tong Y, Yang H. 2019. Specific mechanism of A*cidithiobacillus caldus* extracellular polymeric substances in the bioleaching of copper-bearing sulfide ore. PLoS ONE. 14:e0213945. doi:10.1371/journal.pone.0213945
34. Boase K, González C, Vergara E, Neira G, Holmes D, Watkin E. 2022. Prediction and inferred evolution of acid tolerance genes in the biotechnologically important *Acidihalobacter* genus. *Front. Microbiol*. 13: 848410. doi:10.3389/fmicb.2022.848410
35. González-Rosales C, Vergara E, Dopson M, Valdés JH, Holmes DS. 2021. Integrative genomics sheds light on evolutionary forces shaping the *Acidithiobacillia* class acidophilic lifestyle. *Front. Microbiol*. 12: 822229. doi:10.3389/fmicb.2021.822229
36. Wang F, Baquero DP, Su Z, Beltran LC, Prangishvili D, Krupovic M, Egelman EH. 2020. The structures of two archaeal type IV pili illuminate evolutionary relationshiP. *Nat. Commun*. 11: 3424. doi:10.1038/s41467-020-17268-4
37. Flores-Ríos R, Moya-Beltrán A, Pareja-Barrueto C, Arenas-Salinas M, Valenzuela S, Orellana O, Quatrini R. 2019. The type IV secretion system of ICEAfe1: Formation of a conjugative pilus in *Acidithiobacillus ferrooxidans*. *Front. Microbiol*. 10: 30. doi:10.3389/fmicb.2019.00030
38. LaVallie ER, DiBlasio EA, Kovacic S, Grant KL, Schendel PF, McCoy JM. 1993. A thioredoxin gene fusion expression system that circumvents inclusion body formation in the *E. coli* cytoplasm. *Nat. Biotechnol.* 11: 187–193. doi:10.1038/nbt0293-187
39. Liu ZQ, Yang PC. 2012. Construction of pET-32 α (+) vector for protein expression and purification. *N. Am. J. Med. Sci.* 4: 651-655. doi:10.4103/1947-2714.104318

40. Laemmli UK. 1970. Cleavage of structural proteins during the assembly of the head of bacteriophage T4. *Nature* 227: 680–685. doi:10.1038/227680a0
41. Jumper J, Evans R, Pritzel A, Green T, Figurnov M, Ronneberger O, *et al.*, 2021. Highly accurate protein structure prediction with AlphaFold. *Nat.* 596: 583–589. doi:10.1038/s41586-021-03819-2
42. Pettersen EF, Goddard TD, Huang CC, Couch GS, Greenblatt DM, Meng EC, Ferrin TE. 2004. UCSF Chimera-a visualization system for exploratory research and analysis. *J. Comput. Chem.* 25: 1605–1612. doi:10.1002/jcc.20084
43. Xue B, Dunbrack RL, Williams RW, Dunker AK, Uversky VN. 2010. PONDR-FIT: A meta-predictor of intrinsically disordered amino acids. *Biochim. Biophys. Acta - Proteins Proteom.* 1804: 996–1010. doi:10.1016/j.bbapap.2010.01.011
44. McGuffin LJ, Bryson K, Jones DT. 2000. The PSIPRED protein structure prediction server. *Bioinformatics* 16: 404–405. doi:10.1093/bioinformatics/16.4.404
45. Hallgren J, Tsirigos KD, Damgaard Pedersen M, Juan J, Armenteros A, Marcatili P, Nielsen H, Krogh A, Winther O. 2022. DeepTMHMM predicts alpha and beta transmembrane proteins using deep neural networks. *bioRxiv*. 2022.04.08.487609 doi:10.1101/2022.04.08.487609
46. Hebditch M, Warwicker J. 2019. Web-based display of protein surface and pH-dependent properties for assessing the developability of biotherapeutics. *Sci. Rep.* 9: 1969. doi:10.1038/s41598-018-36950-8
47. Gasteiger E, Hoogland C, Gattiker A, Duvaud S, Wilkins MR, Appel RD, Bairoch A. 2005. Protein identification and analysis tools on the ExPASy server, pp 571–607. *In* Walker JM (ed.), *The Proteomics Protocols Handbook*. Springer Berlin. doi:10.1385/1-59259-890-0:571
48. Fink AL, Calciano LJ, Goto Y, Kurotsu T, Palleros DR. 1994. Classification of acid denaturation of proteins: intermediates and unfolded states. *Biochemistry* 33: 12504–12511. doi: 10.1021/bi00207a018
49. Almutairi GO, Malik A, Alonazi M, Khan JM, Alhomida AS, Khan MS, Alenad AM, Altwaijry N, Alafaleq NO. 2022. Expression, purification, and biophysical characterization of recombinant MERS-CoV main (Mpro) protease. *Int. J. Biol. Macromol*. 209: 984–990. doi: 10.1016/j.ijbiomac.2022.04.077

50. Jazaj D, Ghadami SA, Bemporad F, Chiti F. 2019. Probing conformational changes of monomeric transthyretin with second derivative fluorescence. *Sci. Rep*. 9: 10988. doi: 10.1038/s41598-019-47230-4
51. Mühlmann M, Forsten E, Noack S, Büchs J. 2017. Optimizing recombinant protein expression via automated induction profiling in microtiter plates at different temperatures. *Microb. Cell Fact.* 16: 220. doi:10.1186/s12934-017-0832-4
52. Bartolo-Aguilar Y, Chávez-Cabrera C, Flores-Cotera LB, Badillo-Corona JA, Oliver-Salvador C, Marsch R. 2022. The potential of cold-shock promoters for the expression of recombinant proteins in microbes and mammalian cells. *J. Genet. Eng. Biotechnol.* 20: 173. doi: 10.1186/s43141-022-00455-9
53. Shanmugasundarasamy T, Karaiyagowder Govindarajan D, Kandaswamy K. 2022. A review on pilus assembly mechanisms in Gram-positive and Gram-negative bacteria. *Cell Surf.* 8: 100077. doi:10.1016/j.tcsw.2022.100077.
54. Sahin C, Reid DJ, Marty MT, Landreh M. 2020. Scratching the surface: native mass spectrometry of peripheral membrane protein complexes. *Biochem. Soc. Trans.* 48: 547–558. doi:10.1042/BST20190787
55. Marchler-Bauer A, Bo Y, Han L, He J, Lanczycki CJ, Lu S, Chitsaz F, Derbyshire MK, Geer RC, Gonzales NR, Gwadz M, Hurwitz DI, Lu F, Marchler GH, Song JS, Thanki N, Wang Z, Yamashita RA, Zhang D, Zheng Ch, Lewis YG, Bryant SH. 2017. CDD/SPARCLE: functional classification of proteins via subfamily domain architectures. *Nucleic Acids Res.* 45(D): 200-3. doi:10.1093/nar/gkw1129
56. Holmes DE, Dang Y, Walker DJF, Lovley DR. 2016. The electrically conductive pili of *Geobacter* species are a recently evolved feature for extracellular electron transfer. *Microb. Genom*. 2(8): e000072. doi:10.1099/mgen.0.000072
57. Nguyen Y, Boulton S, McNicholl ET, Akimoto M, Harvey H, Aidoo F, Melacini G, Burrows LL. 2018. A highly dynamic loop of the *Pseudomonas aeruginosa* PA14 type IV pilin is essential for pilus assembly. *ACS Infect. Dis.* 4: 936–943. doi:10.1021/acsinfecdis.7b00229
58. Giltner CL, Nguyen Y, Burrows LL. 2012. Type IV pilin proteins: versatile molecular modules. *Microbiol. Mol. Biol. Rev.* 76: 740–772. doi:10.1128/MMBR.00035-12

59. Harvey H, Habash M, Aidoo F, Burrows LL. 2009. Single-residue changes in the c-terminal disulfide-bonded loop of the *Pseudomonas aeruginosa* type IV pilin influence pilus assembly and twitching motility. *J. Bacteriol.* 191: 6513–6524. doi:10.1128/JB.00943-09
60. Lee KK, Sheth HB, Wong WY, Sherburne R, Paranchych W, Hodges RS, Lingwood CA, Krivan H, Irvin RT. 1994. The binding of *Pseudomonas aeruginosa* pili to glycosphingolipids is a tip-associated event involving the C-terminal region of the structural pilin subunit. *Mol. Microbiol.* 11: 705–713. doi:10.1111/j.1365-2958.1994.tb00348.x.
61. Li J, Egelman EH, Craig L. 2012. Structure of the *Vibrio cholerae* type IVb pilus and stability comparison with the *Neisseria gonorrhoeae* type IVa pilus. *J. Mol. Biol.* 418: 47–64. doi:10.1016/j.jmb.2012.02.017
62. Zhang RM, Snyder GH. 1989. Dependence of formation of small disulfide loops in two-cysteine peptides on the number and types of intervening amino acids. *J. Biol. Chem.* 264: 18472–18479. doi:10.1016/S0021-9258(18)51490-3
63. Hartung S, Arvai AS, Wood T, Kolappan S, Shin DS, Craig L, Tainer JA. 2011. Ultrahigh resolution and full-length pilin structures with insights for filament assembly, pathogenic functions, and vaccine potential. *J. Biol. Chem.* 286: 44254–44265. doi:10.1074/jbc.M111.297242
64. Rojas-Chapana JA, Tributsch H. 2000. Bio-leaching of pyrite accelerated by cysteine. *Process Biochem.* 35: 815–824. doi:10.1016/s0032-9592(99)00142-9
65. Ye J-P, Wang S-Q, Zhang P-Y, Nabi M, Tao X, Zhang H-B, Liu Y-W. 2020. L-cysteine addition enhances microbial surface oxidation of coal inorganic sulfur: Complexation of cysteine and pyrite, inhibition of jarosite formation, environmental effects. *Environ. Res.* 187: 109705. doi:10.1016/j.envres.2020.109705
66. Luzar A. 2000. Resolving the hydrogen bond dynamics conundrum. *J. Chem. Phys.* 113: 10663–10675. doi:10.1063/1.1320826
67. Zahn S, Wendler K, Delle Site L, Kirchner B. 2011. Depolarization of water in protic ionic liquids. *Phys. Chem. Chem. Phys.* 13: 15083. doi:0.1039/c1cp20288j

68. Bezrodnyi V, Shavykin O, Mikhtaniuk S, Neelov IM, Markelov DA. 2020. Molecular Dynamics and Spin-Lattice NMR Relaxation α- and ε-Polylysine. *Appl*. *Magn*. *Reson*. 51: 1669–1679. doi:10.1007/s00723-020-01260-8
69. Zhou H-X, Pang X. 2018. Electrostatic interactions in protein structure, folding, binding, and condensation. *Chem. Rev.* 118: 1691–1741. doi:10.1021/acs.chemrev.7b00305
70. Watanabe H, Yoshida C, Ooishi A, Nakai Y, Ueda M, Isobe Y, Honda S. 2019. Histidine-mediated intramolecular electrostatic repulsion for controlling pH-dependent protein–protein interaction. *ACS Chem. Biol.* 14: 2729–2736. doi:10.1021/acschembio.9b00652
71. Niemann T, Stange P, Strate A, Ludwig R. 2019. When hydrogen bonding overcomes Coulomb repulsion: from kinetic to thermodynamic stability of cationic dimers. *Phys. Chem. Chem. Phys.* 21: 8215–8220. doi:10.1039/c8cp06417b

Supplementary information of Chapter III

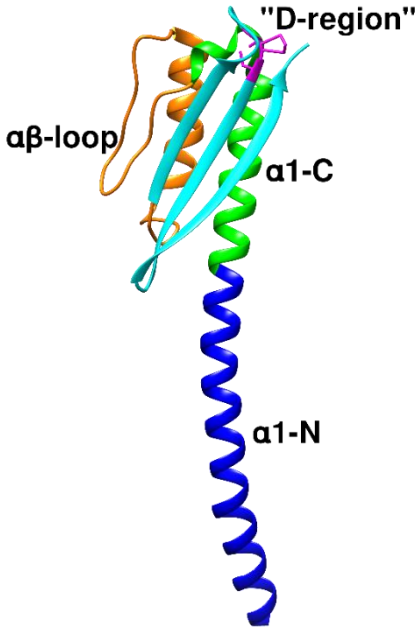

Fig. S1. Predicted tertiary structure of minor pilin PilV of *At. thiooxidans* showing its regions. The α-helix is divided in two sections: the most hydrophobic segment α1-N (blue) and less hydrophobic α1-C (green). The αβ-loop is in orange and the putative D-region in magenta.

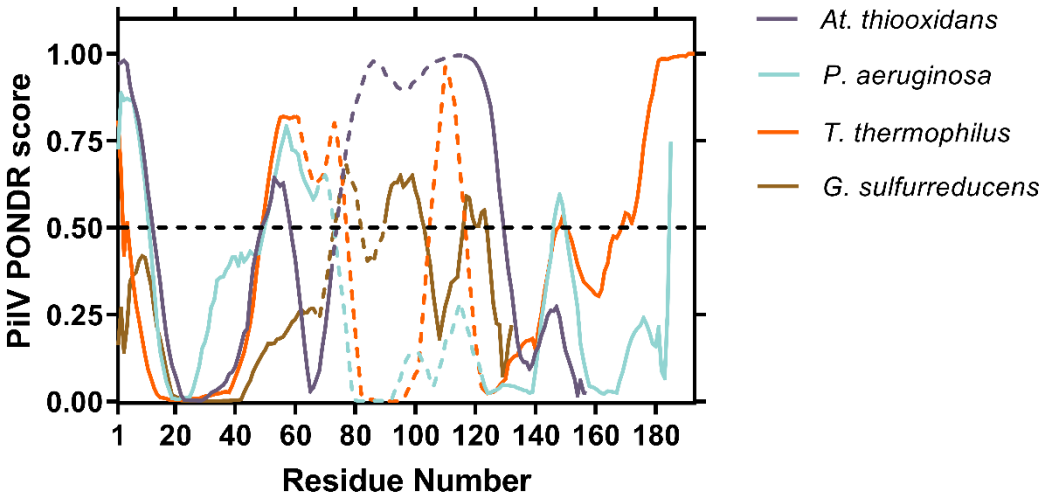

Fig. S2. PONDR scores indicate disorder prediction of PilV pilins from *At. thiooxidans* (purple), *P. aeruginosa* (light blue), *T. thermophilus* (orange) and *G. sulfurreducens* (brown). The dotted lines indicate the segments corresponding to αβ loop. The VL-XT algorithm on the PONDR® server was used, values above 0.5 indicate a tendency for disorder.

CHAPTER IV

The adhesin PilY1 of *Acidithiobacillus thiooxidans*

Araceli Hernández-Sánchez, Edgar D. Páez-Pérez, Elvia Alfaro-Saldaña, J. Viridiana García-Meza

Geomicrobiología, Metalurgia, UASLP, Sierra Leona 550, San Luis Potosí, 78210, SLP, México

Abstract

Thirty years since the first report on the PilY1 protein in bacteria, only the C-terminal domain has been crystallized; there is no study in which the N-terminal domain, let alone the complete protein, has been crystallized. In our laboratory, we are interested in characterizing the Type IV Pili (T4P) of *Acidithiobacillus thiooxidans*. While continuing our experimental work, we have decided to begin the *in silico* characterization of PilY1 and other pilins of the T4P of this acidophilic bacterium. Here, it is presented a description of the particularities of *At. thiooxidans* PilY1 protein through predictor software and homology data. Our results suggest that PilY1 from *At. thiooxidans* may have the same role as has been described for other proteins (non-pilins) associated with T4P in neutrophilic bacteria; also, its C-terminal interacts (interface interaction) with the minor pilins PilX, PilW and PilV. The N-terminal region comprises domains such as the vWA and the beta-propeller folding, involved in signaling, ligand-binding, and protein-protein interaction. In fact, the vWA domain has intrinsically disordered regions that enable it to maintain its structure over a wide pH range, not only at extreme acidity to which *At. thiooxidans* is adapted.

Key Words: acidophile, PilY1 interaction, vWA domain, protein structure, protein disorder, circular dichroism spectra

Introduction

Acidithiobacillus thiooxidans has a significant role in the acidophilic bioleaching process (Yin et al. 2019; Jiménez-Paredes et al. 2021; Kamizela et al. 2021). The conditions and adaptive mechanisms which the *Acidithiobacillus* genus has developed to maintain the integrity of its cellular functions (pH < 3, high redox potentials) provide a good model for studying the resilience of extracellular proteins. For bioleaching, cell adherence and biofilm formation are key factors. Biofilm formation involves surface sensing and the production of extracellular polymeric substances (EPS) (García-Meza et al. 2013), exchange of flagellar and pili motility, and multiple cellular signaling cascades and gene regulation (Díaz-Beneventi et al. 2018). Previous studies have shown that Type IV Pili (T4P) are involved in biofilm formation in *Acidithiobacillus ferrooxidans* and *At. thiooxidans* (Díaz et al. 2017; Tang et al. 2018). Functional and biochemical assays as well as tertiary structure analyses of several pilins of T4P of various prokaryotic pathogens have been carried out, but not for *Acidithiobacillus* sp.

Based on information obtained from bacteria of clinical or biotechnological interest, more than a dozen different key proteins forming part of the T4P structure and system are currently known, e.g. proteins called major pilins (PilA forming the stem of the pilum) and minor pilins on the pili tip (FimU, PilV, PilW, PilX, PilY/PilC). In *At. thiooxidans*, a cluster with a structure similar to the canonical operon found in *Pseudomonas aeruginosa*, which primes the T4P pilus, has been identified. This cluster encodes four minor pilins *fimT*, *pilV*, *pilW*, and *pilX*, in the same orientation with respect to *pilY1* (Páez-Pérez et al. 2023). PilY1 is a high molecular weight protein associated with the pili tip and also found in extracellular membrane (Burdman et al. 2011; Lou et al. 2015; Giltner et al. 2010; Craig et al. 2019).

Specifically, PilY1 was identified by Alm et al. (1996) in *Pseudomonas aeruginosa* and described as a PilC2 gonococcal homologue due to the fact that the C-terminal domain of both are similar. The 127 kDa PilY1 protein was found in membrane and in sheared pili, and the deletion of the *pilY1* gene triggers loss of twitching motility and the disruption of pili biogenesis in mutants, suggesting a priming role in pili assembly. Therefore, the authors suggested that PilY1 participates before and during pilus assembly and is part of pili (Alm et al. 1996). One year earlier, Rudel et al. (1995) reported PilC2 and identified it as the T4P tip

adhesin from purified pilus in the genus *Neisseria*; they indicated that the PilC adhesion property is essential for cell adherence and subsequent infection. The C-terminal similarity and its location at the pili tip were the reasons why PilY1 was also defined as an adhesin.

The PilY1 C-terminal is a conserved domain and folds into an eight-beta-propeller structure (usually named *Neisseria* PilC beta-propeller domain) similar to that predicted in PilC2, which interacts with the minor pili complex. Additionally, this C-terminal domain of PilC2 and PilY1 contains an EF-hand Ca-binding motif where the release of Ca serves as a signal for the regulation of pili retraction, affecting PilT ATPase (Morand et al. 2004; Clapham 2007; Orans et al. 2010; Treuner-Lange et al. 2020).

The N-terminal of PilY1 is not conserved, but diverse bacteria contain a domain that participates in crucial roles such as sensing, cell recognition, or adhesion. This domain includes the von Willebrand A-like factor (vWA) and the metal ion-dependent adhesion site (MIDAS) motif (Siryaporn et al. 2014; Alfaro-Saldaña et al. 2019; Webster et al. 2021; Sacharok et al. 2023). The vWA "is structurally similar to the A2 domain of the human vW factor, a force-sensing glycoprotein important in stopping bleeding" (Webster et al. 2022). In bacteria, this domain is involved in migration, mechanosensing, signaling, adhesion, and biofilm formation (Webster et al. 2022; Islam et al. 2023), while the MIDAS motif resembles the cellular adhesion role of the vWA in α-β integrin chains (Gotwals et al. 1999; Springer 20006).

PilY1 contributes not only to the structure of pili but also to signaling cascades that regulate twitching motility, pilus biogenesis and retraction, and bacterial behavior on surfaces such as cell adhesion processes through molecular binding, sulfur bridges, hydrogen bonds, electrostatic forces, and sense of shear force (Tuson et al. 2013; Siryaporn et al. 2014; Luo et al. 2015; Nguyen et al. 2015; Laventie and Jenal, 2020; Webster et al. 2021). To date, PilY1 has been well studied in pathogens (Kuchma et al. 2010; Orans et al. 2010; Cruz et al. 2014; Hoppe et al. 2017; Marko et al. 2018; Webster et al. 2021; Herfurth et al. 2022; Xue et al. 2022), but its investigation in extremophiles such as acidophiles has been limited to the reporting of their expression (Makarova et al. 2016; Alfaro-Saldaña et al. 2019). In fact, only the tertiary structure of the PilY1 C-terminal domain is currently known (Orans et al. 2010), and no information regarding the N-terminal or full-length structure has been reported. In

recent reports, we confirmed, sequenced, and analyzed PilY1 of *At. thiooxidans* (Alfaro-Saldaña et al. 2019). Our primary and secondary structure analyses revealed that PilY1 amino acid composition and disorder region are associated with pH resilience and stability (Páez-Pérez et al. 2023). Here, we conduct in silico analyses of the predicted tertiary structure of PilY1. First, we describe the conserved C-terminal and its homology with *P. aeruginosa* and *Neisseria* PilC2, enabling us to delineate a potential interaction interface with the minor pilins. We then describe the N-terminal domain of *At. thiooxidans*, focusing on the vWA. The tertiary structure analyses and sequence alignments were conducted comparing vWA' PilY1 and its homologues in neutrophilic bacteria and eukaryotes. Further computational characterization shows that despite the complexity of this protein, it is designed to withstand the hostile environment where *At. thiooxidans* thrives.

Methodology

Structure prediction and sequence analysis of PilY1

The sequence for the PilY1 protein of *At. thiooxidans* ATCC 19377 was AWP39905.1. The sequences for PilY1 of *P. aeruginosa* PAO1AAA93502.1, as well as AFA53726.1 for PilC of *Neisseria meningitides* were used for comparisons. Sequences were obtained from GenBank (https://www.ncbi.nlm.nih.gov/genbank/).

Secondary structure and structural disorder of PilY1 were predicted using, respectively, the FELLS server (http://old.protein.bio.unipd.it/fells/) (Piovesan et al. 2017) and the PONDR® server (http://www.pondr.com/), applying the VL-XT algorithm (Xue et al. 2010).

Predictions of tertiary structure of the PilY1 and its vWA domain from *At. thiooxidans*, *P. aeruginosa* PAO1 and *N. meningitides* were obtained using the AlphaFold2 program ColabFold V1.5.2 (https://alphafold.ebi.ac.uk/) following default recommendations (Jumper et al. 2021; Mirdita et al. 2022). The complete amino acid sequence of PilY1 and PilC2 and the sequence of vWA without the signal peptide of both PilY1 were submitted and predicted with default parameters in each prediction run, yielding PDB files of each structure and the predicted local distance difference test (pLDDT). The C-terminal domain of PilY1 crystal structure (3HX6) (Orans et al. 2010) was obtained from the RCSB Protein Data Bank (RCSB PDB) (https://www.rcsb.org/). Tertiary structure alignments and domain localization were

visualized and computed using UCSF Chimera 1.16 (www.cgl.ucsf.edu/chimera/) (Pettersen et al. 2004).

To align the tertiary predicted structure of PilC2 with similar proteins, we used FoldSeek Server (https://search.foldseek.com/search) (van Kempen et al. 2023). This software compares tertiary structures with protein that have similar shapes, giving us quantitative data about TM-align and RMSD scores.

SignalP-6.0 (https://dtu.biolib.com/SignalP-6) was employed to identify the presence of a signal peptide in PilY1 and PilC2 (Teufel et al. 2022). The calcium binding motifs were predicted using the MIB2 Metal Ion-Binding site prediction and modeling server (http://combio.life.nctu.edu.tw/MIB2/), which uses structural and sequence information to identify protein-metal interaction sites (Lu et al. 2022).

Prediction of functional interaction partners and interface interaction with PilY1

To find potential interaction partners, the STRING database (https://string-db.org/) was utilized. STRING is a comprehensive database specialized in cataloging known and anticipated protein-protein interactions, including both direct (physical) and indirect (functional) associations. It amalgamates evidence from diverse sources such as automated text mining, interaction experiments, annotated complexes/pathways, and computational predictions. With its forthcoming version 11.5, STRING aims to achieve extensive coverage, encompassing over 14,000 organisms (Szklarczyk et al. 2021). Subsequently, the BIPSPI (xgBoost Interface Prediction of Specific Partner Interactions) web server (https://bipspi.cnb.csic.es/) was used to identify which residues are involved in the interaction between PilY1 and the minor pilins predicted by STRING. It employs the XGBoost algorithm and is designed as a three-step workflow involving XGBoost classifiers and a scoring function to convert interacting pair predictions into binding site residue scores. BIPSPI has shown high performance compared to other methods (Sanchez-Garcia et al. 2019).

Primary structure and phylogenetic analysis of vWA

We analyzed the phylogenetic relationships using the protein sequences of the vWA of the PilY1/PilC family of some *Acidithiobacillus* spp. To polarize the obtained tree, the vWA containing the integrin sequence of *Homo sapiens* was used. The sequences obtained from

NCBI were aligned with those obtained in this work using MEGA11 software (Tamura et al. 2021).

Molecular dynamic and circular dichroism at different pH values

The PQR files for the PilY1 vWA domain in different protonation states were initially generated from the PDB file using the PDB2PQR web server (https://server.poissonboltzmann.org/pdb2pqr) (Jurrus et al. 2018). PQR files contain the vWA structure modified by incorporating protons, added at pH values of 1 to 8. Molecular dynamics (MD) simulations of the vWA domain exposed to different pHs were carried out using WebGRO, an online automated program which uses the GROMACS package for MD simulations (https://simlab.uams.edu/index.php) (Abraham et al. 2015). The stability of PilY1 vWA was assessed based on changes, primarily in the RMSD (root mean square deviation), RMSF (root mean square fluctuation) and Rg (radius of gyration). MD runs were carried out with the default parameters, including the GROMOS96 43a1 force field, a triclinic water box with simple point charge (SPC), neutralized system with 150 mM of NaCl, the protein energy minimizations with a maximum of 5000 steps, and constant temperature (300 K) and pressure (1.0 bar). The trajectories were saved at 1000 frames in each simulation and the simulation time was 50 ns.

Circular dichroism spectra of the vWA domain were calculated with the PDBMD2CD program (Drew and Janes 2020) at the web server (https://pdbmd2cd.cryst.bbk.ac.uk/), starting from the molecular dynamic simulation data (e.g. MD trajectories) and generating spectra for each of the structures provided at each pH evaluated.

Results and Discussion

The PilY1 structure

Upon analyzing and comparing the predicted 3D structure of PilY1 of *At. thiooxidans*, *P. aeruginosa*, and PilC2 of *Neisseria meningitides*, two well differentiated domains can be identified: the N- and C-terminal. (Fig. 18). The pLDDT graphics for the three adhesin models show peaks near 100% with sudden drops. These drops are more abundant in the *At. thiooxidans* PilY1 model and in the first 400 residues of PilC2 model, indicating that some regions are difficult to predict (data not shown) because of the lack of counterparts/homologues. The inter-chain predicted alignment error (inter-PAE) indicates

that both PilY1 models have two well-structured regions (one in about the 500 first amino acids and the other in the remaining residues), the N- and C-terminal domains (Figs. 18a and 18b). The inter-PAE of PilC2 of *Neisseria meningitides* has an N-terminal domain of 330 residues (Fig. 18c). To quantify the similarity between N- and C- terminals of PilY1 proteins and PilC2, we use the FoldSeek Search algorithm to compare predicted PilC and PilY1 structures against other structures deposited in the European Bioinformatics Institute and the ESM Atlas (van Kempen et al. 2023). The PilC2 predicted structure (Fig. 18c) was the query structure; the FoldSeek results showed that the query structure of PilC2 fits with the pilus assembly protein of *Neisseria gonorrhoeae* (PilC), covering the complete structure with a RMSD of 2.33; while for PilY1 of *P. aeruginosa* it is 6.35, due to the structure covering only the residues 347–1044 of the query structure; i.e. the N-terminal of our query structure does not overlap with it. These results confirm that the N-terminal domain of PilC proteins is dissimilar to the corresponding domain in PilY1.

The interactions of the C-terminal domain of PillY1

The predicted C-terminal domains for PilY1 of *At. thiooxidans* and *P. aeruginosa* and PilC2 of *N. meningitides* were compared (Fig. 19). The β-propeller shape was found in both PilY1 structures but as expected, the PilY1 C-terminal domain of *P. aeruginosa* (Fig. 19b) showed the higher match score (RMSD: 2.30) and that of *At. thiooxidans* (Fig. 2a) has the lowest (RMSD: 14.39). The difference between the RMSD values reflects that the arrangement of the secondary structures is not precisely identical, while the tertiary structure of the β-propeller folding is maintained (Fig. 19).

Additional insights into the C-terminus of PilY1 (Fig. 19d) and the PilC protein were reported by Parker et al. (2015), highlighting an EF-hand Ca2+-binding motif. This motif is involved in calcium ion signaling, which regulates the extension and retraction of pili in *P. aeruginosa* (Orans et al. 2010; Maier et al. 2017) and Kingella kingae (Porsch et al. 2013). This calcium binding motif is a conserved sequence (Dx[DNx]xDGxxD) in PilY1 homologues (Parker et al. 2015). Thus, we specifically search for divalent cations (Ca2+, Mg2+ and Mn2+) binding motifs in the PilY1 C-terminal region and in accordance with structure homology with *P. aeruginosa*, we found two possible motifs: DASGN (D929-N933), and DNTGN (D938-N942) (Fig. 19c).

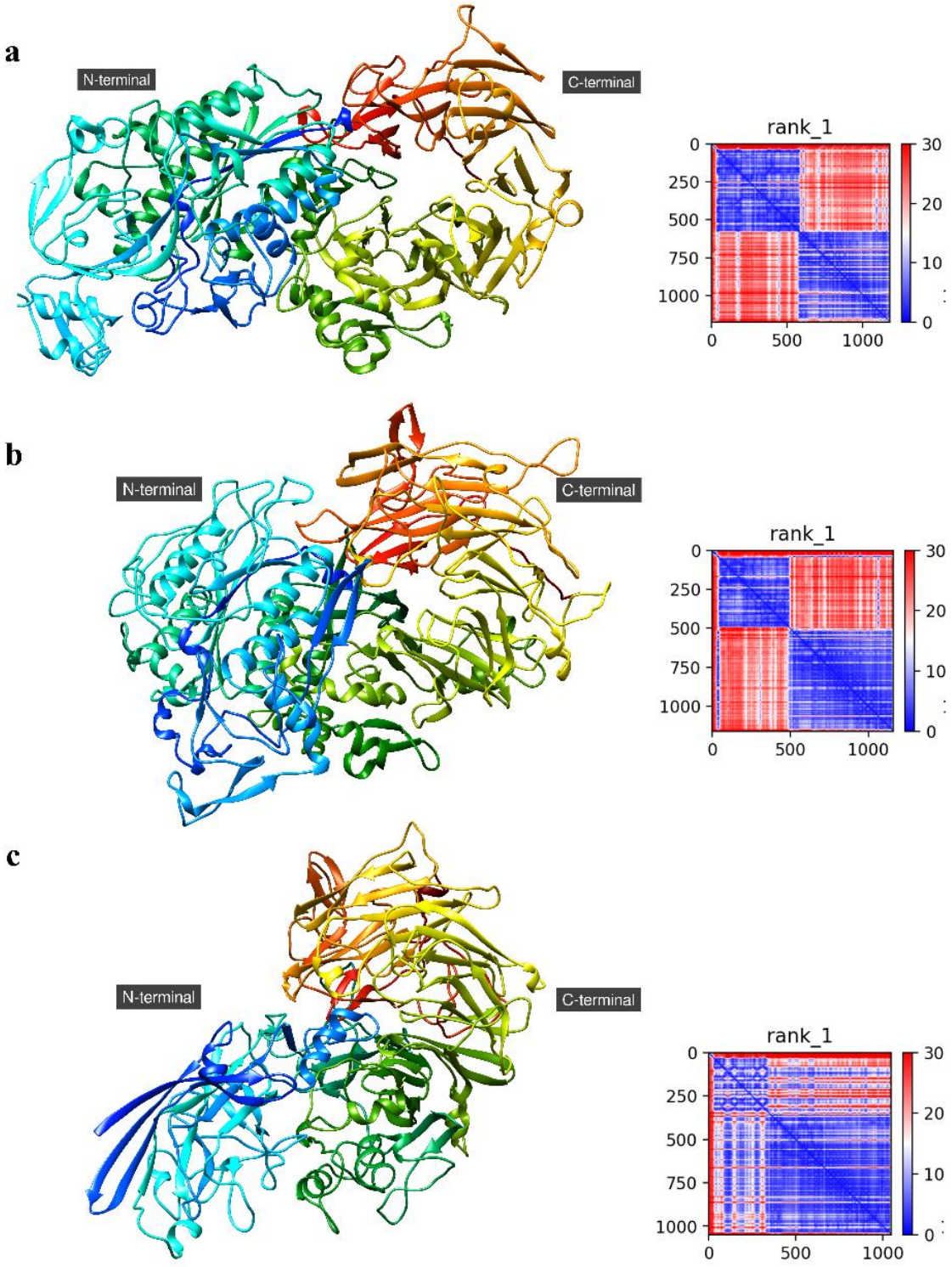

Figure 18. Alpha Fold predicted tertiary structure of PilY1 and PilC2. **a** PilY1 of *At. thiooxidans* (1176 residues), **b** PilY1 of *P. aeruginosa* (1161) residues and of **c** PilC2 of *N. meningitides* (1048 residues). The three structures are colored used rainbow N→C terminal gradient. At right, it shows the inter-chain predicted alignment error (inter-PAE) for each model prediction provided by ColabFold program.

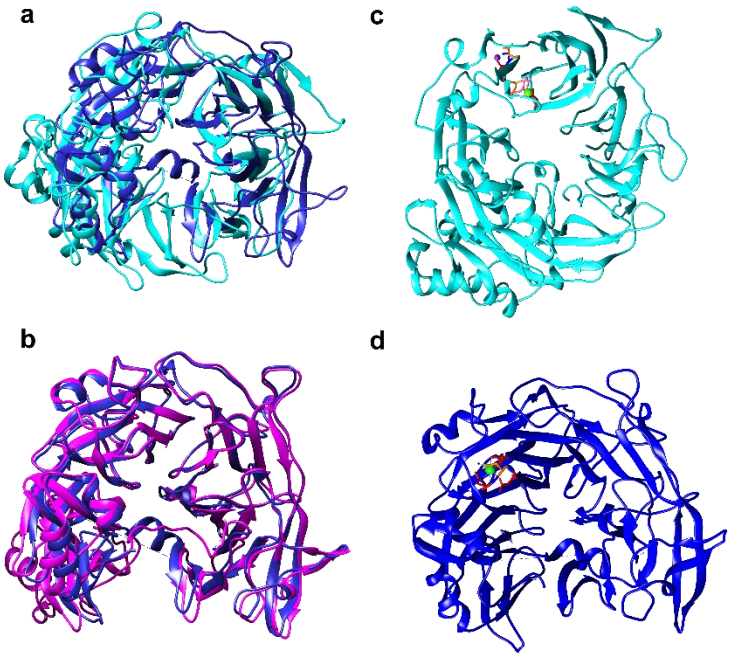

Figure 19 C-terminal domain overlapping of PilY1 crystal structure (Orans et al., 2010) *versus* AlphaFold predicted structures. **a** PilY1 C-terminal of *At. thiooxidans* (cyan), **b** PilY1 C-terminal of *P. aeruginosa* (in magenta). divalent cations binding sites predicted to *At. thiooxidans* PilY1(**c**) and founded in crystalized PilY1 (**d**) The C-terminal crystal structure is the dark blue one in **a**, **b,** and **d**

According to the models, the PilY1 C-terminal domain of *At. thiooxidans* contains six well-formed blades and one incomplete blade consisting of only two β-strands (Fig. 19a) similar to the seven β-propeller fold in the PilY1 C-terminal domain of *P. aeruginosa* (Orans et al. 2010 and Fig. 19b). The β-propeller is a circular fold formed by four to ten repeats that may result from the diversification of an ancestral four-stranded or β-blade implied in protein-protein interactions (Chaudhuri et al. 2008; Chen et al. 2011). In *M. xanthus* and *P. aeruginosa*, the interaction between PilY1 and the minor pilins complex occurs among the PilY1 C-terminal and PilX and PilW (Nguyen et al. 2015; Treuner-Lange et al. 2020), which could suggest the role of the β-propeller in the interaction of PilY1 with minor pilins. In fact, STRING analyses of PilY1 from *At. thiooxidans*, show functional associations with various proteins, some of which are members of the PilMOP machinery, which refers to a minimal system capable of assembling periplasmic T4P (Goosens et al. 2017). Interestingly, the other proteins with which an interaction is predicted are the minor pilins PilX, PilW, and PilV, with scores (predicted functional partners) of 0.933, 0.903, and 0.833 respectively, these also

being the highest in the interaction network predicted by this program. To date, the possible interaction interface of PilY1 with the minor pilins has not been reported (Fig. 20).

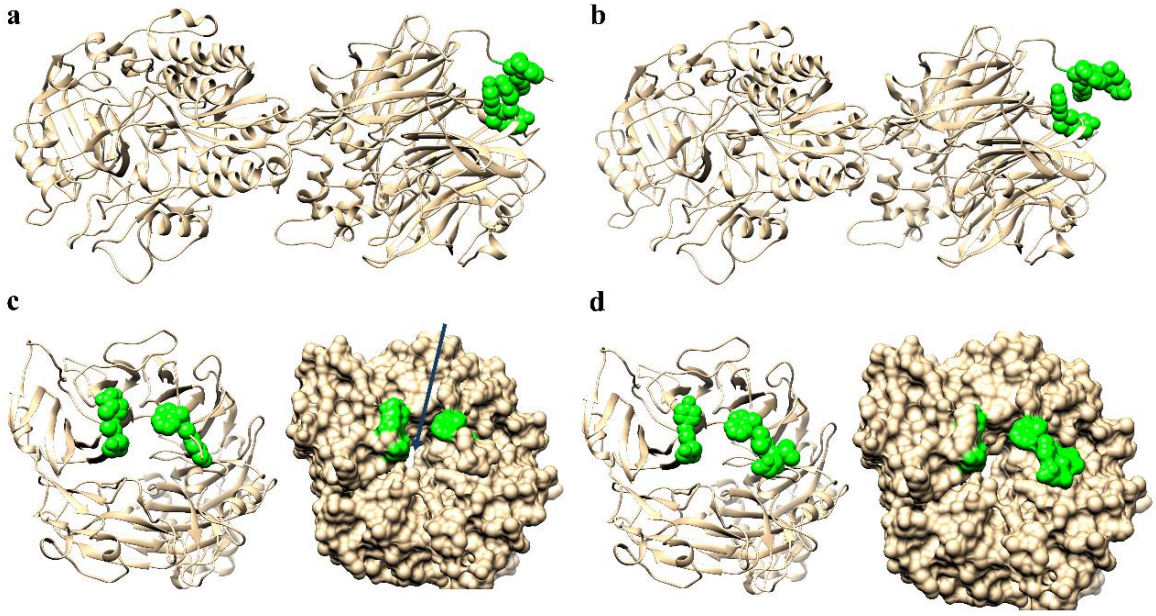

Figure 20. Interface interaction between the C-terminal domain of PilY1 and two minor pilins. a and b Residues (sphere representation) involved in the interaction between minor pilins and PilY1 (PilW and PilX, respectively). c and d Front view of the C-terminal domain in ribbon and surface representation, showing the delimited area for the potential interaction between PilY1 and minor pilins

We are aware of the complications involved in using molecular docking to find potential interaction interfaces due to the lack of experimental information on this and other protein-protein interaction systems. To address this issue, we decided to utilize the BIPSPI method to identify the potential residues of PilY1 for interacting with the minor pilins PilW and PilX.

Interestingly, despite the full-length structure of PilY1 being submitted to the BIPSPI server, the residues with the highest scores (threshold ≥ 0.6) for interaction between the minor pilins and the protein are located around what we could call the "orifice" on the outer face of the C-terminal domain.

The prediction showed that residues Y1000, Y1001, G1771, W1172, and K1173 of PilY1 could potentially interact with both minor pilins, with only residues Q1002 for PilW and residues L1174 and V1175 for PilX being different between the minor pilins. This delimited zone by these shared interaction residues between the two pilins indicates a likely hot spot

for synergistic interaction of PilY1 with the minor pilins, since the results from BIPSPI regarding PilY1 and PilV using the same precision threshold also indicate that residues Q1002, G1771, and W1172 are predicted to interact with this minor pilin.

The former suggested that the C-terminal domain of PilY1 of *At. thiooxidans* may have the same functions as have been reported for homologues of PilY1 and PilC of *P. aeruginosa* and *Neisseria spp*

PilY1 possess a signal peptide type I

For major and minor pilins, their matured form is due to the PilD peptidase, which has cleavages in the well-conserved signal peptide type III (Jacobsen et al. 2020). For the *P. aeruginosa* PilY1, the signal peptide type was predicted by Lewenza et al. (2005) as a prepilin signal peptide with a type III signal peptide processed by PilD. However, type I signal peptides have been reported in PilY1 of *P. aeruginosa* (Nguyen et al. 2015) and in PilY1.1, PilY1.2 and PilY1.3 of *M. xanthus* (Treuner-Lange et al. 2020). Our results suggest that PilY1 of *At. thiooxidans* had a type I signal peptide (confidence score >96%) and its predicted cleavage site occurs between G32–A33. We used the *P. aeruginosa* PilY1 to compare and the predicted signal peptide is indeed type I, while the cleavage occurs between A32–L33. The above data suggests that *At. thiooxidans* PilY1 is matured and cleaved by a type I peptidase as its homologues *P. aeruginosa* and *M. xanthus*.

The vWA is a conserved domain in PilY1 of *At. thiooxidans*

In addition to the signal peptide type I, the PilY1 N-terminal domain contains a vWA domain (Alfaro-Saldaña et al. 2019; Treuner-Lange et al. 2020; Webster et al. 2021). The vWA is widely spread along the three life domains and it had been implicated in sensing, cell recognition, and shear force (Whittaker-Hynes 2002; Zhang et al. 2009; Lancelloti et al. 2019; Hoffmann et al. 2020; Qin et al. 2020; Steinert et al. 2020; Webster et al. 2022).

The vWA of *At. thiooxidans* structure shows five β-sheets surrounded by six α-helices (Fig.21a), known as α/β Rossman folds (Rossman et al. 1974, Lee et al. 195; Hanukoglu et al. 2015). The vWA domains of PilY1 in both *At. thiooxidans* and *P. aeruginosa* (Fig. 21b) show the basic and global structure, but those of *P. aeruginosa* have only four β-sheets and four surrounded α-helices (Fig. 21). Remarkably, the folding of the vWA domain of human integrin alpha 1 is similar (RMSD: 1.07) (Fig. 21c).

Analysis of the primary structure of the *At. thiooxidans* PilY1 protein reveals that the vWA domain (residues 42 to 581) includes the conserved metal-ion-dependent adhesion site (MIDAS) motif (DXSXS…T…D, residues 153-187) (Alfaro-Saldaña et al. 2019) (Fig. 21a). The MIDAS motif is a metal-ion binding site similar to the vWA domain found in the integrins I-domain of eukaryotes, voltage-gated Ca^{2+}, and other intra-extra cellular proteins (Whittaker et al. 2002; Cantí et al. 2005; Zhang and Chen 2012), and it has been reported in other PilY1 vWA domains and other proteins involved in binding extracellular proteins acting as integrin-like switches (Battacharya et al. 2004; Springer 2006; Wang et al. 2020; Webster et al. 2022). Thus, during the mineral *At. thiooxidans* interaction (adhesion, biofilm formation), the MIDAS motif may participate in binding divalent metallic ions such as Ca^{2+}, Mn^{2+} or Mg^{2+} through loops expanded from the vWF, exposed on the protein surface.

MIDAS is involved in conformational changes of the vWA structure but the cysteines stabilize the domain (Baldus and Gräner 2012; Webster et al. 2022). Such cysteines are also involved in mechanosensing; e.g. the glycoprotein vWA factor of eukaryotic cells sense the force across the breaking of sulfide bonds that are usually formed via cysteines interaction, modifying the protein redox state (Baldus and Gräner, 2012, Webster et al. 2022). The PilY1' vWA of *At. thiooxidans* comprises five of seven cysteines (C120, C133, C230, C244 and C444), which may play a vital role during its mechanosensing and attachment to inorganic surfaces such as sulfur minerals such as sphalerite or chalcopyrite (ZnS or $CuFeS_2$, respectively).

Even though MIDAS motif plays a role in conformational changes in the vWA structure, the cysteine residues that it contains are important to stabilize the domain, therefore how much cysteine residues had a vWA domain is pivotal for this role (Baldus and Gräner 2012; Webster et al., 2022).

During the biofilm formation, bacterial adhesins participate in cell adhesion, process that includes molecule-binding, sulfur bridges, hydrogen bonds, electrostatic forces (Tuson et al., 2013, Laventie and Jenal, 2020). For pathogenic bacteria, the role of PilY1 in adhesion has been demonstrated as well as sensing the shear force (Siryaporn et al., 2014). Recently, PilY1 was proposed as mechanosensing protein through the vWA domain (Webster et al., 2021, Webster et al., 2022). e.g. in eukaryotic cells the glycoprotein vWA factor (which includes

three vWA domains) senses the force across breaking of sulfide bonds that are usually formed via cysteines interaction, modifying the protein redox state (Baldus and Gräner, 2012, Webster et al., 2022). The vWA domain of the PilY1 of *At. thiooxidans* comprises five of seven Cys (Cys120, Cys133, Cys230, Cys244 and Cys444), that may play a vital role during its mechanosensing and attachment to inorganic surfaces as sulfur minerals as sphalerite or chalcopyrite (ZnS or CuFeS2, respectively).

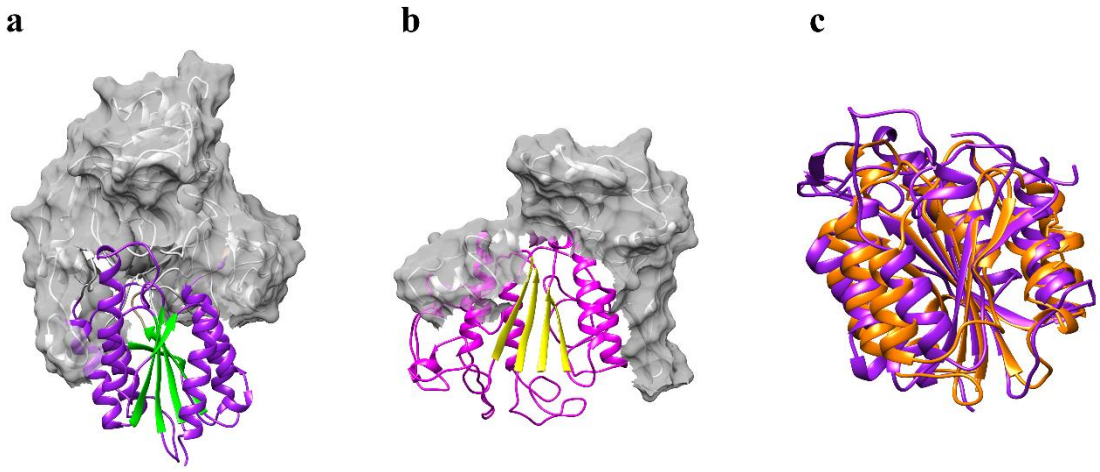

Figure 21 The PilY1 von Willebrand A domain. a The vWA of *At. thiooxidans* structure includes six α-helixes (purple) and five β-sheets (green). b The vWA structure of *P. aeruginosa* has only four α-helixes (magenta) and three β-sheets (yellow). c Merge between *At. thiooxidans* PilY1 (purple) and the von Willebrand domain of the integrin α1 for *H. sapiens* (orange)

Previously, we reported that the phylogeny analysis of the PilY1 complete sequence of *At. thiooxidans* clusters with other iron/sulfur oxidizing microorganisms (Alfaro-Saldaña et al. 2019). Thus, as in other acidophiles, the vWA domain of *At. thiooxidans* must have intrinsic properties that allow it to maintain its structure and function under acidic conditions. The phylogenetic analysis of the vWA indeed showed that the acidophiles form a separate group within the *Acidithiobacillus* genus. They form a cohesive group, except for the thermoacidophilic Archaea *Sulfolobus acidocaldarious* (Fig. 22). Also, the phylogenetic tree reveals that the vWA domain of PilY1 of some acidophiles and non-acidophiles are indeed homologues.

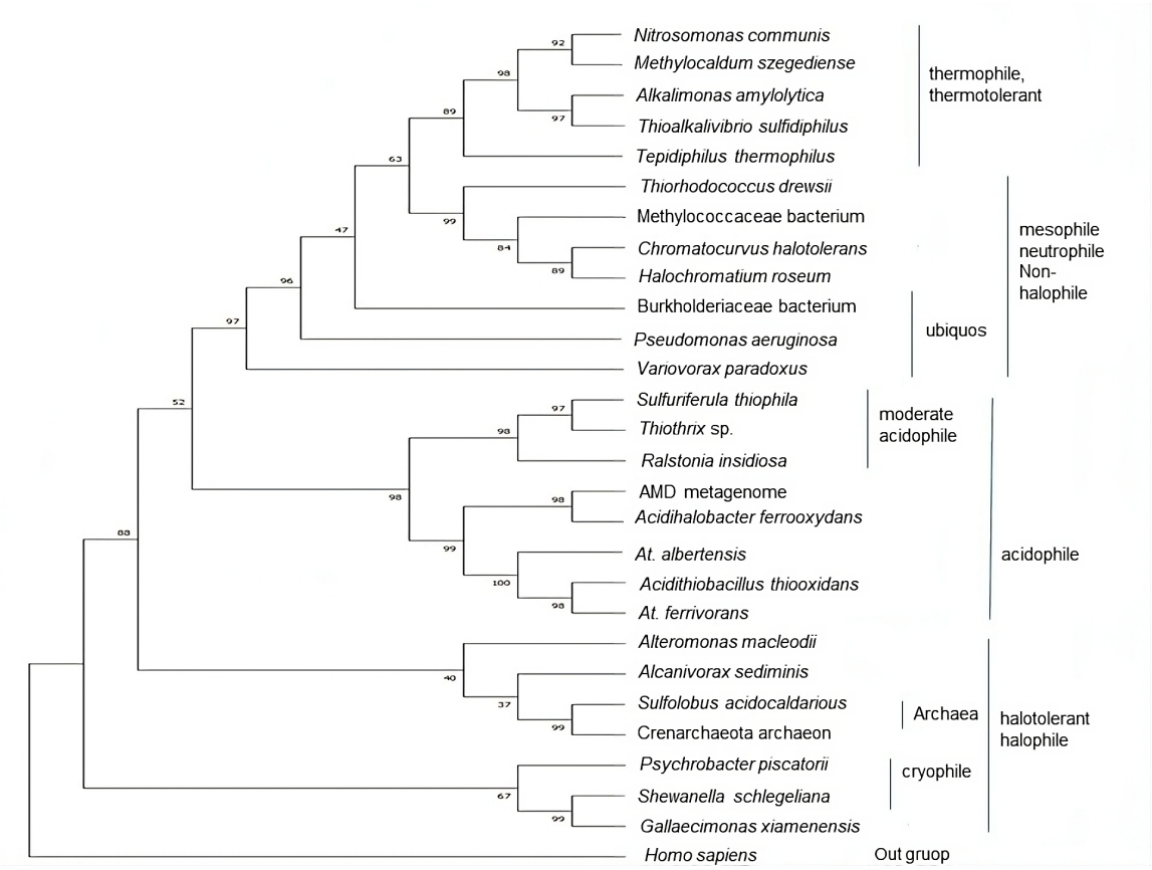

Figure 22 Phylogenetic analysis of the vWA motif present in PilY/PilC Phylogenetic analysis of the vWA motif present in the PilY/PilC family of some Bacteria, in the archaellum regulatory network of an Archaea (*Sulfolobus acidocaldarious*) and in the integrin of an Eukarya, *Homo sapiens*. Evolutionary history obtained by ML log likelihood and the JTT matrix-based model. Bootstrap consensus tree inferred after 1000 replicates; the discrete Gamma distribution was used to model evolutionary rate differences among sites (5 categories (+G, parameter = 3.2697)). The rate variation model allowed for some sites to be evolutionarily invariable ([+I], 1.40% sites). Analysis of 28 amino acid sequences, 713 positions in the final dataset. Evolutionary analyses were conducted in MEGA11 (Jones et al. 1992; Tamura et al. 2021). Accession numbers in Supplementary Table S1)

The PilY1 vWA domain has intrinsic disorder and displays pH resilience

Intrinsic disorder has been identified in extracellular pilins and PilY1 of *At. thiooxidans* that could confer an advantage in acidic environments (Páez-Pérez et al. 2023). Assuming that the structure of the vWA domain must be maintained under harsh conditions, we decided to evaluate the intrinsic disorder and other features of the PilY1 vWA domain in more detail. Our results show a segment between G42 and I171 that is predicted to transition from

disorder to order, probably due to the presence of a ligand or cofactors. This region includes a portion of the MIDAS motif and an α helix of vWA (Fig. 23a).

Focusing on the vWA domain and investigating whether this disorder could be important in other PilY1 vWA domains, we perform a disorder analysis between the vWA domains of acidophiles and non-acidophiles. The data on disorder showed statistically significant differences in acidophiles versus non acidophiles (Fig. 23b). We applied a one-way ANOVA with the mean PONDR score of these domains. We found that in general, the structural disorder of the vWA domain in acidophiles is significantly higher ($p<0.0001$) compared to their non-acidophilic counterparts. For the non-acidophiles, the vWA domain of the sulfur-oxidizing *Sulfuriferula* sp. AH1 is also significantly higher compared to the protein of *P. aeruginosa*.

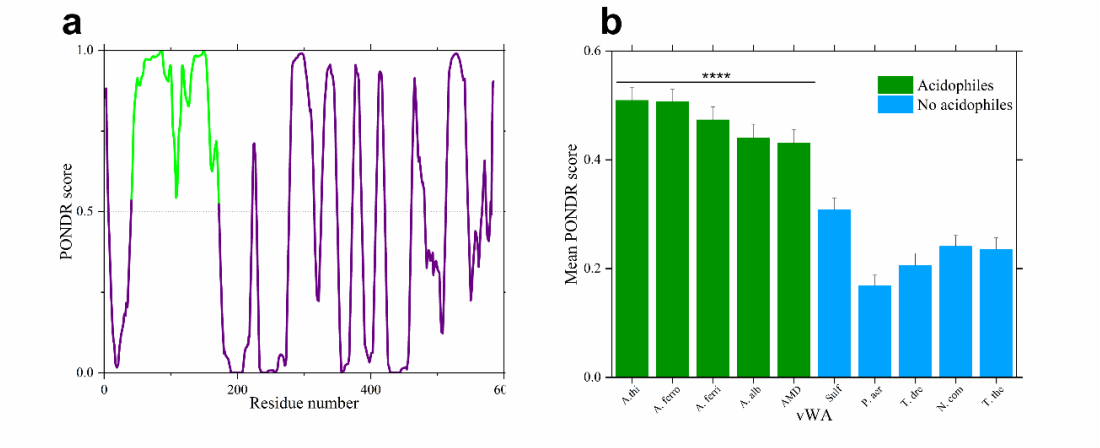

Figure 23 PONDR disorder analysis of PilY1 N-terminal domain. **a** Disorder prediction of PilY1 N-terminal (1-581), values above dotted line indicates high probability for disorder. Green line points out the order-disorder transition region predicted by PONDR using VL-XT algorithm. **b** Comparison between predicted disorder in vWA domains from acidophiles (olive green) and their non-acidophiles counterparts (blue), graphic shows the one way ANOVA comparison with $p<0.0001$

The vWA in PilY1 of *At. thiooxidans* must be a pH-resistant protein. Three characteristics have been proposed to explain why the structure and function of extracellular proteins are maintained in acidophiles: presence of structural disorder, the enrichment of hydroxy and amide residues, and low surface charge (Páez-Pérez et al. 2023). Full-length PilY1 sequences keep these characteristics, but the stability of its vWA exposed to the acidic environment has not been evaluated. If the vWA domain is key in sensing surfaces for *At. thiooxidans*, an

unchanged structure is expected.The stability of the vWA domain at different pH (1–8) was evaluated through molecular dynamics simulations. The results from the simple root mean square deviation (RMSD) and root mean square fluctuation (RMSF) exhibit closely aligned values, with a difference of scarcely < 0.15 nm between successive pH values. This suggests that the globular structure of the vWA maintains stability across different pH levels. To confirm this, we conducted predicted circular dichroism (CD) analysis from molecular dynamics trajectories. The CD analysis showed characteristic peaks of α/β proteins at approximately 210 and 222 nm across different pH values (Fig. 24a). Notably, at pH levels 1 and 2, there was a slight increase in α-helix peaks and a decrease in β-sheet peaks. Interestingly, disorder persisted across all pH levels, with the lowest values observed at pH 2 and 8 (Fig. 24b).

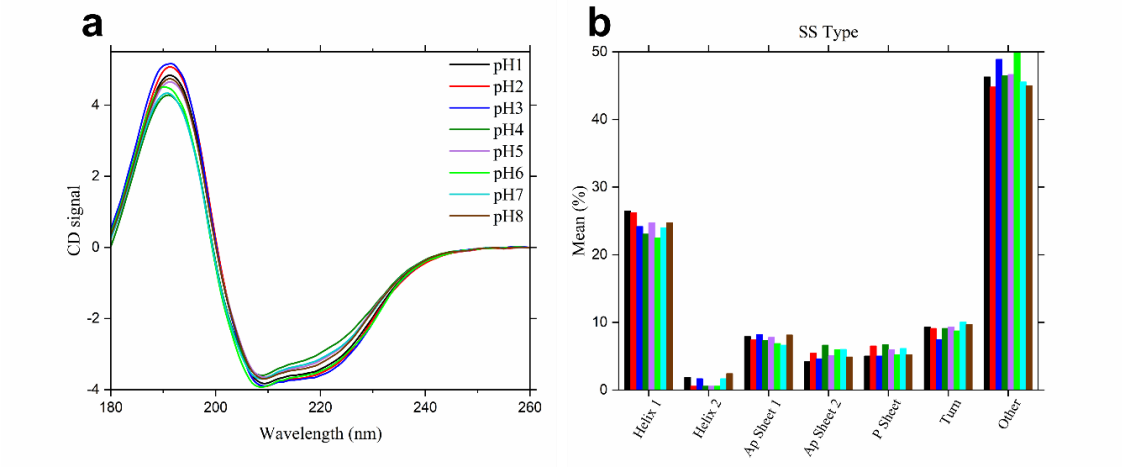

Figure 24 Conserved structure of *At. thiooxidans* vWA domain. **a** Circular dichroism spectrum for the vWA structure of *At. thiooxidans* at different pH values. **b** Percent of secondary structures predicted by CD, in horizontal axis it showed the secondary structure type and in vertical axis the percent, color code in b is the same that in **a.** AP: antiparallel, P: parallel

Thus, the molecular dynamics for the PilY1 vWA domain of *At. thiooxidans* showed that tertiary and secondary structures remain stable through different pH values. This is probably due to its tendency to disorder as was found in other acidophiles (Páez-Pérez et al. 2023).

The molecular dynamics simulations conducted on the vWA domain of PilY1 in *At. thiooxidans* revealed remarkable stability in both tertiary and secondary structures across a spectrum of pH levels. This robustness can likely be attributed to the inherent tendency of the protein towards disorder, a characteristic shared with other acidophiles as highlighted in previous work (Páez-Pérez et al. 2023). These findings underscore the resilience of the vWA

domain in maintaining its structural integrity, further reinforcing our earlier conclusions regarding the adaptive mechanisms of acidophiles to thrive in extreme environments.

Conclusions

Even though the acidophilic bacteria *At. thiooxidans* and neutrophilic bacteria live in under different environmental conditions, both have the pili tip associated protein PilY1. The PilY1 protein structure of *At. thiooxidans* possesses the same representative domains as its non-acidophile homologues, e.g. the N-terminal vWA domain with MIDAS motif and the C-terminal domain with the β-propeller folding, which mainly interact with the minor pilins PilX and PilW. The vWA domain of PilY1 is conserved, being comparable to other vWA domains mainly in its three-dimensional folding and the sequence of the ligand-binding MIDAS motif. The enriched presence of cysteines in vWA suggests its active role in adhesion and sensing. To maintain its structure and function in acidic environments, the vWA domain has intrinsically disordered regions; our results of molecular dynamics and circular dichroism indicate that the structure of this domain is maintained over a wide pH range (1–8), as a resilient domain.

References Chapter IV

Abraham MJ, Murtola T, Schulz R, et al (2015) GROMACS: High performance molecular simulations through multi-level parallelism from laptops to supercomputers. SoftwareX. 1–2:19–25. http://dx.doi.org/10.1016/j.softx.2015.06.001

Aim RA, Hallinan JP, Watson AA, et al (1996) Fimbrial biogenesis genes of *Pseudomonas aeruginosa*: *pilW* and *pilX* increase the similarity of type 4 fimbriae to the GSP protein-secretion systems and *pilY1* encodes a gonococcal PilC homologue. Mol Microbiol. 22:161–173. http://dx.doi.org/10.1111/j.1365-2958.1996.tb02665.x

Alfaro-Saldaña E, Hernández-Sánchez A, Patrón-Soberano OA et al (2019) Sequence analysis and confirmation of the type IV pili-associated proteins PilY1, PilW and PilV in *Acidithiobacillus thiooxidans*. PLoS One. 14:e0199854. http://dx.doi.org/10.1371/journal.pone.0199854

Bhattacharya AA, Lupher ML Jr, Staunton DE, Liddington RC (2004) Crystal structure of the A domain from complement factor B reveals an integrin-like open conformation. Structure. 12:371–378. http://dx.doi.org/10.1016/j.str.2004.02.012

Bohn Y-ST, Brandes G, Rakhimova E et al (2009) Multiple roles of *Pseudomonas aeruginosa* TBCF10839 PilY1 in motility, transport and infection. Mol Microbiol. 71:730–747. http://dx.doi.org/10.1111/j.1365-2958.2008.06559.x

Burdman S, Bahar O, Parker JK, De La Fuente L (2011) Involvement of type IV Pili in pathogenicity of plant pathogenic bacteria. Genes (Basel). 2:706–735. http://dx.doi.org/10.3390/genes2040706

Cantí C, Nieto-Rostro M, Foucault I, et al (2005) The metal-ion-dependent adhesion site in the Von Willebrand factor-A domain of $\alpha_2\delta$ subunits is key to trafficking voltage-gated Ca^{2+} channels. Proc Natl Acad Sci USA. 102:11230–11235. http://dx.doi.org/10.1073/pnas.0504183102

Chaudhuri I, Söding J, Lupas AN (2008) Evolution of the β-propeller fold. Proteins. 71:795–803. http://dx.doi.org/10.1002/prot.21764

Clapham DE (2007) Calcium signaling. Cell. 131:1047–1058. http://dx.doi.org/10.1016/j.cell.2007.11.028

Craig L, Forest KT, Maier B 82019) Type IV pili: dynamics, biophysics and functional consequences. Nat Rev Microbiol. 17:429–440. http://dx.doi.org/10.1038/s41579-019-0195-4

Cruz LF, Parker JK, Cobine PA, de la Fuente L (2014) Calcium-enhanced twitching motility in *Xylella fastidiosa* is linked to a single PilY1 homolog. Appl Environ Microbiol. 80:7176–7185. http://dx.doi.org/10.1128/AEM.02153-14

Díaz M, Castro M, Copaja S, Guiliani N (2018) Biofilm formation by the acidophile bacterium *Acidithiobacillus thiooxidans* involves c-di-GMP pathway and Pel exopolysaccharide. Genes (Basel). 9:113. http://dx.doi.org/10.3390/genes9020113

Doerr S, Harvey MJ, Noé F, De Fabritiis G (2016) HTMD: High-throughput molecular dynamics for molecular discovery. J Chem Theory Comput. 12:1845–1852. http://dx.doi.org/10.1021/acs.jctc.6b00049.

Drew ED, Janes RW (2020) PDBMD2CD: providing predicted protein circular dichroism spectra from multiple molecular dynamics-generated protein structures. Nucleic Acids Res. 48:W17–W24. http://dx.doi.org/10.1093/nar/gkaa296

García-Meza JV, Fernández JJ, Lara RH, González I (2013) Changes in biofilm structure during the colonization of chalcopyrite by *Acidithiobacillus thiooxidans*. Appl Microbiol Biotechnol. 97:6065–6075. http://dx.doi.org/10.1007/s00253-012-4420-6

Giltner CL, Habash M, Burrows LL (2010) *Pseudomonas aeruginosa* minor pilins are incorporated into type IV pili. J Mol Biol. 398:444–461. http://dx.doi.org/10.1016/j.jmb.2010.03.028

Goosens VJ, Busch A, Georgiadou M, Castagnini M, Forest KT, Waksman G, Pelicic V (2017) Reconstitution of a minimal machinery capable of assembling periplasmic type IV pili. Proc Natl Acad Sci USA. 114:E4978-E4986. Doi: 10.1073/pnas.1618539114

Hallgren J, Tsirigos KD, Pedersen MD et al (2022) DeepTMHMM predicts alpha and beta transmembrane proteins using deep neural networks. bioRxiv. http://dx.doi.org/10.1101/2022.04.08.487609

Hanukoglu I (2015) Proteopedia: Rossmann fold: A beta-alpha-beta fold at dinucleotide binding sites: Rossmann Fold in FAD, NAD and NADP Binding Domains. Biochem Mol Biol Educ. 43:206–209. http://dx.doi.org/10.1002/bmb.20849

Herfurth M, Treuner-Lange A, Glatter T et al (2022) A noncanonical cytochrome c stimulates calcium binding by PilY1 for type IVa pili formation. Proc Natl Acad Sci USA. 119(6). http://dx.doi.org/10.1073/pnas.2115061119

Hoffmann L, Anders K, Bischof LF et al (2019) Structure and interactions of the archaeal motility repression module ArnA-ArnB that modulates archaellum gene expression in *Sulfolobus acidocaldarius*. J Biol Chem. 294:7460–7471. http://dx.doi.org/10.1074/jbc.RA119.007709

Hoppe J, Ünal CM, Thiem S et al (2017) PilY1 promotes *Legionella pneumophila* infection of human lung tissue explants and contributes to bacterial adhesion, host cell invasion, and twitching motility. Front Cell Infect Microbiol. 7. http://dx.doi.org/10.3389/fcimb.2017.00063

Jones DS, Roepke EW, Hua AA et al (2017) Complete genome sequence of *Sulfuriferula* sp. Strain AH1, a sulfur-oxidizing autotroph isolated from weathered mine tailings from the Duluth complex in Minnesota. Genome Announc. 5. http://dx.doi.org/10.1128/genomeA.00673-17

Jones DT, Taylor WR, Thornton JM (1992) The rapid generation of mutation data matrices from protein sequences. Comput Appl Biosci. 8:275–282. http://dx.doi.org/10.1093/bioinformatics/8.3.275

Jonsson AB, Nyberg G, Normark S (1991) Phase variation of gonococcal pili by frameshift mutation in pilC, a novel gene for pilus assembly. EMBO J. 10:477–488. http://dx.doi.org/10.1002/j.1460-2075.1991.tb07970.x

Jumper J, Evans R, Pritzel A et al (2021) Highly accurate protein structure prediction with AlphaFold. Nature. 596:583–589. http://dx.doi.org/10.1038/s41586-021-03819-2

Jurrus E, Engel D, Star K et al (2018) Improvements to the APBS biomolecular solvation software suite. Protein Sci. 27:112–128. http://dx.doi.org/10.1002/pro.3280

Kamizela T, Grobelak A, Worwag M (2021) Use of *Acidithiobacillus thiooxidans* and *Acidithiobacillus ferrooxidans* in the recovery of heavy metals from landfill leachates. Energies. 14:3336. http://dx.doi.org/10.3390/en14113336

van Kempen M, Kim SS, Tumescheit C et al (2023) Fast and accurate protein structure search with Foldseek. Nat Biotechnol. http://dx.doi.org/10.1038/s41587-023-01773-0

Kuchma SL, Ballok AE, Merritt JH, et al (2010) Cyclic-di-GMP-mediated repression of swarming motility by *Pseudomonas aeruginosa*: the pilY1 gene and its impact on surface-associated behaviors. J Bacteriol. 192:2950–2964. http://dx.doi.org/10.1128/JB.01642-09

Laventie B-J, Jenal U (2020) Surface sensing and adaptation in bacteria. Annu Rev Microbiol. 74:735–760. http://dx.doi.org/10.1146/annurev-micro-012120-063427

Lewenza S, Gardy JL, Brinkman FSL, Hancock REW (2005) Genome-wide identification of *Pseudomonas aeruginosa* exported proteins using a consensus computational strategy combined with a laboratory-based PhoA fusion screen. Genome Res. 15:321–329. http://dx.doi.org/10.1101/gr.3257305

Luo Y, Zhao K, Baker AE, et al (2015) A hierarchical cascade of second messengers regulates *Pseudomonas aeruginosa* surface behaviors. MBio. 6. http://dx.doi.org/10.1128/mBio.02456-14

Lu CH, Chen CC, Yu CS et al (2022) MIB2: metal ion-binding site prediction and modeling server. Bioinformatics. 38:4428–4429. http://dx.doi.org/10.1093/bioinformatics/btac534

Makarova KS, Koonin EV, Albers SV (2016) Diversity and evolution of type IV pili systems in Archaea. Front Microbiol. 7:667. http://dx.doi.org/10.3389/fmicb.2016.00667

Marko VA, Kilmury SLN, MacNeil LT, Burrows LL (2018) *Pseudomonas aeruginosa* type IV minor pilins and PilY1 regulate virulence by modulating FimS-AlgR activity. PLoS Pathog. 14:e1007074. http://dx.doi.org/10.1371/journal.ppat.1007074

McGuffin LJ, Bryson K, Jones DT (2000) The PSIPRED protein structure prediction server. Bioinformatics. 16:404–405. http://dx.doi.org/10.1093/bioinformatics/16.4.404

Mirdita M, Schütze K, Moriwaki Y et al (2022) ColabFold: making protein folding accessible to all. Nat Methods. 19:679–682. http://dx.doi.org/10.1038/s41592-022-01488-1

Morand PC, Bille E, Morelle S et al (2004) Type IV pilus retraction in pathogenic *Neisseria* is regulated by the PilC proteins. EMBO J. 23:2009–2017. http://dx.doi.org/10.1038/sj.emboj.7600200

Nguyen Y, Sugiman-Marangos S, Harvey H et al (2015) *Pseudomonas aeruginosa* minor pilins prime type IVa pilus assembly and promote surface display of the PilY1 adhesin. J Biol Chem. 290:601–611. http://dx.doi.org/10.1074/jbc.M114.616904

Orans J, Johnson MDL, Coggan KA et al (2010) Crystal structure analysis reveals *Pseudomonas* PilY1 as an essential calcium-dependent regulator of bacterial surface motility. Proc Natl Acad Sci USA. 107:1065–1070. http://dx.doi.org/10.1073/pnas.0911616107

Páez-Pérez ED, Hernández-Sánchez A, Alfaro-Saldaña E, García-Meza JV (2023) Disorder and amino acid composition in proteins: their potential role in the adaptation of extracellular pilins to the acidic media, where *Acidithiobacillus thiooxidans* grows. Extremophiles. 27:31. http://dx.doi.org/10.1007/s00792-023-01317-z

Parker JK, Cruz LF, Evans MR, De La Fuente L (2015) Presence of calcium-binding motifs in PilY1 homologs correlates with Ca-mediated twitching motility and evolutionary history across diverse bacteria. FEMS Microbiol Lett. 362:1–9. http://dx.doi.org/10.1093/femsle/fnu063

Pettersen EF, Goddard TD, Huang CC et al (2004) UCSF Chimera—A visualization system for exploratory research and analysis. J Comput Chem. 25:1605–1612. http://dx.doi.org/10.1002/jcc.20084

Piovesan D, Walsh I, Minervini G, Tosatto SCE (2017) FELLS: fast estimator of latent local structure. Bioinformatics. 33:1889–1891. http://dx.doi.org/10.1093/bioinformatics/btx085

Porsch EA, Johnson MDL, Broadnax AD et al (2013) Calcium binding properties of the *Kingella kingae* PilC1 and PilC2 proteins have differential effects on type IV pilus-mediated adherence and twitching motility. J Bacteriol. 195:886–895. http://dx.doi.org/10.1128/jb.02186-12

Qin N, Sun H, Lu M et al (2020) A single von Willebrand factor C-domain protein acts as an extracellular pattern-recognition receptor in the river prawn *Macrobrachium nipponense*. J Biol Chem. 295:10468–10477. http://dx.doi.org/10.1074/jbc.RA120.013270

Rahman M, Källström H, Normark S, Jonsson AB (1997) PilC of pathogenic *Neisseria* is associated with the bacterial cell surface. Mol Microbiol. 25:11–25. http://dx.doi.org/10.1046/j.1365-2958.1997.4601823.x

Rossmann MG, Moras D, Olsen KW (1974) Chemical and biological evolution of a nucleotide-binding protein. Nature. 250:194–199. http://dx.doi.org/10.1038/250194a0

Rudel T, Scheuerpflug I, Meyer TF (1995) *Neisseria* PilC protein identified as type-4 pilus tip-located adhesin. Nature. 373:357–359. http://dx.doi.org/10.1038/373357a0

Sacharok AL, Porsch EA, St Geme JW 3rd (2023) The *Kingella kingae* PilC1 MIDAS motif is essential for type IV pilus adhesive activity and twitching motility. Infect Immun. 91:e0033822. http://dx.doi.org/10.1128/iai.00338-22

Sanchez-Garcia R, Sorzano COS, Carazo JM, Segura J (2019) BIPSPI: a method for the prediction of partner-specific protein-protein interfaces. Bioinformatics. 35:470-477. Doi: 10.1093/bioinformatics/bty647

Siryaporn A, Kuchma SL, O'Toole GA, Gitai Z (2014) Surface attachment induces *Pseudomonas aeruginosa* virulence. Proc Natl Acad Sci USA. 111:16860–16865. http://dx.doi.org/10.1073/pnas.1415712111

Szklarczyk D, Gable AL, Nastou KC, Lyon D, Kirsch R, Pyysalo S, Doncheva NT, Legeay M, Fang T, Bork P, Jensen LJ, von Mering C (2021) The STRING database in 2021:

customizable protein-protein networks, and functional characterization of user-uploaded gene/measurement sets. Nucleic Acids Res. 8:D605-D612. doi: 10.1093/nar/gkaa1074

Springer TA (2006) Complement and the multifaceted functions of VWA and integrin I domains. Structure. 14:1611–1616. http://dx.doi.org/10.1016/j.str.2006.10.001

Steinert M, Ramming I, Bergmann S (2020) Impact of Von Willebrand factor on bacterial pathogenesis. Front Med (Lausanne). 7:543. http://dx.doi.org/10.3389/fmed.2020.00543

Tamura K, Stecher G, Kumar S (2021) MEGA11: molecular evolutionary genetics analysis version 11. Mol Biol Evol. 38:3022–3027. http://dx.doi.org/10.1093/molbev/msab120

Tang D, Gao Q, Zhao Y et al (2018) Mg^{2+} reduces biofilm quantity in *Acidithiobacillus ferrooxidans* through inhibiting Type IV pili formation. FEMS Microbiol Lett. 365. http://dx.doi.org/10.1093/femsle/fnx266

Teufel F, Almagro Armenteros JJ, Johansen AR et al (2022) SignalP 6.0 predicts all five types of signal peptides using protein language models. Nat Biotechnol. 40:1023–1025. http://dx.doi.org/10.1038/s41587-021-01156-3

Treuner-Lange A, Chang YW, Glatter T et al (2020) PilY1 and minor pilins form a complex priming the type IVa pilus in *Myxococcus xanthus*. Nat Commun. 11:5054. http://dx.doi.org/10.1038/s41467-020-18803-z

Tuson HH, Weibel DB (2013) Bacteria–surface interactions. Soft Matter. 9:4368. http://dx.doi.org/10.1039/c3sm27705d

Wang Qin, Chen Y, Li S et al (2020) Ca^{2+}-based allosteric switches and shape shifting in RGLG1 VWA domain. Comput Struct Biotechnol J. 18:821–833. http://dx.doi.org/10.1016/j.csbj.2020.03.023

Webster SS, Lee CK, Schmidt WC et al (2021) Interaction between the type 4 pili machinery and a diguanylate cyclase fine-tune c-di-GMP levels during early biofilm formation. Proc Natl Acad Sci USA. 118:e2105566118. http://dx.doi.org/10.1073/pnas.2105566118

Webster SS, Mathelié-Guinlet M, Verissimo AF et al (2021) Force-induced changes of PilY1 drive surface sensing by *Pseudomonas aeruginosa*. MBio. 13:e0375421. http://dx.doi.org/10.1128/mbio.03754-21

Webster SS, Wong GCL, O'Toole GA (2022) The power of touch: type 4 pili, the von Willebrand A domain, and surface sensing by *Pseudomonas aeruginosa*. J Bacteriol. 204:e0008422. http://dx.doi.org/10.1128/jb.00084-22

Whittaker CA, Hynes RO (2002) Distribution and evolution of von Willebrand/integrin A domains: Widely dispersed domains with roles in cell adhesion and elsewhere. Mol Biol Cell. 13:3369–3387. http://dx.doi.org/10.1091/mbc.e02-05-0259

Xue B, Dunbrack RL, Williams RW et al (2010) PONDR-FIT: A meta-predictor of intrinsically disordered amino acids. Biochim Biophys Acta Proteins Proteom. 1804:996–1010. http://dx.doi.org/10.1016/j.bbapap.2010.01.011

Xue S, Mercier R, Guiseppi A et al (2022) The differential expression of PilY1 proteins by the HsfBA phosphorelay allows twitching motility in the absence of exopolysaccharides. PLoS Genet. 18:e1010188. http://dx.doi.org/10.1371/journal.pgen.1010188

Yin Z, Feng S, Tong Y, Yang H (2019) Adaptive mechanism of *Acidithiobacillus thiooxidans* CCTCC M 2012104 under stress during bioleaching of low-grade chalcopyrite based on physiological and comparative transcriptomic analysis. J Ind Microbiol Biotechnol. 46:1643–1656. http://dx.doi.org/10.1007/s10295-019-02224-z

Zhang Q, Zhou YF, Zhang CZ et al (2009) Structural specializations of A2, a force-sensing domain in the ultralarge vascular protein von Willebrand factor. Proc Natl Acad Sci USA. 106:9226–9231. http://dx.doi.org/10.1073/pnas.0903679106

Supplementary information of Chapter IV

Table S1 Accession numbers (GeBank) of sequences used in this work

Bacteria (PilY/PilC family)*	
Acidihalobacter ferrooxydans	WP_232225000
Acidithiobacillus thiooxidans	AWP39905
At. albertensis	WP_075322776
At. ferrivorans	WP_085537817
Alcanivorax sediminis	A0A6N7M0E9
Alkalimonas amylolytica	WP_091344945
Alteromonas macleodii	AFS38035.1
AMD metagenome	CBI05240
Burkholderiaceae bacterium	MCO5101957
Chromatocurvus halotolerans	WP_117315296
Gallaecimonas xiamenensis	EKE68266
Halochromatium roseum	WP_201221026
Methylocaldum szegediense	WP_026611218
Methylococcaceae bacterium	MDD5033544
Nitrosomonas communis	SDW55994
Pseudomonas aeruginosa	AAA93502
Psychrobacter piscatorii	WP_058025667
Ralstonia insidiosa	WP_048935080
Shewanella schlegeliana	WP_202720381
Sulfuriferula thiophila	WP_189941779
Tepidiphilus thermophilus	CUB07558
Thioalkalivibrio sulfidiphilus	WP_187148405
Thiorhodococcus drewsii	EGV31806
Thiothrix sp.	WP_301017903
Variovorax paradoxus	ADU40052
Archaea (vWA containing archaellum regulatory network)	
Sulfolobus acidocaldarious	AAY80555
Crenarchaeota archaeon	OLD13196
Eukarya (vWA containing integrin)	
Homo sapiens	AAA59491

* Equivalent PilC pilin in *P. aeruginosa*

CHAPTER V

General conclusions

- *Acidithiobacillus thiooxidans* type 4 pili belongs to subtype a (T4aP)
- The pilins FimT, PilV, PilW, and PilX are the minor pilins in T4P of *At. thiooxidans*
- The minor pilins are coded in the same cluster, along PilY1
- The pilins and PilY1 proteins of T4P of *At. thiooxidans* posse more structural disorder that their counterparts non-acidophiles
- The pilins and PilY1 proteins of T4P of *At. thiooxidans* are enriched in hydroxyl and amide residues that their counterparts non-acidophiles
- The pilins and PilY1 proteins of T4P of *At. thiooxidans* are reduced in positive and negative charge surface residues that their counterparts non-acidophiles
- Disorder and amino acids variability are suggested as mechanisms for resilience to acidic environments in extracellular proteins
- The correct heterologous expression of proteins from extremophiles requires a deeply *in silico* analysis and specific well-designed protocols
- Experimental and *in silico* analysis for PilV and PilY1 corroborate that these proteins maintain secondary and tertiary structure when are exposed to different pH values
- vWA domain in PilY1 of *At. thiooxidans* have structural but not sequence homology with other bacterial pili associated proteins

CHAPTER VI

Perspectives

To achieve the last of objectives of this thesis, we have been working on the manufacture of a device that allows us to indirectly obtain the conductance of proteins in solution.

Below is a brief description of the ongoing project:

Device for the electrochemical characterization of pilins of *At. thiooxidans*

As in metallic electron transfer, tunneling in biomolecules occurs because donor and acceptor atoms are proximal (Shih et al., 2008); the cellular machinery used to tunnel as short-charge transfer mechanisms, under physiological conditions. If a protein as a α-helix increases in length, the electron transfer may switch from tunneling to sequential steps of hopping (Shih et al., 2008; Creasey et al., 2018), and the electron transfer in peptides and proteins may lead to reactivity at a distal point, involving fast molecular motions (in fs scale in peptides) mainly between neighboring amino acids *circa* the Ramachandran angles (ψ and ϕ in a model peptide) (Schlag et al., 2007). Thus, bio-redox reactions "takes the advantage of hopping to transfer charge in dynamic (solution) environments" (Creasey et al., 2018).

We describe the predicted structure of PilV of *At. thiooxidans* (Chapter III). The PilV of *At. thiooxidans* comprises nine aromatic amino acids (three phenylalanine, F, two tryptophan, W, and 4 tyrosine, Y). The physicochemical stable PilV may be an electroactive protein as other non-redox active proteins (Zhang et al., 2020) like PilA of *G. sulfurreducens* that conducts electrons. The electrical (conductive) properties of individual or polymeric proteins have been extensively evaluated using scanning tunneling *(*STM), atomic force microscope (AFM) or transmission electron microscope (TEM). However, these technical require a greats and sophistical treatments for the electrodes and samples, some which may be far from their natural responses (Zhang et al., 2020; Myers et al., 2023; Szmuc et al., 2023).

Applying the concept of Costa-Krämer et al., (1995) and Briones Hernández (2004), we designed and construct a mechanically controlled break junction device (MCBJ) to forming and breaking metallic Cu-Cu contacts using macroscopic wires. The currents (I) between contacts were amplified, recorded as electrical potential (V), and detected using an oscilloscope, enable us to calculate protein conductance after Cu-Cu contact has been formed

and broken (Fig 25). The assayed protein was the pilin PilV of *At. thiooxidans* and the thioredoxin (Trx) protein, since Trx is a thiol-reducing (redox-active) protein with electron-rich amino acids like cysteine, tyrosine, and tryptophan (Cys-Gly-Pro-Cys-) in its exposed active center (Holmgren 1985).

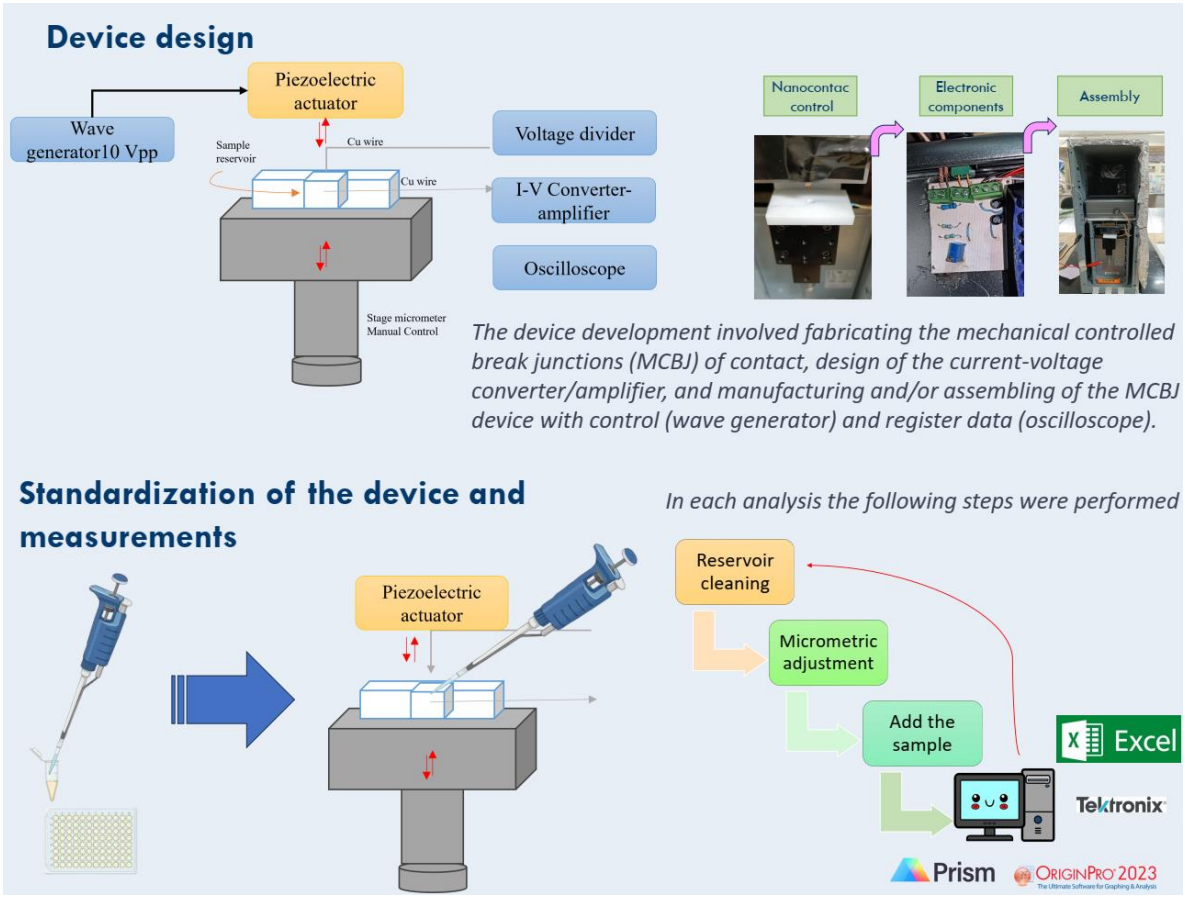

Figure 25. Brief description of MCBJ device: design, standardization and analysis.

Until the publication of this thesis, our group still continues with the data analysis and theoretical adjustment.

References Chapter VI

Briones Hernández, Joel; 2004. Conductancia eléctrica en el régimen balístico a través de contactos atómicos metálicos 42543 (Instituto de Física "Manuel Sandoval Vallarta").

Creasey RC, Mostert AB, Nguyen TA, Virdis B, Freguia S, Laycock B. 2018. Microbial nanowires–electron transport and the role of synthetic analogues. Acta Biomater 69:1-30. doi:1016/j.actbio.2018.01.007

Costa-Krämer JL, García N, García-Mochales P, Serena PA. 1995. Nanowire formation in macroscopic metallic contacts: quantum mechanical conductance tapping a table top. Surf Sci. 1–3:L1144–L1149. doi:10.1016/0039-6028(95)00967-1

Hernández-Sánchez A, Páez-Pérez ED, Alfaro-Saldaña E, Olvares-Iliana V, García-Meza JV 2024. Understanding a core pilin of the type IVa pili of *Acidithiobacillus thiooxidans*, PilV

Holmgren A. 1985. Thioredoxin. Annu Rev Biochem 54:237-271. doi:10.1146/annurev.bi.54.070185.001321

Schlag EW, Sheu SY, Yang DY, Selzle HL, Lin SH. 2007. +, Angew Chem Int Ed 46:3196–3210. Doi: 10.1002/anie.200601623

Shih C, Museth AK, Abrahamsson M et al., 2008) Tryptophan-accelerated electron flow through proteins. Science 320:1760-1762. doi:10.1126/science.1158241

Szmuc E, Walker DJF, Kireev D, Akinwande D, Lovley DR, Keitz B, Ellington A. 2023. Engineering *Geobacter* pili to produce metal: organic filaments. Biosens Bioelectron. 114993:114993. doi:10.1016/j.bios.2022.114993

ANNEXE

SPRINGER NATURE LICENSE
TERMS AND CONDITIONS

Apr 10, 2024

This Agreement between Mrs. Araceli Hernández Sánchez ("You") and Springer Nature ("Springer Nature") consists of your license details and the terms and conditions provided by Springer Nature and Copyright Clearance Center.

License Number	5765671018083
License date	Apr 10, 2024
Licensed Content Publisher	Springer Nature
Licensed Content Publication	Extremophiles
Licensed Content Title	Disorder and amino acid composition in proteins: their potential role in the adaptation of extracellular pilins to the acidic media, where Acidithiobacillus thiooxidans grows
Licensed Content Author	Edgar D. Páez-Pérez et al
Licensed Content Date	Oct 17, 2023
Type of Use	Thesis/Dissertation
Requestor type	academic/university or research institute
Format	print and electronic